



National Library
of Canada

Bibliothèque nationale
du Canada

Canadian Theses Service

Services des thèses canadiennes

Ottawa, Canada
K1A 0N4

CANADIAN THESES

THÈSES CANADIENNES

NOTICE

The quality of this microfiche is heavily dependent upon the quality of the original thesis submitted for microfilming. Every effort has been made to ensure the highest quality of reproduction possible.

If pages are missing, contact the university which granted the degree.

Some pages may have indistinct print especially if the original pages were typed with a poor typewriter ribbon or if the university sent us an inferior photocopy.

Previously copyrighted materials (journal articles, published tests, etc.) are not filmed.

Reproduction in full or in part of this film is governed by the Canadian Copyright Act, R.S.C. 1970, c. C-30.

**THIS DISSERTATION
HAS BEEN MICROFILMED
EXACTLY AS RECEIVED**

AVIS

La qualité de cette microfiche dépend grandement de la qualité de la thèse soumise au microfilmage. Nous avons tout fait pour assurer une qualité supérieure de reproduction.

S'il manque des pages, veuillez communiquer avec l'université qui a conféré le grade.

La qualité d'impression de certaines pages peut laisser à désirer, surtout si les pages originales ont été dactylographiées à l'aide d'un ruban usé ou si l'université nous a fait parvenir une photocopie de qualité inférieure.

Les documents qui font déjà l'objet d'un droit d'auteur (articles de revue, examens publiés, etc.) ne sont pas microfilmés.

La reproduction, même partielle, de ce microfilm est soumise à la Loi canadienne sur le droit d'auteur, SRC 1970, c. C-30.

**LA THÈSE A ÉTÉ
MICROFILMÉE TELLE QUE
NOUS L'AVONS REÇUE**

THE UNIVERSITY OF ALBERTA

PARTITION FUNCTION ZEROS IN STATISTICAL MECHANICS:
A REVIEW AND SOME NEW RESULTS

by

Jan C.W. Van Aalst

A THESIS

SUBMITTED TO THE FACULTY OF GRADUATE STUDIES AND RESEARCH

IN PARTIAL FULFILMENT OF THE REQUIREMENTS FOR THE DEGREE

OF MASTER OF SCIENCE

IN

THEORETICAL PHYSICS

DEPARTMENT OF PHYSICS

EDMONTON, ALBERTA

SPRING, 1986

Permission has been granted to the National Library of Canada to microfilm this thesis and to lend or sell copies of the film.

The author (copyright owner) has reserved other publication rights, and neither the thesis nor extensive extracts from it may be printed or otherwise reproduced without his/her written permission:

L'autorisation a été accordée à la Bibliothèque nationale du Canada de microfilmer cette thèse et de prêter ou de vendre des exemplaires du film.

L'auteur (titulaire du droit d'auteur) se réserve les autres droits de publication; ni la thèse ni de longs extraits de celle-ci ne doivent être imprimés ou autrement reproduits sans son autorisation écrite.

ISBN 0-315-30227-5

THE UNIVERSITY OF ALBERTA

RELEASE FORM

NAME OF AUTHOR: Jan C.W. Van Aalst
TITLE OF THESIS: Partition Function Zeros in Statistical
..... Mechanics: A Review and Some New
..... Results
DEGREE: Master of Science
YEAR THIS DEGREE GRANTED 1986

Permission is hereby granted to THE UNIVERSITY OF ALBERTA LIBRARY to reproduce single copies of this thesis and to lend or sell such copies for private, scholarly or scientific research purposes only.

The author reserves other publication rights, and neither the thesis nor extensive extracts from it may be printed or otherwise reproduced without the author's written permission.

.....
(Student's signature)

Student's Permanent Address:
3783 Killarney Street
.....
Port Coquitlam, B.C.
.....
V3B 3G5
.....

Date: 7 , 1986

THE UNIVERSITY OF ALBERTA

FACULTY OF GRADUATE STUDIES AND RESEARCH

The undersigned certify that they have read, and recommend to the Faculty of Graduate Studies and Research for acceptance, a thesis entitled "Partition Function Zeros in Statistical Mechanics: A Review and Some New Results," submitted by Jan C.W. Van Aalst in partial fulfilment of the requirements for the degree of Master in Science in Theoretical Physics.

.....
Supervisor

.....
Date: 1986

Voor Mijn Ouders,

A.J. Van Aalst - Van Thiel en C.J. Van Aalst

ABSTRACT

This thesis consists of two fairly independent parts. The first part contains an overview of what is known about the Ising model and other models from the exact solutions and series expansions.

In Chapter II we restrict ourselves to the Ising model and discuss the series expansions, exact solutions, critical behavior, and several related topics.

In Chapter III we discuss the theorems on the magnetization and the location of the fugacity zeros given by Lee and Yang at some length. Then we discuss fugacity zeros distributions, some of the extensions of the theorems, Fisher's conjectures regarding the temperature zeros, and examples of zeros distributions in a temperature variable.

In Chapter IV we discuss the analytical development of Stephenson and Couzens near the critical points in the complex temperature plane. They found a variable w , in terms of which they were able to extract the density of zeros. Near the critical points the distribution of zeros is proportional to $|y|$, the distance from the real axis. For the antiferromagnetic lattice with the two weakest interactions equal, zeros lie on circles centered on $w = -1$, approximately. The density of zeros varies as r^{-1} , where

r is the radius of such a circle.

In Chapter V we write the square of the partition function as a polynomial and compute numerically some zero distributions in the complex temperature plane. All distributions (quadratic and triangular) contain the unit circle in the w -plane. For some lattices the polynomial contains even powers of the z -variable only, giving rise to unphysical real zeros in the w -plane.

Chapter 1 provides a general introduction.

ACKNOWLEDGEMENT

Many individuals helped in one way or another, to make the completion of this work possible. It is a pleasure to thank them for their contributions, encouragement, and continual support.

I have greatly benefitted from the examples, as teachers, which many professors have provided over the duration of my studies here. They displayed a genuine love of students and the pursuit of truth, and they taught me with warmth. They include Professors A.Z. Capri, the late A.B. Bhatia, F. Baragar, N.A. Page, and J. Crowther. I also gratefully acknowledge the encouragement I received from Dr. T. Toyoda and Dr. T. Arimitsu, through many discussions.

Secondly, I am indebted to my advisor, Professor J. Stephenson, for his untiring and patient supervision. The thesis project which he suggested has been a very rewarding one, and he guided me on several other projects as well. I gratefully acknowledge the help which Baltazar Aguda provided in drawing some of the illustrations for Chapters II and III.

Thirdly, I record my gratitude toward those who helped incessantly to make my stay in Edmonton a more pleasant one, and those who guided me in my volunteer activities. They include David Hinz, Joanne Weber, Peter Lyons,

Marianne Malo, Loretta Fowley and Jean Forest.

By far the greatest debt is toward my parents. Their continual support and encouragement were tremendous. Regrettably they received far too little in return for it, often having to wait long for a letter from me. I dedicate this thesis to them, hoping it is worthy of such a dedication. Finally, I gratefully acknowledge the contribution which W.J. Van Thiel made toward my education, in sponsoring my immigration into Canada, and in a variety of other ways.

TABLE OF CONTENTS

| Chapter | | page |
|---------|--|------|
| I | INTRODUCTION | 1 |
| II | THE ISING MODEL | 5 |
| | 2.1 Introduction | 5 |
| | 2.2 Series Expansions | 10 |
| | 2.3 Transformations of Ising Lattices | 14 |
| | 2.4 Exact Solutions | 19 |
| | 2.5 Two-spin Correlations | 23 |
| | 2.6 Critical Behavior | 26 |
| | BIBLIOGRAPHY | 34 |
| III | A REVIEW OF PARTITION FUNCTION ZEROS IN STATIS- TICAL MECHANICS | 37 |
| | 3.1 Introduction | 37 |
| | 3.2 Numerical Studies | 43 |
| | 3.3 Further Rigorous Developments | 47 |
| | 3.4 Lee-Yang Edge | 51 |
| | 3.5 Temperature Zeros | 53 |
| | 3.6 Connection with Thermodynamics | 55 |
| | BIBLIOGRAPHY | 62 |
| IV | SOME NEW ANALYTICAL RESULTS ON THE TEMPERATURE ZEROS | 64 |
| | 4.1 Introduction | 64 |
| | 4.2 General Development Near the Curie Point | 64 |

| Chapter | page |
|--|------|
| 4.3 Examples | 70 |
| 4.4 Development Near the Néel Point | 76 |
| 4.5 Temperature Zeros for $J_1 < J_2 = J_3 < 0$ | 77 |
| BIBLIOGRAPHY | 82 |
| V | |
| SOME NUMERICAL RESULTS ON THE TEMPERATURE ZEROS | 83 |
| 5.1 Location of the Temperature Zeros | 83 |
| 5.2 Anisotropic Quadratic Lattices | 87 |
| 5.3 Class (1) Lattices | 88 |
| 5.4 Partly Anisotropic Ferromagnetic Lattices ... | 91 |
| 5.5 Partly Anisotropic Antiferromagnetic Lattices | 93 |
| VI | |
| DISCUSSION AND CONCLUSIONS | 118 |
| BIBLIOGRAPHY | 121 |

LIST OF TABLES

| Table | | page |
|-------|---|------|
| 2.1 | Critical exponents, their definitions, and scaling laws | 30 |
| 5.1 | Classification of lattices, and transforma- tions used to prove symmetry under $z \rightarrow -z$ and to reduce the range of ϕ_r and/or ϕ_s required in numerical calculations | 95 |
| 5.2 | Lattice classification data, critical point values z_C , z_N and associated unphysical real w zeros for selected quadratic and triangular lattices | 96 |

LIST OF FIGURES

| Figure | | page |
|--------|---|------|
| 2.1 | H-T diagram for Ising model anti-ferromagnet | 31 |
| 2.2 | The star-triangle transformation | 32 |
| 2.3 | Inversion of triangle | 33 |
| 2.4 | H-T diagram for Ising ferromagnet | 33 |
| 3.1 | Analytical structure of fugacity plane | 60 |
| 3.2 | Density of fugacity zeros on unit circle | 60 |
| 3.3 | Zeros in the $X = \exp(-K)$ plane computed by Abe and Katsura | 61 |
| 3.4 | Boundary conditions for lattices (A) and (B) in Section 3.5 | 61 |
| 3.5 | Temperature zeros obtained by Ono <u>et al.</u> for the 4x6 quadratic lattice | 61 |
| 4.1 | Circles centered on $-\beta = \frac{\alpha}{\alpha-1}$ | 81 |
| 5.1 | Zero distribution for (310) in the z-plane | 97 |
| 5.2 | Zero distribution for (320) in the z-plane | 97 |
| 5.3 | Zero distribution for (210) in the z-plane | 98 |
| 5.4 | Zero distribution for (310) in the w-plane | 99 |
| 5.5 | Zero distribution for (320) in the w-plane | 100 |
| 5.6 | Zero distribution for (210) in the w-plane | 101 |
| 5.7 | Zero distribution for (331) in the z-plane | 102 |
| 5.8 | Zero distribution for (113) in the z-plane | 103 |
| 5.9 | Zero distribution for (311) in the z-plane | 104 |

| Figure | | page |
|--------|---|------|
| 5.10 | Zero distribution of the completely isotropic lattice (111) in the z-plane | 104 |
| 5.11 | Zero distributions for (311) in the w-plane | 105 |
| 5.12 | Zero distribution for (113) in the w-plane | 106 |
| 5.13 | Zero distribution for (311) in the w-plane | 107 |
| 5.14 | Zero distribution for (311) in the w-plane | 108 |
| 5.15 | Zero distribution for (221) in the z-plane | 109 |
| 5.16 | Zero distribution for (112) in the z-plane | 109 |
| 5.17 | Zero distribution for (221) in the w-plane | 110 |
| 5.18 | Zero distribution for (112) in the w-plane | 111 |
| 5.19 | Zero distribution for (332) in the z-plane | 112 |
| 5.20 | Zero distribution for (223) in the z-plane | 112 |
| 5.21 | Zero distribution for (332) in the w-plane | 113 |
| 5.22 | Zero distribution for (223) in the w-plane | 114 |
| 5.23 | Zero distribution for (211) in the w-plane | 115 |
| 5.24 | Zero distribution for (322) in the w-plane | 116 |
| 5.25 | Zero distribution for (211) in the z-plane | 117 |
| 5.26 | Zero distribution for (322) in the z-plane | 117 |
| 5.27 | Zero distribution for the completely anisotropic lattice (321) in the z-plane | 118 |
| 5.28 | Zero distribution for (321) in the w-plane | 119 |

CHAPTER I
INTRODUCTION

When helium is cooled below 2.17K it separates into two fluid phases. One is the normal fluid that also exists above this temperature, and the other is a superfluid, which has a vanishing viscosity. The coexistence of water and ice at 0°C is well known. These substances are said to exhibit a phase transition. Water and ice both consist of H₂O molecules, but have very different features. The specific volume of ice is much larger than that of water; ice has a crystalline structure, etc.

Some materials are ferromagnetic. This means that the microscopic magnetic moments do not average out to zero, but tend to line up in a certain direction. It may be less obvious than for condensation, but here, too, there is a transition involved. Below the critical point there is long-range order. This means that two magnetic moments far apart know what the orientation of the other magnetic moment is and will align in such a way as to minimize the free energy. Above the critical point this does not happen. The reason some materials seem to be naturally ferromagnetic is that the critical point is quite high for these materials.

By studying phase transitions one hopes to gain some

knowledge concerning the mechanisms by which these transitions take place. Above and below the critical point the physics is not very interesting. Heating water from 30°C to 40°C does not yield an understanding of the physical interactions. Of course one can make a measurement of this type to obtain the specific heat for a certain temperature range, and this may be of interest in an engineering situation. From the point of view of physics the interesting thing is that H₂O molecules can either behave as a fluid, or else as a solid, depending on the temperature.

The aim of statistical mechanics is, starting from certain assumptions about the interatomic (or intermolecular) interactions, to predict the macroscopic behavior of a material. To be specific, consider a lattice of N sites, with an atom of magnetic moment $\vec{m} = g\mu_B \vec{J}$, where \vec{J} is the total angular momentum. According to quantum mechanics this magnetic moment can be oriented in $2J + 1$ directions in space. The lattice as a whole then has $(2J + 1)^N$ distinct configurations. With each configuration one associates an energy E which arises from the interactions between the atoms, and of the atoms with an external magnetic field. One could then calculate the partition function in the canonical ensemble, and obtain the magnetization from the derivative of the free energy with respect to the magnetic field. If one then takes the limit $H \rightarrow 0$ one could find, for a certain range of temperatures, that $M_0 \equiv M(H=0, T) \neq 0$.

Unfortunately it is possible to calculate the partition function exactly only for a much restricted class of models, and one must resort to a more indirect approach. One such approach is to expand the partition function in a perturbation series, and obtain the desired information from these series. This approach has been very fruitful.

Detailed analysis near criticality has shown that the critical exponents are independent of the structure of the lattice and depend only on its dimensions. It turns out that one can also construct invariants of certain of the critical amplitudes. These results have led to the universality hypothesis. Critical problems may be divided into classes which are differentiated by (a) the dimensionality of the system, (b) the symmetry of the interactions, and perhaps some other criteria. Within such a universality class the critical parameters are to be the same, or at worst continuous functions of few parameters. If one compares the diagrams we show in Chapter V in the z -plane, one observes the essential features are similar for quadratic and triangular lattices. The critical points are at different locations for different lattices, and the interactions can change the diagrams significantly, e.g. when two of the interactions become equal.

A second result known from the analysis of series and from the exact solutions of the Ising model is the concept of scaling. The scaling laws discussed in Section 2.6 arise from thermodynamic scaling. Because at the

critical point fluctuations at all length scales are important to the thermodynamic functions, one might expect invariance under a scaling of the length. This scaling of the length will give scaling laws involving the critical exponents of the correlation function.

In Chapter II we give an overview of what is known about the Ising model on the basis of series expansions, not including scaling and universality.

A second approach was put forward by Lee and Yang, and is reviewed in Chapter III. For a finite lattice the partition function is a polynomial. The analytic structure of the partition function can then be discussed in terms of the roots of this polynomial. This approach does not give the partition function, but it does give information regarding the onset of a phase transition, and can be used to estimate the critical temperature and some of the critical exponents independently of the series analysis.

In Chapters IV and V we then discuss some new results regarding the temperature zeros.

CHAPTER II
THE ISING MODEL

2.1 Introduction

In this chapter we give an overview of what is known about the Ising model on the basis of the exact solutions and series expansions. This overview is a selective one, but sufficient to provide the content within which we can discuss the partition function zeros. Exactly solved models in statistical mechanics have been treated by Baxter.¹ A comprehensive review of the theory of critical phenomena was edited in the 1970s by Domb and Green; it contains contributions from many authors.^{a)}

Following Pathria² we consider a lattice of N sites with a spin capable of two spatial orientations at each site. Such a lattice has 2^N distinct configurations. Let us make the following assumptions:

1. Translational invariance;
2. Only two-body interactions between nearest neighbor spins are important, and these interactions are sufficiently weak to be treated as perturbations.

^{a)} C. Domb and M.S. Green (eds.), Phase Transitions and Critical Phenomena, Academic Press. Reference will be made to the individual contributions in this series, as they are needed in the text.

As a first approximation one can then treat the lattice as a system of N non-interacting fermions, and obtain the wavefunction in terms of the Slater determinant involving the N wavefunctions $\psi_i(\vec{x}_i)$ centered on the sites i . The interaction energy between the i -th site and the j -th site can then be obtained using first order perturbation theory.

After integration over the $N-2$ irrelevant coordinates there are two situations to consider: the spatial part of the (remaining part of the) wavefunction can be odd or even.

The even state is a singlet and corresponds to two antiparallel spins; the odd state is a triplet and corresponds to parallel spins. The interaction energy reduces to

$K_{ij} \pm J_{ij}$, where the upper sign refers to the antiparallel state. K_{ij} is the Coulomb energy and J_{ij} the quantum mechanical exchange energy. If $V(|\vec{x}_i - \vec{x}_j|)$ is the interatomic potential,

$$K_{ij} = \int d^3x_i d^3x_j \psi_i^*(\vec{x}_i) \psi_j^*(\vec{x}_j) V(|\vec{x}_i - \vec{x}_j|) \psi_i(\vec{x}_i) \psi_j(\vec{x}_j) \quad (2.1)$$

and

$$J_{ij} = \int d^3x_i d^3x_j \psi_i^*(\vec{x}_i) \psi_j^*(\vec{x}_j) V(|\vec{x}_i - \vec{x}_j|) \psi_i(\vec{x}_j) \psi_j(\vec{x}_i). \quad (2.2)$$

Let ϵ_{++} be the interaction energy of a pair of parallel spins and ϵ_{+-} of a pair of antiparallel spins. Algebraically,

$$\epsilon_{++} - \epsilon_{+-} = -2J_{ij}. \quad (2.3)$$

If $J_{ij} > 0$, the parallel state is the energetically favored one, and if $J_{ij} < 0$, the antiparallel state. The first situation corresponds to ferromagnetism, and the last to anti-ferromagnetism. Consider the expression

$$2\vec{s}_i \cdot \vec{s}_j = (\vec{s}_i + \vec{s}_j)^2 - \vec{s}_i^2 - \vec{s}_j^2 = S(S+1) - 2S(S+1).$$

If the spins are parallel $S = 1$ and this expression is positive; if they are antiparallel $S = 0$ and it is negative.

Therefore the interaction energy can be written in terms of the spins as $-2J_{ij}\vec{s}_i \cdot \vec{s}_j + \text{const}$. The total interaction energy for a lattice of spin $\frac{1}{2}$ particles is therefore ^{b)}

$$E = \text{const} - 2 \sum_{nn} J_{ij} \vec{s}_i \cdot \vec{s}_j. \quad (2.4)$$

The model based on this interaction energy is known as the Heisenberg model. If only the z-components of the spins are kept the Ising model results. The z-component is the only one which is diagonal; the x- and y-components are given in terms of the raising and lowering operators. Suppressing the x- and y-components also reduces the model to a classical one.

Ising³ showed that the one-dimensional model does not exhibit a spontaneous magnetization, but was not able to obtain the partition function in two dimensions.

If the interactions between the spins are all chosen to be of the same strength, say J , and periodic boundary conditions are employed, then the hamiltonian of the one-dimensional Ising model is symmetric in the spins. If the

b) One can generalize for other values of the spin. Instead of equ. (2.4), Heisenberg wrote down the expression

$$E = \text{const} - 2 \sum_{nn} J_{ij} \vec{s}_i \cdot \vec{s}_j.$$

spins interact with the magnetic field H , and the magnetic moment is m , the hamiltonian is

$$\hat{H}_N = -J \sum_{i=1}^N \sigma_i \sigma_{i+1} - \frac{1}{2} mH \sum_{i=1}^N (\sigma_i + \sigma_{i+2}) \quad (2.5)$$

Here σ_i is an eigenvalue of the Pauli matrix τ^z for the i -th spin. Introducing

$$K = J/kT \quad \text{and} \quad h = mH/kT \quad (2.6)$$

the partition function is written as

$$Z_N(H, T) = \sum_{\sigma_1} \cdots \sum_{\sigma_N} \exp \left\{ \sum_{i=1}^N (K \sigma_i \sigma_{i+1} + \frac{1}{2} h (\sigma_i + \sigma_{i+1})) \right\} \quad (2.7)$$

This can be written as the trace of a matrix. Let V be the matrix whose elements V_{ij} are defined by

$$V_{ij} = \langle \sigma_i | V | \sigma_j \rangle = \exp \{ K \sigma_i \sigma_j + \frac{1}{2} h (\sigma_i + \sigma_j) \} \quad (2.8)$$

then

$$\begin{aligned} Z_N(H, T) &= \sum_{\sigma_1} \cdots \sum_{\sigma_N} \langle \sigma_1 | V | \sigma_2 \rangle \langle \sigma_2 | V | \sigma_3 \rangle \cdots \langle \sigma_N | V | \sigma_1 \rangle \\ &= \text{tr } V^N \end{aligned} \quad (2.9)$$

Let λ_1 and λ_2 be the eigenvalues of V . Then

$$Z_N(H, T) = \lambda_1^N + \lambda_2^N. \quad \text{Asymptotically the partition function}$$

is obtained from the largest eigenvalue. In the present

case one obtains for the free energy per spin

$$\frac{-f}{kT} = \ln \{ e^K \cosh(\beta H) + \sqrt{e^{-2K} + e^{2K} \sinh^2(\beta H)} \}^{1/2} \quad (2.10)$$

It is easy to check that the magnetization vanishes when the

limit $H \rightarrow 0$ is taken.

In 1936, Peierls⁴ showed that the two-dimensional Ising model does have a spontaneous magnetization, so that it might be regarded as a valid model of ferromagnetism. Griffiths⁵ improved Peierls' argument slightly in 1964.

The solution of the two-dimensional Ising model turned out to be much more difficult than the one-dimensional case. Onsager⁶ gave the exact solution on a finite quadratic lattice, in the absence of a magnetic field, in 1944. The exact solution with a magnetic field is still an open problem. The first major step toward the Onsager solution was a paper by Kramers and Wannier⁷ in 1941. They introduced the matrix method we already used in this section to solve the one-dimensional problem. They were also able to conjecture the transition temperature of the Ising lattice, by realizing that a certain dual relationship exists between lattices of the same dimensionality but otherwise different geometrical features. We will discuss the dual transformation they discovered in Section 2.3.

Several authors, including Bethe, Braggs and Williams, and Gugenheim developed closed-form approximations,⁸⁻¹⁰ but these were rejected later, when it was clear they gave only a few of the terms of the series expansions correctly.¹¹ Series expansions had been obtained by Kramers and Wannier to check these closed-form approximations, but in 1949 Domb¹⁵ suggested that these expansions could be used to determine the critical behavior if sufficiently many terms are known.

In the next section we briefly discuss these series expansions. The calculations are quite formidable, and for a fuller discussion the reader is referred to the reviews by Domb^{12,13} in Domb and Green. We want to discuss these series here because they are an important tool in studying critical phenomena. Results from the partition function zeros must be corroborated with what is known from other approaches.

2.2 Series Expansions

At high temperatures $\beta = 1/kT$ is a small parameter, so we can expand the partition function in a perturbation series in terms of β . Let $\langle \cdot \cdot \cdot \rangle$ denote the trace over all the configurations. Then

$$Z_N = \langle e^{-\beta \hat{H}} \rangle = 1 - \beta \langle \hat{H} \rangle + \frac{1}{2!} \beta^2 \langle \hat{H}^2 \rangle - \dots \quad (2.11)$$

If $\ln Z_N$ is expanded instead of Z_N , we obtain the so-called cumulant expansion

$$\begin{aligned} \ln Z_N = & -\beta \langle \hat{H} \rangle + \frac{1}{2!} \beta^2 [\langle \hat{H}^2 \rangle - \langle \hat{H} \rangle^2] \\ & - \frac{1}{3!} \beta^3 [\langle \hat{H}^3 \rangle - 3\langle \hat{H}^2 \rangle \langle \hat{H} \rangle + 2\langle \hat{H} \rangle^3] + \dots \end{aligned} \quad (2.12)$$

A convenient form of this type of series is^{c)}

$$\ln Z_N = N \ln(2 \cosh h) + \frac{1}{2} N q \ln(\cosh K) + \sum_{r=1}^{\infty} w^r \psi_r(\tau), \quad (2.13)$$

with

^{c)} q is the coordination number.

$$w = \tanh K \quad , \quad \tau = \tanh h \quad (2.14)$$

The $\psi_r(\tau)$ are polynomials of degree r in τ , which contain only even powers of τ . The reason no odd powers occur is that when the trace in equation (2.12) is taken, the contributions arising from odd powers of h cancel.

To estimate the critical behavior from series of this type, Domb and Sykes^{14,15} assumed that the susceptibility has a branch point singularity at the critical point of the form

$$\chi(T) \sim A(T - T_c)^{-\gamma} \quad , \quad (2.15)$$

which defines the critical susceptibility exponent and the critical amplitude A . When more terms in the susceptibility series became available, they modified this to a singularity of the Darboux form:¹⁶

$$\chi(T) \sim (T - T_c)^{-\gamma} A(T) + B(T) \quad , \quad (2.16)$$

where A and B are analytic at T_c .

Mathematically, no rigorous results can be expected if only a finite number of terms are calculated. Nevertheless the susceptibility series is quite smooth, and a good estimate of the susceptibility critical exponent can be obtained from a small number of its terms. In 1957, Domb suggested a value for γ of exactly $7/4$ for the simple quadratic and plane triangular lattices. In 1959, Fisher¹⁷ justified this value; his arguments were made more rigorous by several authors¹⁸⁻²² after the publication of the scaling equation of state in the critical region.²³ Domb and

Sykes²⁴ then suggested that for all three-dimensional lattices $\gamma = 5/4$. This was an important step toward Kadanoff's universality hypothesis (see Chapter I).

Besides the high temperature limit there are two other situations in which we can make perturbation expansions. Physically, at high temperature, the lattice is oriented at random. As the temperature is lowered slightly some of the spins will align.

In a very strong magnetic field all the spins will be aligned. If we subsequently lower the field some of the spins will turn over and form clusters of turned-over spins.

Now

$$z = e^{-2h} \quad (2.17)$$

is a small parameter, so $\ln Z_N$ can be expanded in terms of z . The result is

$$\ln Z_N \approx -\frac{1}{2} N \ln z - \frac{qN}{8} \ln u + \sum_{r=1}^{\infty} z^r G_r(u) \quad (2.18)$$

The function $G_r(u)$ is related to the cluster integral for a cluster consisting of r overturned spins; u is an appropriate temperature variable. For the quadratic lattice with periodic boundary conditions $u = \exp(-4K)$. This kind of expansion is very similar to the cluster expansions used in Mayer's cluster integral theory of fluids.

At sufficiently low temperatures the spins will align even in the absence of a magnetic field. Then one has the possibility that some of the spins turn over, raising

the energy of the lattice. Now one obtains a series of the

form

$$\ln Z_N = N \ln 2 - \frac{1}{8} \frac{q}{N} \ln u + \sum_{r=1}^{\infty} B_r^{(0)} u^r \quad (2.19)$$

The term $N \ln 2$ arises from the high temperature limit.

In three dimensions the signs of the coefficients $B_r^{(0)}$ alternate, which means that

$$\sum_{r=1}^{\infty} B_r^{(0)} u^r \quad (2.20)$$

has a singularity on the negative real axis, corresponding to an imaginary temperature. Generally this (unphysical) singularity makes it difficult to extract the critical behavior from a finite number of terms. ^{d)}

In 1961, ²⁵ Baxter introduced the so-called Padé approximant method to those series to obtain information about the critical behavior. He could bypass the singularity on the negative real axis, and was able to estimate the exponent β of the spontaneous magnetization (see below). Since then the Padé approximant has been a useful tool in analyzing series of the Ising model, and has also been applied to other models.

The antiferromagnetic lattice can in principle be discussed by changing $J \rightarrow -J$ and then insisting that $J > 0$. The last term in the high temperature series is now an

^{d)} Note that imaginary interactions on the hexagonal corresponds to a real temperature on the antiferromagnetic triangular lattice.

alternating series. Instead of equation (2.13), one has

$$\ln Z_N = N \ln(2 \cosh h) + \frac{1}{2} N q \ln(\cosh K) + \sum_{r=1}^{\infty} (-1)^r w^r \psi_r(1). \quad (2.21)$$

The high field series (2.17) remains valid but the range of u is different. Instead of the ferromagnetic range $0 < u < 1$, u is in $1 < u < \infty$.

At low temperatures, the situation is more complicated because the ground states change. We show the conjectured T-H diagram of the antiferromagnetic lattice in Figure 2.1.

2.3 Transformations of Ising Lattices

Since the matrix V in equation (2.8) is a 2×2 matrix, it can be expressed in terms of the Pauli matrices and the unit matrix. If $h = 0$, $V|1\rangle = e^K|1\rangle + e^{-K}|-1\rangle$ and $V|-1\rangle = e^{-K}|1\rangle + e^K|-1\rangle$, so

$$V = e^K \mathbb{1} + e^{-K} \tau^x, \quad (2.22)$$

with

$$\tau^x = \begin{pmatrix} 0 & 1 \\ 1 & 0 \end{pmatrix} \quad \text{and} \quad \mathbb{1} = \begin{pmatrix} 1 & 0 \\ 0 & 1 \end{pmatrix}.$$

Usually one deals with V^N , where N is a large number. The leading term of V^N , with $K > 0$ is $e^{NK} \mathbb{1}$; this is a very large number times the unit matrix. One could reduce this number by writing $K^* = \ln K$, in which case the leading

term becomes $(K^*)^{N\uparrow}$. Assuming that J is fixed, the lattice has gone from one at a low temperature to one at a high temperature when $K \rightarrow K^*$.

If K^* is defined by the relation

$$K^* = \frac{1}{2} \ln \coth K = \tanh^{-1} (e^{-2K}) \quad (2.23)$$

instead, then, one can show that

$$\sinh 2K \sinh 2K^* = 1. \quad (2.24)$$

Notice that this last equation is symmetric with respect to K and K^* . In terms of K^* the matrix V becomes

$$V = (2 \sinh 2K)^{1/2} \exp(K^* \tau^x). \quad (2.25)$$

Onsager⁶ used this form of V in calculating the partition form of the finite, square Ising lattice, in the absence of a magnetic field. The addition of one row of N spins to the lattice is represented by

$$V_1 = (2 \sinh K_1)^{N/2} \cdot \exp(K_1^* \sum_{j=1}^N \tau_j^x), \quad (2.26)$$

where

$$\tau_j^x = \uparrow \times \uparrow \times \dots \times \tau^x \times \uparrow \times \dots \times \uparrow, \quad (2.27)$$

and the Pauli matrix τ^x is in the j -th position. The interaction energy within a row is expressed by

$$V_2 = \exp(K_2 \sum_{j=1}^N \tau_j^z \tau_{j+1}^z). \quad (2.28)$$

The partition function is then obtained from the largest eigenvalue of V^N , where

$$V = V_1 V_2. \quad (2.29)$$

Onsager showed that asymptotically the partition functions of a lattice with interactions (K_1^*, K_2^*) and a lattice with interactions (K_1, K_2) are related by

$$\lambda_{\max}(K_1^*, K_2^*) = (\sinh 2K_1 \sinh 2K_2)^{-N/2} \lambda_{\max}(K_1, K_2) . \quad (2.30)$$

The lattice with interaction strengths (K_1^*, K_2^*) has ferromagnetic short-range order, and the one with interaction strengths (K_1, K_2) long-range order. If the physical lattice exhibits only these two phases, the phase boundary must be given by the condition

$$\sinh 2K_1 \sinh 2K_2 = 1 , \quad (2.31)$$

since then $\lambda_{\max}(K_1^*, K_2^*) = \lambda_{\max}(K_1, K_2)$.

The so-called dual transformation defined by equation (2.21) was discovered by Kramers and Wannier⁷ in 1941, and they used equation (2.31) to estimate the critical temperature. Their result is a precursor to the idea of the fixed point.

Next we discuss the star-triangle transformation. We restrict ourselves, following Syozi's²⁶ review, to the isotropic case. The more general, anisotropic case has been discussed by Domb²⁷ in 1960 in his review, and by Green and Hurst.²⁸

Suppose any spin σ interacts with three surrounding spins σ_1 , σ_2 , and σ_3 with equal interaction strengths (see Figure 2.2), and that $H = 0$. The partition function contains

factors

$$\sum_{\sigma=\pm 1} \exp(K\sigma(\sigma_1 + \sigma_2 + \sigma_3)) = 2 \cosh [K(\sigma_1 + \sigma_2 + \sigma_3)] . \quad (2.32)$$

We want to write this in terms of the sum of the interactions between σ_1 , σ_2 , and σ_3 , as follows:

$$2\cosh(K(\sigma_1 + \sigma_2 + \sigma_3)) = \Delta \exp\{R(\sigma_1\sigma_2 + \sigma_2\sigma_3 + \sigma_3\sigma_1)\} . \quad (2.33)$$

Here Δ and R are to be determined.

If $\sigma_1 = \sigma_2 = \sigma_3 = \pm 1$, equation (2.33) yields

$$2\cosh 3K = \Delta e^{3R} . \quad (2.34)$$

On the other hand, if $\sigma_1 = \sigma_2 = 1$ and $\sigma_3 = -1$, or cyclic permutations hereof, one obtains the expression

$$2\cosh K = \Delta e^{-R} . \quad (2.35)$$

Dividing equation (2.34) by the last equation yields

$$e^{4R} = 2\cosh 2K - 1, \quad (2.36)$$

and multiplying them,

$$\Delta^4 = 16 \cosh 3K \cosh^3 K = e^{4R} (e^{4R} + 3)^2 . \quad (2.37)$$

The last two equations define the star-triangle transformation for this special case.

Because we have summed over $\sigma = \pm 1$, σ no longer occurs in the partition function. Consequently the star consisting of σ and the three spins σ_1 , σ_2 , and σ_3 has been reduced to a triangle with σ_1 , σ_2 , and σ_3 at its vertices. The interactions R now correspond to the edges of this triangle. If

the star-triangle transformation is applied to half of the spins on a hexagonal lattice, a triangular lattice results.

The dual and star-triangle transformations are useful in relating the partition functions of geometrically different lattices. The square lattice is self-dual in the sense that applying the dual transformation to a square lattice results again in a square lattice. However, the boundary conditions may change; not all square lattices are exactly self-dual. We have seen that the star-triangle transformation changes a hexagonal lattice into a triangular one. It can be shown that the dual transformation also changes the hexagonal lattice to a triangular lattice.

In order to estimate the critical temperature of the triangular lattice, one first applies the star-triangle transformation to the triangular lattice to get a hexagonal lattice, and subsequently applies the dual transformation to get a triangular lattice. This succession of transformations is called inversion. The two triangular lattices here are not topologically equivalent, since the triangles in the final lattice are upside down (see Figure 2.3). If the original (triangular) lattice is at high temperature the inverted lattice is at low temperature. To obtain a triangular lattice which is topologically equivalent to the original one, one must apply inversion twice.

2.4 Exact Solutions

Onsager obtained the partition function and boundary tension of the anisotropic square lattice by calculating the eigenvalues of the matrix V in equation (2.29). From the largest eigenvalue of V he found that

$$\ln Z = N \ln 2 + \frac{N}{8\pi^2} \int_0^{2\pi} \int_0^{2\pi} \ln(C_1 C_2 - S_1 \cos \omega - S_2 \cos \omega_2) d\omega_1 d\omega_2, \quad (2.38)$$

where

$$C_i = \cosh 2K_i \quad \text{and} \quad S_i = \sinh 2K_i. \quad (2.39)$$

The boundary tension is given by

$$\sigma = 2(K_2 - K_1^*) = 2J_2 - kT \ln(\coth(J_1/kT)). \quad (2.40)$$

The details of Onsager's solution are rather formidable! Several authors have attempted to elucidate his method. Kaufman²⁹ considered a set of $2n$ 2^n -dimensional matrices Γ_k obeying the commutation rules

$$\{\Gamma_\ell, \Gamma_k\} = 2\delta_{\ell k}, \quad (2.41)$$

and showed that the dual transformation interchanges the role of K_1 and K_2 (when applied to the square lattice) via a complex rotation in the $2n$ -space spanned by the Γ_k . Onsager had obtained the eigenvalues of V in terms of a product of the eigenvalues of the rotation matrix. Kaufman also pointed out that another representation of the algebra (2.40) is a rotation in 2^n -dimensional spin space and discussed Onsager's work in the framework of this representation.

Green and Hurst²⁸ have also given a simplified derivation of Onsager's solution, and more recently Baxter and Enting³⁰ gave a derivation using the star-triangle rotation recursively. For a more complete overview of the exact solutions we refer the reader to the review article by Temperley³¹ in Domb and Green. This article also contains a discussion of the pfaffian method, in which the partition function is expressed as a pfaffian.^{e)}

In 1964, Schultz, Mattis, and Lieb³² gave a derivation of the partition function in the density matrix formalism. Their derivation makes use of the commutation relations of the spin operators in a more natural way, and elucidated why Onsager's method cannot yield the partition function of a finite lattice in a magnetic field. It is already clear from the discussion in Section 2.1 that this is because the hamiltonian cannot be separated if $H \neq 0$. The method of Schultz et al. is also likely to be more comprehensible to the modern student of the Ising model. Instead of Onsager's quaternion algebra, one introduces second quantization and creation and annihilation operators, a procedure very familiar from the theory of superconductivity, lattice vibrations, and field theory.

By the application of Wick's theorem these authors showed also that the two-spin correlations on an axis can be expressed in terms of a single Toeplitz determinant.

^{e)} A pfaffian^s is the analogous quantity to the determinant for a triangular array.

Onsager and Kaufman obtained a sum of two Toeplitz determinants, and Montroll, Potts and Ward³³ showed the equivalence of these results only with considerable effort.

Below we briefly discuss the derivation due to Schultz et al. A fuller discussion can be found in Callaway's³⁴ book. Consider a lattice of N rows and M columns. It is assumed that the ends in the vertical direction of the lattice are free. One may employ periodic boundary conditions in the horizontal direction, but this is not necessary. If N is large, it is reasonable to assume that the probability of finding the N -th row in a certain configuration, if one averages over the configurations of the other $N-1$ rows, is independent of N . One may then look for a recursion relation between the probability of a given configuration of the last row of lattices with N rows and $N-1$ rows, respectively.

Schultz et al. found that such a recursion relation was not possible as an operator equation, but was possible if applied to a particular state. They chose the state $|0\rangle$ in which all the spins point downwards. Let Σ_N denote a row of spins and $\rho_N(\Sigma_N)$ the density matrix of the lattice after taking the trace over the configurations of the first $N-1$ rows. Schultz et al. call $\rho_N(\Sigma_N)$ the reduced density matrix. They show that

$$\text{tr } \rho_N(\Sigma_N) = 2^M \langle 0 | \rho_N(\Sigma_N) | 0 \rangle, \quad (2.42)$$

so knowledge of the action of the recursion relation on $|0\rangle$ is sufficient for knowledge of the partition function.

Next they introduce fermion operators A_m^+ and A_m defined by

$$A_m^+ = \left[\exp\left(\pi i \sum_{j=1}^{m-1} \sigma_j^+ \sigma_j^-\right) \right] \sigma_m^+ \quad (2.43)$$

$$A_m = \left[\exp\left(\pi i \sum_{j=1}^{m-1} \sigma_j^+ \sigma_j^-\right) \right] \sigma_m^- \quad (2.44)$$

Here the σ_m^\pm are raising and lowering operators in one row. The transformation from the σ_m^\pm to the fermion operators leaves the parts in V due to the interactions between the spins in a quadratic form, but the part due to the interaction of the spins with the magnetic field is not left in a simple form. It is this difficulty which prohibits the solution of the Ising model in a magnetic field by this method. In addition, if second nearest neighbor interactions are allowed, V_2 involves higher-order terms than quadratic, preventing diagonalization of V .

Restricting themselves to nearest neighbor interactions and $H = 0$, Schultz et al. were able to diagonalize V and obtain the free energy per spin in one row:

$$F = -kT \ln(2 \sinh K_1)^{1/2} + \frac{1}{4\pi} \int_{-\pi}^{\pi} \epsilon_q dq \quad (2.45)$$

Here ϵ_q is a parameter which depends on K_1^* and K_2 , masking the dependence of F on K_2 slightly.

This method of obtaining the partition function is in principle not restricted to the two-dimensional lattice. To solve the three-dimensional lattice one would attempt to construct a recursion relation between the last planes of

the lattices. However, no such attempts seem to have been published.

2.5 Two-Spin Correlations

The correlation length is an interesting quantity since it is a measure of the extent to which order exists in the lattice. For future convenience, we briefly discuss the two-spin correlations here.

Schultz et al. obtained the correlations between two spins on the same row from Wick's theorem. The result can be expressed in terms of a determinant as follows:

$$\begin{aligned}
 \langle \tau_{nm}^z \tau_{nm'}^z \rangle &= \lim_{M \rightarrow \infty} \langle 0 | \tau_{nm}^z \tau_{nm'}^z | 0 \rangle \\
 &= \sum (-1)^P a_{m, P(m)} \cdots a_{m'-1, P(m'-1)} \\
 &= \begin{vmatrix} a_{m,m} & a_{m,m+1} & \cdots & a_{m,m'-1} \\ a_{m+1,m} & & & \\ & & & \\ & & & \\ a_{m'-1,m} & \cdots & \cdots & a_{m'-1,m'-1} \end{vmatrix} \quad (2.46)
 \end{aligned}$$

Here,

$$a_{ij} = \langle 0 | A_i^y A_{j+1}^x | 0 \rangle \quad (2.47)$$

If periodic boundary conditions are applied in the horizontal direction, a_{ij} depends on i and j only through

$i-j$. In this case the determinant in equation (2.46) is called a Toeplitz determinant. Below the critical point the asymptotic value of equation (2.46) was calculated by Montroll, Potts, and Ward,³⁸ and is given by

$$\lim_{m \rightarrow \infty} \lim_{M, N \rightarrow \infty} \langle \tau_{nm}^z \tau_{nm'}^z \rangle = \left[1 - \frac{(1 - \tanh^2 K_1)(1 - \tanh^2 K_2)}{16 \tanh^2 K_1 \tanh^2 K_2} \right]^{1/4} \quad (2.48)$$

Notice that this expression is completely symmetrical in K_1 and K_2 . Consequently the two-spin correlations are asymptotically similar along the lattice axes. Above T_c they vanish asymptotically.

Stephenson³⁵ classified the triangular lattices on the basis of the correlation functions. Let J_1 and J_2 be the interactions along the horizontal and vertical axes of a square lattice, and J_3 along the diagonals. If J_3 is the weakest interaction the Toeplitz determinant has the following symmetry properties along this axis:

$$\begin{aligned} a_{ij}(J_1, J_2, J_3)_3 &= a_{ij}(-J_1, -J_2, J_3)_3 \\ &= (-1)^{i-j+1} a_{ij}(-J_1, J_2, -J_3)_3 \\ &= (-1)^{i-j+1} a_{ij}(J_1, -J_2, -J_3)_3. \end{aligned} \quad (2.49)$$

The subscript 3 refers to the (3) axis. The correlations along this axis are invariant under the changes $J_1 \rightarrow -J_1$ and $J_2 \rightarrow -J_2$.

For the antiferromagnetic triangular lattice with $J_1 < J_2 < J_3 < 0$, Stephenson found that there is a disorder temperature $T_D < T_N$ determined by the condition

$$z_1 z_2 - z_2 z_3 - z_3 z_1 = -1, \quad (2.50)$$

where $z_\ell = \exp(-2J_\ell/kT)$.

Domb³⁰ has discussed that the Néel temperature T_N is determined by

$$z_1 z_2 - z_2 z_3 - z_3 z_1 = 1 \quad (2.51)$$

The ferromagnetic lattice with $J_1 > J_2 > J_3 > 0$ has a Curie point T_C determined by

$$z_1 z_2 + z_2 z_3 + z_3 z_1 = 1. \quad (2.52)$$

Notice that if the two weaker interactions are equal, equation (2.51) has no real solution.

In the ferromagnetic lattice the correlations are similar along all of the axes. Below T_C there is ferromagnetic long-range order, and above T_C short-range order.

To discuss the antiferromagnetic lattice below T_N one needs to distinguish between the axis with the weakest interaction (J_3) and the other two interactions. Along the (3) axis there is ferromagnetic long-range order. This is evident from the first line in equation (2.49). Along the two axes with the stronger interactions the correlations are similar to each other and there is antiferromagnetic long-range order.

Above T_N the correlations are again similar along all axes. If $T_N < T < T_D$ the pair correlations decay

monotonically, giving rise to antiferromagnetic short-range order. Above T_D the correlations also decay exponentially but within this decaying envelope there are oscillations which complicate the correlations slightly. Notice that T_D does not separate regions of order and disorder, as do T_N and T_D ; it separates two regions of disorder. The existence of T_D is related to the fact that there are triangles in the lattice. The antiferromagnetic quadratic lattice does not have a disorder point, and can be discussed by changing $J_1 \rightarrow -J_1$ and $J_2 \rightarrow -J_2$. In this case the Néel temperature is numerically equal to the Curie temperature.

2.6 Critical Behavior

Finally we describe the analytical behavior of the thermodynamic functions near the critical point. The critical behavior of a model is its most crucial test. Mean field theory correctly predicts that the Ising Lattice exhibits a phase transition, but it gives the critical exponents incorrectly. The reason for this is that the fluctuations are ignored in mean field theory, and they become infinite at the critical point. In the next chapters we will see how the zeros of the partition function can give information about the analytical structure of the partition function and the thermodynamic functions, so it will be useful to know what critical behavior we should expect from the zeros distributions.

At the critical point one usually assumes that the

thermodynamic functions have a branch point, as we discussed for the susceptibility in Section 2.2. This assumption allows one to introduce critical exponents and amplitudes. If it happens that the thermodynamic function under consideration is known to have a jump discontinuity at the critical point (e.g. on the basis of experimental evidence) then one must at first assume different critical exponents below and above T_c . In Table 2.1 we list the definitions of the critical exponents, their currently accepted values, and the scaling relations between them.

The magnetization of the ferromagnetic lattice is given by

$$M = m \left[1 - 2N^{-1} \sum_{r=1}^{\infty} z^r G_r(u) \right] . \quad (2.53)$$

Here $G_r(u)$ is the same as in the high field series (2.18).

Evaluating M at the critical temperature defines the M-H relation along the critical isotherm.

The terms of the series in equation (2.53) all have consistent signs, so there is a dominant singularity at $z = +1$, or $H = 0$. The critical exponent δ is then determined by the asymptotic values of the coefficients $G_r(u)$. Gaunt, Fisher, Sykes, and Essam³⁶ obtained $\delta = 15.00 \pm 0.08$ in two dimensions and $\delta = 5.20 \pm 0.15$ in three dimensions. They conjectured that $\delta = 15$ exactly for all two-dimensional lattices.

In view of the singularity in M at $z = +1$, the T-H-plane is cut along $H = 0$ from $T = 0$ to $T = T_c$. Above T_c

all the thermodynamic functions are analytic. The spontaneous magnetization has been discussed in detail by Griffiths,³⁷ especially some difficulties with its definition. We show the T-H diagram in Figure 2.4.

On the basis of thermodynamics alone, Rushbrooke³⁸ derived the inequality

$$\alpha' + 2\beta + \gamma' \geq 2, \quad (2.54)$$

and Griffiths^{39,40}

$$\alpha' + \beta(\delta + 1) \geq 2. \quad (2.55)$$

The ' here indicates that the significant critical exponent is the one for $T < T_C$. The last inequality was verified experimentally by Roach and Douglass.⁴¹ The inequalities (2.54) and (2.55) are very general. Their derivation does not require a lattice; it depends only on the requirement that the free energy is a convex function. For a particular model the inequalities can become equalities, as happens with the Ising model.

These relations suggest that the critical exponents are not all independent. Widom⁴² found a homogeneous equation of state from which such relations between the critical exponents, and many others could be derived. Subsequently these relations have been called scaling laws and the equation Widom discovered the scaling equation of state. Almost simultaneously Patashinskii and Pakrovskii⁴³ arrived at an equation of the same form by introducing coarse graining. In the critical region large blocks of

spins are then replaced by a single spin. Also simultaneously with these developments, Domb and Hunter introduced the gap exponent Δ in the even derivatives of the susceptibility.

Writing

$$\frac{d^{2r} \bar{\chi}_0}{d\bar{H}^{2r}} = C_{2r}^+ (1-t)^{-\gamma-2r\Delta}, \quad (2.56)$$

where $\bar{\chi}_0 = kT\chi/m^2$ and $\bar{H} = \beta mH$ they derived an equation of state of the same form as the one of Widom and Pataskinskii and Pakrovskii:

$$\bar{H}t^{-\Delta} = X^+(Mt^{\gamma-\Delta}). \quad (2.57)$$

Here X^+ is a power series containing only odd powers of its argument. It can be shown that $\gamma-\Delta = \beta$.

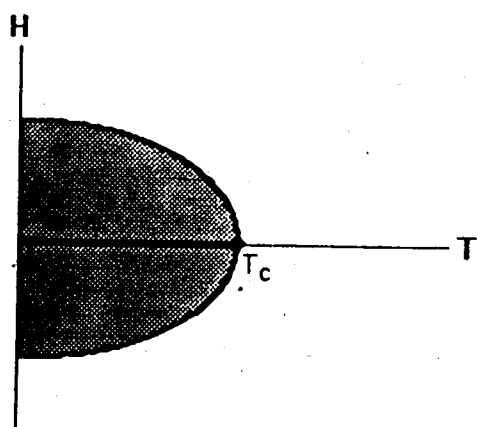
It should be emphasized that equation (2.57) is only valid in the critical region. It depends on only two critical exponents and a single function X^+ . A detailed discussion of this equation of state has been given by Domb¹¹ and others. This equation was derived from three very different perspectives. It is remarkable that these three approaches gave the same equation of state, and this fact led Kadanoff to his scaling hypothesis.

Table 2.1
 Critical exponents, their definitions, and scaling laws.
 (Adapted from references 2, 11, 34, 44, and references 32 and 33 of Chapter III)

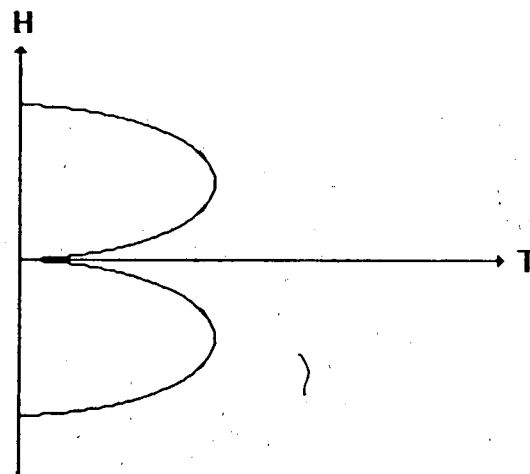
| Critical Exponent | Definition | Scaling Law | d=∞ | d=2 | d=3 |
|-------------------|--|-------------------------------------|----------------|----------------|--|
| β | $M \sim (-t)^\beta$ | | $\frac{1}{2}$ | $\frac{1}{8}$ | 0.313 ± 0.04 |
| γ | $x \sim t^{-\gamma}$ | | 1 | $\frac{7}{4}$ | 1.250 ± 0.001 |
| γ' | $x \sim (-t)^{-\gamma'}$ | | 1 | $\frac{7}{4}$ | 1.31 ± 0.05 |
| δ | $M \sim H^{1/\delta}$ | | 3 | 15 | 5.2 ± 0.15 |
| α | $C_H \sim t^{-\alpha}$ | $\alpha = 2 + \gamma - 2\delta$ | 0 ^a | 0 ^b | 0.125 ± 0.002 |
| α' | $C_H \sim (-t)^{-\alpha'}$ | | 0 ^a | 0 ^b | 0.07 ± 0.16 -0.04 |
| Δ | $\frac{d^2 r \bar{x}_0}{dH^2} \sim (1-t)^{-\gamma'} - 2r\alpha'$ | $\Delta = 2 + \gamma = \beta\delta$ | $\frac{3}{2}$ | 15/8 | $\sim 25/16$ |
| σ | $g \sim H^\sigma$ | | $\frac{1}{2}$ | ≥ -0.232 | 0.12 ± 0.05 |
| ν | $\xi \sim g^{-\nu}$ | | $\frac{1}{2}$ | 1 | 0.643 ± 0.003 0.683 ± 0.002 |

^aFrom finite jump-discontinuity in C_H .

^bLogarithmic singularity.



(a) quadratic lattice



(b) triangular lattice

Figure 2.1. H-T diagram for Ising antiferromagnet.

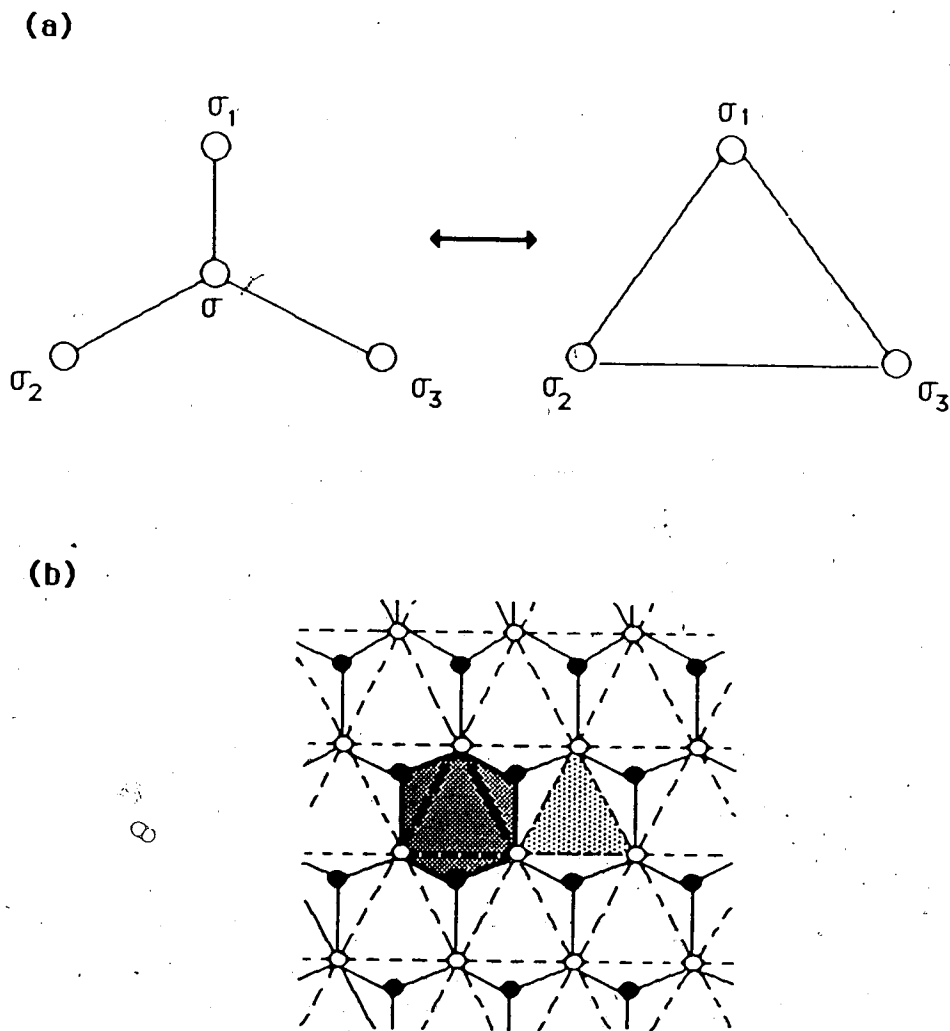


Figure 2.2. The star-triangle transformation.

(a) definition.

(b) If this transformation is applied to the black spins in this hexagonal lattice, a triangular lattice is obtained.

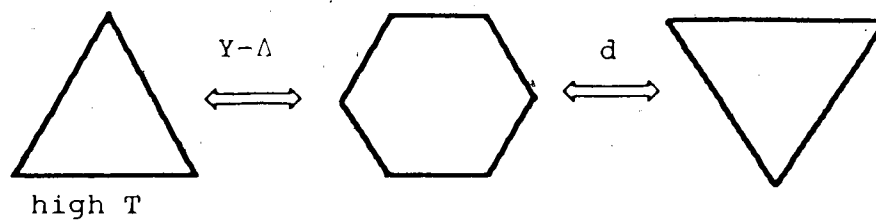


Figure 2.3. Inversion of triangle.

The inversion takes the triangle at high temperature to one which is upside down at low temperature.

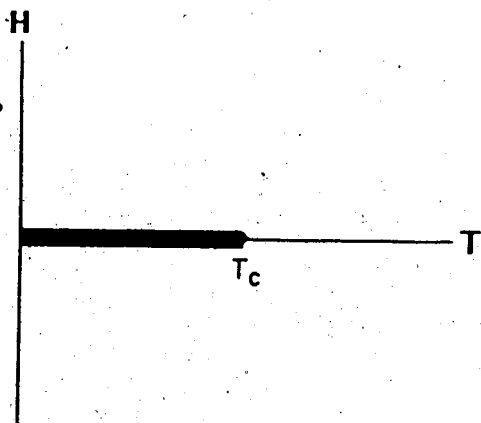


Figure 2.4 H-T diagram for Ising ferromagnet.

BIBLIOGRAPHY

1. R.J. Baxter, Exactly Solved Models in Statistical Mechanics. Academic Press, 1982.
2. R.K. Pathria. Statistical Mechanics. Pergamon Press, 1972.
3. E. Ising. Z. Phys. 31(1925), 253.
4. R.E. Peierls, Proc. Camb. Phil. Soc. 32(1936), 477.
5. R.B. Griffiths, J. Math Phys. 5(1964), 1215.
6. L. Onsager, Phys. Rev. 65(1944), 117.
7. H.A. Kramers and G.H. Wannier, Phys. Rev. 60(1941), 242; Ibid., 263.
8. W.L. Bragg and E.J. Williams, Proc. R. Soc. A145(1934), 699.
9. H.A. Bethe, Proc. R. Soc. A216(1935), 304.
10. E.A. Gugenheim, Proc. R. Soc. A148(1935), 304.
11. C. Domb, in C. Domb and M.S. Green, eds., Phase Transitions and Critical Phenomena, Vol. III, p. 357, Academic Press, 1974.
12. C. Domb, Proc. R. Soc. A199(1949), 199.
13. C. Domb, in C. Domb and M.S. Green, eds., Phase Transitions and Critical Phenomena, Vol. III, p. 1, Academic Press, 1974.
14. C. Domb and M.F. Sykes, Phys. Rev. 108(1957), 1415.
15. C. Domb and M.F. Sykes, Proc. R. Soc. A240(1957), 214.
16. C. Domb, Adv. Phys. 19(1970), 329.
17. M.E. Fisher, Physica 25(1959), 521.
18. G.V. Ryazanov, Sov. Phys. JETP 22(1966), 789.
19. L.P. Kadanoff, Nuovo Cimento 44(1966), 276.
20. T.T. Wu, Phys. Rev. 149(1966), 380.

21. H. Cheng and T.T. Wu, Phys. Rev. 164(1967), 163.
22. P.B. Abraham, Phys. Lett. 43A(1973), 163.
23. C. Domb and D.L. Hunter, Proc. Phys. Soc. 86(1965), 1147.
24. C. Domb and M.F. Sykes, J. Math Phys. 2(1961), 63.
25. G.A. Baker Jr., Phys. Rev. 124(1961), 768.
26. I. Syozi, in C. Domb and M.S. Green, eds., Phase Transitions and Critical Phenomena, Vol. 1, p. 269, Academic Press, 1972.
27. C. Domb, Adv. in Phys. 9(1960), 149.
28. H.S. Green and C.A. Hurst. Order-Disorder Phenomena, Wiley, 1964.
29. B. Kaufman, Phys. Rev. 76(1949), 1232.
30. R.J. Baxter and I.G. Enting, J. Phys. A. Math Gen. 11(1978), 2463.
31. H.N.V. Temperley, in C. Domb and M.S. Green, eds., Phase Transitions and Critical Phenomena, Vol. 1, p. 227, Academic Press, 1972.
32. T.D. Schultz, D.C. Mattis, and E.H. Lieb, Rev. Mod. Phys. 36(1964), 856.
33. E.W. Montroll, R.B. Potts, and J.C. Ward, J. Math Phys. 4(1963), 308.
34. J. Callaway, Quantum Theory of the Solid State. Academic Press, 1974.
35. J. Stephenson, J. Math. Phys. 11(1970), 420.
36. D.S. Gaunt, M.E. Fisher, M.F. Sykes, and J.W. Essam, Phys. Rev. Lett. 13(1964), 713.
37. R.B. Griffiths, Phys. Rev. 152(1966), 240.
38. G.S. Rushbrooke, J. Chem. Phys. 39(1963), 542.
39. R.B. Griffiths, Phys. Rev. Lett. 14(1965), 623.
40. R.B. Griffiths, J. Chem. Phys. 43(1965), 1958.
41. P.R. Reach and D.H. Douglass, Phys. Rev. Lett. 19(1967), 287.

42. B. Widom, J. Chem. Phys. 43(1965), 3898.
43. A.Z. Patashinskii and V.L. Pokrovskii, Soviet Physics JETP 23(1966), 292.
44. E. Stanley, Phase Transitions and Critical Phenomena, Clarendon Press, 1971.

CHAPTER III
A REVIEW OF PARTITION FUNCTION ZEROS
IN STATISTICAL MECHANICS

3.1 Introduction

In 1952, Yang and Lee¹ showed how, for the problem of condensation, the analytic properties of the pressure and density can be obtained from knowledge of the zeros of the partition function. In a separate paper² in the same year, they showed that the problems of the lattice gas and the Ising ferromagnet are mathematically equivalent. They also obtained a theorem regarding the locations of these zeros in the complex fugacity plane (Theorem 3.2). In this chapter, we review the progress that has been made in the theory of phase transitions on the basis of this work of Lee and Yang.

Consider a monatomic gas which is contained in a base of volume V and is kept at a fixed temperature T . If the gas is allowed to exchange atoms with a reservoir which is at the chemical potential μ , then the probability of having N atoms in the container as $Q_N y^N / N!$. Here Q_N is the configurational part of the partition function and

$$y = \left(\frac{2\pi mkT}{h^2} \right)^{3/2} \exp(\mu/kT) \quad (3.1)$$

If the volume V is finite, a maximum number of atoms N_m can be packed into it. In this case the partition function is a polynomial of degree N_m in y :

$$Z_V = \sum_{N=0}^{N_m} \frac{Q_N}{N!} y^N, \quad (3.2)$$

and can be factored in terms of its roots y_i :

$$Z_V = \prod_{i=1}^{N_m} (1 - y/y_i). \quad (3.3)$$

The pressure and density are determined by

$$\frac{P}{kT} = \lim_{V \rightarrow \infty} \frac{1}{V} \ln Z_V \quad (3.4)$$

and

$$\rho = \lim_{V \rightarrow \infty} \frac{\partial}{\partial \ln y} \left(\frac{1}{V} \ln Z_V \right). \quad (3.5)$$

Since all of the coefficients $Q_N/N!$ in equation (3.2) are positive, the partition function does not have any zeros on the positive real axis. However, in the thermodynamic limit, zeros can pinch the positive real axis. If the interatomic potential is sufficiently well-behaved the following theorem holds.

Theorem 3.1 (Yang and Lee)

If in the complex y -plane a region R containing a segment of the positive real axis is free of roots, then in this region, when $V \rightarrow \infty$,

$$\frac{1}{V} \ln Z_V, \frac{\partial}{\partial \ln y} \frac{1}{V} \ln Z_V, \frac{\partial^2}{(\partial \ln y)^2} \frac{1}{V} \ln Z_V, \dots$$

approach limits which are analytic in y .

Suppose first that no zeros close into the positive real axis as $V \rightarrow \infty$, so that R contains the entire positive real axis. In that case everywhere in R one can interchange the operations $\frac{\partial}{\partial \ln y}$ and $\lim_{V \rightarrow \infty}$, and the density is given by

$$\rho = \frac{\partial}{\partial \ln y} \left(\frac{P}{kT} \right). \quad (3.6)$$

The pressure and density are then monotonic and analytic functions of y on the positive real axis, and the gas exhibits a single phase in R .

Next, suppose that zeros do close in on the positive real axis at isolated points, say at $y = t_1$ and $y = t_2$, as $V \rightarrow \infty$. Now there are three regions R_1 , R_2 , and R_3 to be considered (see Figure 3.1). In each of these regions, it follows by the above argument that the gas exhibits a single phase. At $y = t_1$ and $y = t_2$ P is continuous, but ρ is discontinuous. As T varies, t_1 and t_2 move along the real axis. If at $T = T_c$ the roots no longer close into one of the points t_1 , t_2 , as T is lowered, then T_c is called the critical temperature. If there exists a temperature for which $t_1 = t_2$, then at this temperature we have a triple point.

Starting from equation (3.3) one can write

$$\frac{1}{V} \ln Z_V = \sum_{\ell=1}^{\infty} b_{\ell}(V) y^{\ell}, \quad (3.7)$$

where

$$b_\ell(V) = \frac{-1}{\ell V} \sum_{j=1}^{N_m} \left(\frac{1}{Y_j}\right)^\ell. \quad (3.8)$$

In Mayer's theory of condensation one considers the series

$$\chi(y) = \sum_{\ell=1}^{\infty} b_\ell(\infty) y^\ell, \quad (3.9)$$

and its analytic continuation along the positive real y -axis. If the first singularity of $\chi(y)$ along this axis is at $y = t_1$, one can show that:

1. For $\rho < \rho_1$, $\rho = \lim_{y \rightarrow t_1} -y \chi'(y)$. (3.10)

The ' denotes differentiation with respect to y . The system is in a single phase for these values of ρ .

2. For $\rho \geq \rho_1$ P is independent of ρ . The P - V diagram is flat for these values of ρ , so Mayer's theory cannot explain the existence of a liquid phase.

In the theory of Yang and Lee, this difficulty does not arise. To see this, draw a circle C inside R_1 , centered at $y = 0$. In C , the series (3.7) converges uniformly. Since for all the zeros y_i , $|y_i| > \sigma$, where σ is the radius of C , equation (3.8) yields

$$|b_\ell| \leq \left(\frac{N_m}{V}\right) \frac{1}{\ell \sigma}. \quad (3.11)$$

If as $V \rightarrow \infty$, N_m/V is bounded, one can conclude that in C ,

$$\lim_{V \rightarrow \infty} \sum_{\ell=1}^{\infty} b_\ell(V) y^\ell = \sum_{\ell=1}^{\infty} b_\ell(\infty) y^\ell. \quad (3.12)$$

One can now conclude that in C the cluster integrals $b_\ell(V)$ given by equation (3.8) are identical with the ones in Mayer's theory, and that $\chi(y) = P/kT$. By analytic continuation this is true everywhere in R_1 . However, the series $\chi(y)$ cannot be analytically continued beyond its singularity at $y = t_1$. The Yang-Lee theory is still correct here, but Mayer's theory is not since the $b_\ell(V)$ cannot be replaced by the $b_\ell(\omega)$.

For a further discussion of Theorem 3.1, we refer the reader to the review article by Griffiths,³ in which a proof based on the Hurwitz Theorem is given.

Lee and Yang² also showed that the lattice gas and Ising ferromagnet with $s = \frac{1}{2}$ are mathematically equivalent. By a lattice gas we mean the following. At each site on a lattice there is either one atom, or else it is empty. Any atom is assumed to interact only with its nearest neighbors through an attractive, bounded interatomic potential. For a real gas this is an approximation, but it is expected to be a good one if the lattice spacing is small. Of course one must also take the kinetic energy of the atoms into account. In the $S = \frac{1}{2}$ Ising model, it is assumed that there is a spin capable of two orientations at each site. For the lattice gas there are two possibilities at a given lattice site; either an atom is present there or no atom is present. The correspondences between the various thermodynamic functions in these two models are well known, and can be found in any text on statistical mechanics.⁴

In view of this equivalence of the $S = \frac{1}{2}$ Ising model and the lattice gas, the previous discussion on the zeros of the partition function can also be applied to the Ising model. Zeros of the partition function now become very interesting because the Ising model with a finite magnetic field has not been solved exactly, not even for the two-dimensional lattices. For finite lattices the partition function zeros approach is exact. It can provide a confirmation of the scaling picture, independent of the series expansions method, and can be used to calculate some of the critical exponents.⁵

The partition function of the isotropic Ising model with a magnetic field H is

$$Z_N(T, H) = \sum_{\{o_i\}} \exp\{K \sum_{ij} o_i o_j + h \sum_i o_i\}. \quad (3.13)$$

This expression is quite complicated. Usually one fixes the temperature or the magnetic field. If the temperature is fixed, one obtains an expression of the form

$$Z_N(h) = Z_N(h=0) \prod_v (1 - z/z_v), \quad (3.14)$$

where $z = \exp(\beta mH)$ and the z_v are roots of $Z_N(z) = 0$.

The z here should be identified with the y in equation (3.1) of the lattice gas. Thus, strictly speaking z is proportional to the fugacity, but usually we will not make the distinction.

For these zeros in the z -plane Lee and Yang² proved the following theorem regarding their location in the z -plane.

Theorem 3.2 (Lee and Yang)

If all the interactions J_{ij} of the $S = \frac{1}{2}$ Ising model satisfy $J_{ij} > 0$, then the roots z_v of $Z_N(z) = 0$ lie on the unit circle:

$$|z_1| = |z_2| = \dots = |z_N| = 1.$$

The proof of this theorem is given in Appendix II of the original paper by Lee and Yang.² Theorem 3.2 is a very strong result. It can be extended in a variety of ways (see below) and does not depend on the lattice.

3.2 Numerical Studies

In this section we review some studies motivated by the ideas of the previous section. First we relate the distribution of zeros to the thermodynamics.

If z_i is a zero of the partition function, so is z_i^* . Therefore, instead of (3.14) we write

$$Z_N = Z_N(h=0) \prod_i (1 - z/z_i)(1 - z/z_i^*) \quad (3.15)$$

If the conditions of Theorem 3.2 are satisfied, one can introduce the one-dimensional distribution of zeros $g(\theta, t)$; the number of zeros between θ and $\theta + d\theta$ is then $g(\theta, t)d\theta$.

Here $t = (T - T_C)/T_C$. Since we have accounted for z_i and z_i^* separately, it is now sufficient to keep θ in the range $0 \leq \theta \leq \pi$. Hence one can derive that

$$-\frac{F}{kT}(z) = \frac{mH}{kT} + \int_0^\pi g(\theta, t) \ln(z^2 - 2z + 1) d\theta \quad (3.16)$$

thermodynamic functions. The zero-field susceptibility and specific heat were calculated in this way by Suzuki.^{6,7}

Assuming that $g(\theta, t)$ has the properties

1. $g(\theta, T=0) = \frac{1}{2}\pi$;
 2. $g(\theta, T \rightarrow \infty) = \delta(\theta - \pi)$,
- (3.17)

Ono, Suzuki, Kawabata and Karaki⁸ showed that it is possible to have a critical angle θ_c above T_c , such that $g(\theta, t) = 0$ for $|\theta| < \theta_c$. Moreover if no such a critical angle exists, $g(\theta, t) = 0$ above T_c . Interpreting g as the independent variable they derive a differential equation for θ in terms of g . The critical angle θ_c is then determined by setting $g = 0$ for $t > 0$. We show $g(\theta, t)$ for several temperatures in Figure 3.2.

Yang⁹ proved in 1952 that the magnetic field zeros of the one-dimensional $S = \frac{1}{2}$ antiferromagnetic Ising lattice all lie on the negative real axis, but noted that this is not true in general for the Ising model. Katsura¹⁰ found that zeros lie on the negative real axis for the 1×6 Heisenberg antiferromagnet. Rather than going to larger lattices, several authors studied the antiferromagnetic Ising lattice with second nearest neighbor interactions. The nnn interactions were expected to be important for the antiferromagnetic state.¹¹⁻¹³

Katsura, Abe and Yamomoto¹⁴ showed that the Ising model with nnn interactions has three different ground states:

- (A) Ferromagnetic, if $J > 0$ and $J' > -\frac{1}{2}J$;
 (B) Antiferromagnetic, if $J < 0$ and $J' > \frac{1}{2}J$;
 (C) Super-antiferromagnetic, if $J < 0$ and $J' < \frac{1}{2}J$, or
 $J > 0$ and $J' < -\frac{1}{2}J$.

Here J' denotes the interaction energy between second nearest neighbor spins. These authors calculated the partition function for 4×4 and 4×6 lattices on the computer, using periodic boundary conditions. The partition function of an $L \times M$ lattice is written as

$$Z_{L \times M}(x, y, z) = \sum a_{lmn} x^l y^m z^n, \quad (3.18)$$

where

$$x = \exp(-2K), \quad y = \exp(-2K'), \quad \text{and} \quad z = \exp(2h). \quad (3.19)$$

When $J > 0$, $J' > 0$ and when $J > 0$, $J' > -\frac{1}{2}J$, zeros were found to lie on the unit circle. For high T zeros are on part of the unit circle, but do not cross the positive real axis. Note that this is in agreement with the work of Ono, Suzuki, Kawabata and Karaki.⁸ For low temperatures, the zeros are distributed uniformly on the unit circle and do cross the positive real axis.

When $J < 0$ and $J' > 0$, zeros lie on two concentric circles which cross the positive real axis at two points-- z_c and $1/z_c$. This suggests that phase transitions occur at the critical fields $\pm H_c$. If $T \rightarrow 0$, H_c tends to $-2J/m$. Above T_c there is a single locus which does not cross the positive real axis, and at $T = T_c$ there is one locus which crosses at $z_c = +1$.

When $J < 0$ and $J' < 0$, these authors found that most of the zeros lie on the negative real axis.

We discuss the case $J < 0$ and $J' > 0$ in more detail. At low temperatures, $x \gg 1$ and $y \ll 1$. The leading terms of the partition function are ($N = L \times M$).

$$z_N \approx x^{-N} y^{-N} (z^{N/2} - z^{-N/2}) + 2x^N y^{-N} + Nx^{N-4} y^{-N+4} (z + 1/z) + \dots \quad (3.20)$$

Zeros of the first two terms are located by

$$z^{N/2} = -x^{2N} \pm \sqrt{x^{4N} - 1} \quad (3.21)$$

or approximately $-2x^{2N}$ or $-1/2x^{2N}$. This yields the two circles

$$z_\ell \approx x^4 \exp(2\pi i \ell / N) \quad \text{and} \quad z_\ell \approx x^{-4} \exp(2\pi i \ell / N). \quad (3.22)$$

The power of 4 here reflects the fact that in a two-dimensional lattice each spin has four nearest neighbors. The neglected term in equation (3.20) is a factor of $\sim N(y/x)^4$ smaller than the term $x^N y^{-N}$, and can be neglected at low temperatures. To this approximation, zeros of the partition function lie on the circles (3.22).

The magnetization is (at low T)

$$M = \frac{z^{N/2} - z^{-N/2}}{z^{N/2} + 2x^{2N} + z^{-N/2}} = \begin{cases} +1, & -2J < mH \\ 0, & 2J < mH < -2J \\ -1, & mH < 2J \end{cases} \quad (3.23)$$

So M is a stepfunction of the magnetic field, and the critical

fields are $H_C = \pm 2J/m$.

The other cases above can be analyzed similarly. We refer the reader to reference 8 for more details.

To conclude this section, we quote some other numerical results. Kawabata and Suzuki¹⁵ verified that zeros lie on the unit circle for the ferromagnetic Ising lattice with spins up to $S = 3/2$. Katsura, Abe and Ohkochi, and others¹⁶⁻¹⁹ have obtained the partition function for lattices, up to 6×6 , of Lieb's and Wu's KDP models. These models are two-dimensional versions of Slater's model of ferro- and antiferroelectricity. Zeros were found to lie on the unit circle in the fugacity plane. This result was proved by Suzuki and Fisher.²⁰

3.3 Further Rigorous Developments

In this section we discuss two important generalizations of the theorems of Lee and Yang. In 1968, Asano^{21,22} and Suzuki^{23,24} proved the Yang-Lee theorem for the $S=1$ and Ising model. In 1969, Griffiths²⁵ gave the proof for the Ising model with general spin.

Griffiths considered particles with spin S which is allowed to take on the values

$$-p, -p+2, \dots, p, \dots, p-2, p. \quad (3.23)$$

The z -component of this spin is $p/2$. He assumed that a particle of spin S is made up of a cluster of $s = \frac{1}{2}$ particles:

$$S = \sum_{j=1}^p \sigma_j. \quad (3.24)$$

Here $\sigma_j = \pm 1$, as usual. One can then express the hamiltonian either in terms of S , or in terms of $\{\sigma_j\}$ making up such a cluster. In this way the problem of general spin S is reduced to that of the $s = \frac{1}{2}$ Ising model, for which Theorems 3.1 and 3.2 have been proved by Lee and Yang. Griffiths' proof is quite detailed, and will not be discussed here. The essential feature is that the partition functions are the same in the S and $\{\sigma_j\}$ description of the problem.

Theorem 3.3 (Griffiths)

(A) If all the interaction strengths J_{ij} in the hamiltonian

$$\hat{H} = - \sum_{i \leq j} J_{ij} S_i S_j - H \sum_i S_i \quad \text{satisfy}^b)$$

$$0 \leq J_{ij} < \infty,$$

then the zeros of the partition function lie on the unit circle $|z| = 1$ in the z -plane, where $z = \exp(-2\beta H)$.

(B) If scaling factors r_1 and r_2 are introduced, such that $J_{ij} \rightarrow r_1 J_{ij}$ and $H \rightarrow r_2 H$, then the following inequality holds:

$$\frac{1}{2} M_p(\frac{1}{2} r_1, \frac{1}{2} r_2) \leq M_p(r_1, r_2) \leq M_1(r_1, r_2).$$

If the $s = \frac{1}{2}$ Ising model has a spontaneous magnetization

b) It is possible to extend Theorem 3.3 further, allowing $J_{ij} = \infty$ also. The restriction $i \leq j$ in the first summation in the hamiltonian ensures that no double-counting occurs.

M, for temperatures $T < T_C(1)$, then the spin- $p/2$ ferromagnet has a Curie point in the range

$$\frac{1}{2}T_C(1) \leq T_C(p) \leq T_C(1) , \quad (3.25)$$

provided that the values of the J_{ij} are the same in both cases.

Asano^{21,22} considered the Heisenberg ferromagnetic lattice consisting of n spins. The hamiltonian is

$$\hat{H} = -\sum_{1 \leq i, j \leq n} J_{ij} \hat{H}_{ij} \quad (3.26)$$

with

$$\hat{H}_{ij} = \frac{1}{2}(\tau_i^z \tau_j^z - 1) + \frac{1}{2}\gamma_{ij}(\tau_i^x \tau_j^x + \tau_i^y \tau_j^y) . \quad (3.27)$$

The factors γ_{ij} introduce an anisotropy between the z -component and the x - and y -components of the interactions. The magnetic field is put in the partition function explicitly through a factor z^M , where $M = \sum_i \sigma_i$:

$$Z(z) = \sum_{\{\sigma\}} \langle \sigma_1 \dots \sigma_n | z^M \exp(-\beta \hat{H}) | \sigma_1 \dots \sigma_n \rangle . \quad (3.28)$$

Asano was not able to extend Theorem 3.2 to the partition function (3.28) directly. Therefore, he considered the expression

$$\Phi(\{z\}) = \sum_{\{\sigma\}} z_1^{\sigma_1} \dots z_n^{\sigma_n} \langle \sigma_1 \dots \sigma_n | \exp(-\beta \hat{H}_i) | \sigma_1 \dots \sigma_n \rangle . \quad (3.29)$$

Let

$$P(N) = \prod_{i < j} \exp(J_{ij} \hat{H}_{ij} / N), \quad (3.30)$$

then using the Trotter formula²⁶ one can show that

$$\phi(\{z\}) = \lim_{N \rightarrow \infty} \phi_N(\{z\}), \quad (3.31)$$

where

$$\phi_N(\{z\}) = \sum_{\{\sigma\}} \left(\prod_{i=1}^n z_i^{\sigma_i} \right) \langle \sigma_1 \dots \sigma_n | P^N(N) | \sigma_1 \dots \sigma_n \rangle. \quad (3.32)$$

For ϕ_N Asano was able to prove an extension of Theorem 3.2.

Theorem 3.4 (Asano)

If $J_{ij} \geq 0$ and $-1 < \gamma_{ij} < 1$ in equation (3.27), then zeros z_v of $\phi_N(\{z\}) = 0$ all lie on the unit circle in the complex z -plane for all N .

By this theorem zeros of $Z_N(z)$ defined by

$$Z_N(z) = \phi_N(z, z, \dots, z) \quad (3.33)$$

then all lie on the unit circle. When $N \rightarrow \infty$, ϕ_N and Z_N approach ϕ and N respectively; therefore zeros of the partition function ϕ are expected to lie on the unit circle if ϕ_N satisfies Theorem 3.4.

There are many other interesting generalizations of the Lee-Yang theory, but a detailed discussion of them is clearly beyond the scope of this thesis. For references regarding these results, see the papers of Lieb and Sokal, and of Ruelle.^{27,28}

3.4 Lee-Yang Edge

In section 3.2, we briefly discussed the existence of a critical angle such that no zeros in $z = \exp(-2H/kT)$ occur for $|\theta| < \theta_c$ above T_c . This zero-free part of the unit circle defines the Lee-Yang edge. The nature of this edge was first investigated by Abe²⁹ and Suzuki⁶ (last paper in this reference). Gallavotti, Miracle-Sole and Robinson³⁰ proved the existence of such a region free of zeros near $z=1$ for sufficiently high temperatures for the isotropic quadratic lattices.

It is sometimes convenient to discuss magnetic field zeros in terms of H itself, rather than z . One then writes $H = H' + iH''$. The unit circle $|z| = 1$ now corresponds to the imaginary axis in the complex H -plane. The width of the Lee-Yang gap in this description is $2H_0(T)$; the edges of this gap are branch points of the magnetization. The magnetization has a jump-discontinuity of $2M_0(T)$,⁶ which is proportional to the density of zeros with $H = 0$.

$$2M_0(T) \sim g(0, T) \quad (3.34)$$

Fisher³¹ introduced an exponent σ to describe the analytic properties of $g(H'', T)$ near the Lee-Yang edge, in the following way:

$$g(H'', T) \sim |H'' - H_0(T)|^\sigma \quad (3.35)$$

This gives rise to a branch point of the form $m \sim h^\sigma$ for the magnetization. (Here we set $m = M - M(iH_0, T)$ and $h = H - iH_0(T)$.) Fisher suggested that the edge singularities

are analogous to the usual critical exponent, and that the exponent σ fits into the scaling picture; e.g.

$$\sigma = \frac{1}{\delta} = \frac{d - 2 + \nu}{d + 2 - \nu} \quad (3.36)$$

Here d is the dimension of the lattice.

For $d=1$, $\sigma = -\frac{1}{2}$ for all T . A consideration of mean field or Landau theory indicates that the "critical point" is associated with a ϕ^3 -theory, instead of a ϕ^4 -theory. It can be shown via the methods of the renormalization group that this leads to a cross-over dimensionality $d^* = 6$ above which the mean field value $\sigma = +\frac{1}{2}$ applies.

The first published numerical investigation of the Lee-Yang edge appears to be the one done by Kortman and Griffiths³² in 1971. They used the high field series, of which fourteen terms had been calculated, to look for a divergence in the susceptibility. If one assumes a relation of the form (3.34), then at the Lee-Yang edge the susceptibility should diverge according to the relation

$$\chi = \left(\frac{\partial M}{\partial H} \right)_T \sim |H'' - M_O(T)|^{\sigma-1} \quad (3.37)$$

In this way, these authors obtained estimates of σ as follows: $\sigma = -0.12 \pm 0.05$ for the square lattice, and $\sigma = +0.12 \pm 0.05$ for the three-dimensional Ising lattice. Recently, Baker, Benofy and Enting³³ used the high field series to obtain a lower bound on σ of -0.232 . The true nature of the branch point in equation (3.36) remains an open problem.

3.5 Temperature Zones

In 1964, Fisher³⁴ suggested that the square of the partition function can be replaced by one term of the Kaufman solution,

$$Z_N = \sum_{i=1}^4 Z_N^{(i)}. \quad \text{He chose the term}$$

$$Z_N^{(1)2} = 2^{2mn} \prod_{r=1}^m \prod_{s=1}^n \left\{ \frac{1+v_1}{1-v_1} \frac{1+v_2}{1-v_2} - \frac{2v_1}{1-v_1} \cos \frac{2\pi r}{m} - \frac{2v_2}{1-v_2} \cos \frac{2\pi s}{n} \right\}, \quad (3.38)$$

where $v_i = \tanh K_i$. The other terms involve $\cos((2r-1)\pi/m)$, $\cos((2s-1)\pi/n)$, and mixed terms. Fisher conjectured that when $J_1 = J_2$ zeros of equation (3.37) lie on two circles centered at $\text{Re } v = \pm 1$, of radius $\sqrt{2}$, that this is true for all four of the terms and that the zeros of the sum Z_N also lie on these zeros.

Fisher's conjectures were tested numerically by Katsura.³⁵ Abe and Katsura³⁶ found that asymptotically Fisher's conjecture was correct, by numerically calculating partition function zeros of $Z_{m \times n}$ in the variable $\exp(-K)$ for the special case $J_1 = J_2$ on 4×6 , 6×6 , 6×8 , 8×8 and 10×10 lattices. They chose the term with

$$\phi_r = 2\pi r/n \quad \text{and} \quad \phi_s = (2s-1)\pi/m, \quad (3.39)$$

and found reasonably good agreement with Fisher's conjectures.

We show the loci these authors obtained in Figure 3.3.

Fisher's conjecture that zeros lie on zeros was proved for special boundary conditions in 1974 by Brascamp and Kunz.³⁷ The result they proved is the following:

1. For the lattices (A) and (B) defined below, temperature zeros lie on the unit circle in the $\sinh 2K$ plane.
2. For the lattice (C) as defined below zeros lie asymptotically on the Fisher loci

$$e^{-2K} = \pm 1 + \sqrt{2}e^{i\phi} \quad . \quad (3.40)$$

The lattices (A), (B) and (C) have the following boundary conditions (see Figure 3.4):

- (A) Periodic in the horizontal direction, with a row of upward spins at the top of the resulting cylinder, and a row of alternating spins at the bottom.
- (B) Periodic in a diagonal direction, with a row of upward spins along the upper edge and free along the bottom of the cylinder.
- (C) Periodic boundary conditions in one direction and an arbitrary homogeneous magnetic field along the lower boundary.

Temperature zeros of the general quadratic Ising lattice are not expected to lie on lines, such as the Fisher circles, but should fill two-dimensional regions in the complex plane. Van Saarloos and Kurtze³⁸ write the partition function of the anisotropic lattice as

$$\begin{aligned}
 Z_N(H=0, T) &= \sum_{k, \ell} m_{k, \ell} (e^{-2K})^k (e^{-2\alpha K})^\ell \\
 &= \sum_{k, \ell} m_{k, \ell} (e^{-2K})^{k + \alpha \ell}
 \end{aligned} \tag{3.41}$$

where

$$K_1 = K \quad \text{and} \quad K_2 = \alpha K.$$

If α is not an integer, $Z_N(0, T)$ is not a polynomial in $\exp(-2K)$. Two parameters are then needed to describe the distribution of zeros.

3.6 Connection with Thermodynamics

In this section we show that the specific heat of the Ising model is obtained from the temperature zeros, and discuss some related numerical results. The specific heat was first discussed in the context of the temperature zeros by Abe.³⁹

In the absence of a magnetic field, the partition function for the isotropic Ising lattice is

$$Z_N(H=0, T) = 2^N (\cosh K)^{Nq/2} \prod_{i=1}^N (1 - w/w_i), \tag{3.43}$$

where the w_i are the roots of the equation

$$F(w) = \sum_n a_n w^n = 0. \tag{3.44}$$

The coefficients a_n are the number of closed graphs that can be constructed with n nearest neighbor bonds, and are all positive. Hence there cannot be any roots w_i on the real, positive axis. However, it is possible that roots

approach the real, positive axis at certain points as $N \rightarrow \infty$. In this limit the factorization of the partition function, as in equation (3.43), is no longer possible, but it is hoped that the zero distribution of the finite lattice, for large N , yields thermodynamic behavior not too different from that of the infinite lattice.

The factors $2^N (\cosh K)^{Nq/2}$ give a contribution $-1/2 qJ$ to the internal energy per site, and will be ignored in this section. If w_i is a zero of equation (3.44), so is w_i^* . Hence the singular part of the internal energy is

$$E_{\text{sing}} = \frac{\partial w}{\partial \beta} \sum_{i=1}^N \left(\frac{1}{w_i - w} + \frac{1}{w_i^* - w} \right) \quad (3.45)$$

Near the critical point zeros are expected to approach the real axis vertically, so here one writes $w_i = w_c + iy$ and introduces the one-dimensional distribution of zeros $g(y)$. The density of zeros $g(y)$ can be extracted from equation (3.38). In Sections 4.3.2 and 4.3.3 we will show that near $y = 0$, $g(y)$ is proportional to $|y|/2\pi$ for the quadratic Ising lattice. The singular part of the internal energy can now be written as

$$E_{\text{sing}} = \left(\frac{\partial w}{\partial \beta} \right) 2(w_c - w) \int_0^{y_0} \frac{g(y) dy}{(w - w_c)^2 + y^2} \quad (3.46)$$

where y_0 is a cut-off parameter. With $g(y) = |y|/2\pi$ the integration yields

$$E_{\text{sing}} = \left(\frac{\partial w}{\partial \beta}\right) \frac{1}{2\pi} (w_c - w) \left\{ 2 \ln y_0 + \ln \left| 1 + \left(\frac{w_c - w}{y_0}\right)^2 \right| - 2 \ln |w_c - w| \right\} . \quad (3.47)$$

The term proportional to $\ln y_0$ is constant and does not contribute to the specific heat. The second term in the braces can be expanded about $w = w_c$ and yields

$$\left(\frac{w_c - w}{y_0}\right)^2, \text{ which can be neglected near the critical point.}$$

Hence the most singular part of the internal energy is independent of the cut-off parameter y_0 :

$$E_{\text{sing}} = -\frac{1}{\pi} \left(\frac{\partial w}{\partial \beta}\right) (w_c - w) \ln |w_c - w| . \quad (3.48)$$

Differentiating with respect to the temperature, and neglecting terms not singular at w_c , the singular part of the specific heat is

$$\frac{C_{\text{sing}}}{Nk} = -\frac{1}{\pi} \left(\beta \frac{\partial w}{\partial \beta}\right)^2 \ln |T - T_c| , \quad (3.49)$$

which diverges logarithmically near the critical point.

The calculation of the density of zeros proved to be a difficult problem. Abe considered the different possibilities near the critical point. If $g(y)$ is assumed constant, it must be discontinuous at $y=0$ because there are no temperature zeros on the positive, real axis. This situation corresponds to a first-order phase transition. Alternatively, if a term proportional to y^2 is assumed, it can be shown that the contribution to the specific heat is proportional to $(w_c - w) \ln |w_c - w|$, which vanishes near the critical point.

Hence one could conjecture that $g(y) \sim |y|$ on the basis of the expected thermodynamic behavior. Stephenson and Couzens showed that the density of zeros can be extracted from equation (3.38) for quadratic and triangular lattices, by choosing a suitable w -variable, in which equation (3.38) is then a quadratic. We discuss their results in detail in Chapter IV.

The specific heat (3.49) is symmetric about T_c . This is not expected to be true for the three-dimensional lattice, because analysis of the series expansions gives an asymmetric specific heat. The reason the specific heat is symmetric in the two-dimensional case is that the zeros approach the real axis vertically — there is no distinction between $w < w_c$ and $w > w_c$. Abe³⁹ has shown that if one assumes that near the critical point roots are located asymmetrically by $w = w_c + y e^{i\phi}$, the specific heat behaves as^{c)}

$$\frac{C}{Nk} \propto \begin{cases} \cos 2\phi \ln|T - T_c| + (\pi - \phi) \sin 2\phi, & T < T_c \\ \cos 2\phi \ln|T - T_c| - \phi \sin 2\phi, & T > T_c. \end{cases} \quad (3.50)$$

Ono, Suzuki, Kawabata, and Karaki⁴⁰ established numerically that for the $3 \times 3 \times 3$ and $3 \times 3 \times 2$ cubic and the $3 \times 3 \times 3$ bcc lattices zeros cross the positive real axis at a certain angle, in the variable $z = \exp(-2K)$, indicating an asymmetric specific heat.

The distribution of temperature zeros can also be

^{c)} Here ϕ is the angle which the locus of zeros near w_c makes with the positive real axis.

used to determine the critical temperature: in the thermodynamic limit zeros cross the positive real axis at $z = z_c$. Ono et al. estimated T_c in this way for several quadratic and three-dimensional isotropic lattices. These authors also found that there are zeros on the imaginary axis, closer to the origin than the value z_c , giving rise to a radius of convergence of the series expansions less than z_c .

In figure 3.5, we show temperature zeros of the 4×6 isotropic lattice, obtained by Ono et al. Figure 3.5(a) shows zeros in the z -plane, which lie on the Fisher loci discussed in the previous section. In figure 3.5(b) we show zero distributions in the z^2 -plane. Zeros appear to lie on the square of side $\sqrt{2}$, the unit circle, and the reflection of this square in the unit circle. The square itself is not authentic, but the fact that its reflection in the unit circle is also a locus of zeros is. This symmetry for the quadratic lattice results from the invariance of the partition function under the transformation $z \rightarrow 1/z$, and extends to the anisotropic quadratic lattice (see Chapter V).

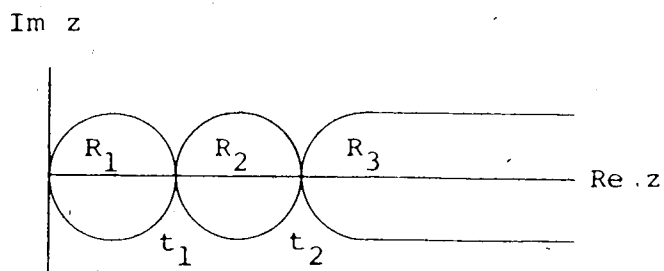


Figure 3.1. Analytical structure of fugacity plane.
The regions R_1 , R_2 , R_3 are free of zeros.

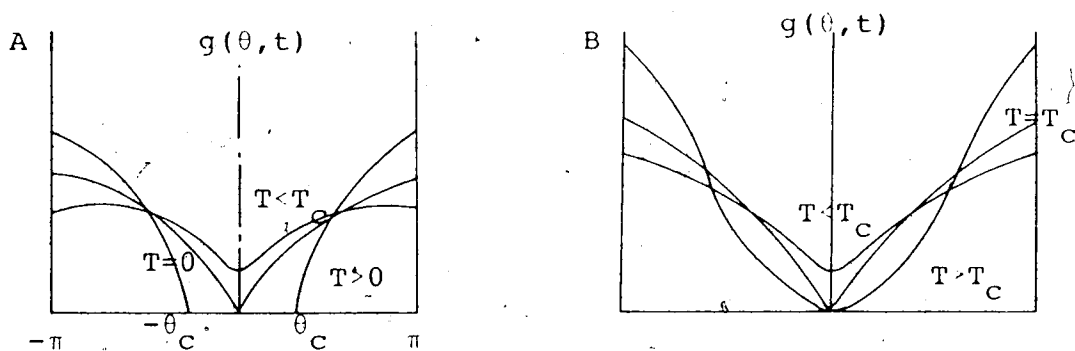


Figure 3.2. Density of fugacity zeros on the unit circle.
(a) there exists a critical angle θ_c above T_c .
(b) no critical angle exists, but $g(\theta, T_c) = 0$
for $T > T_c$.

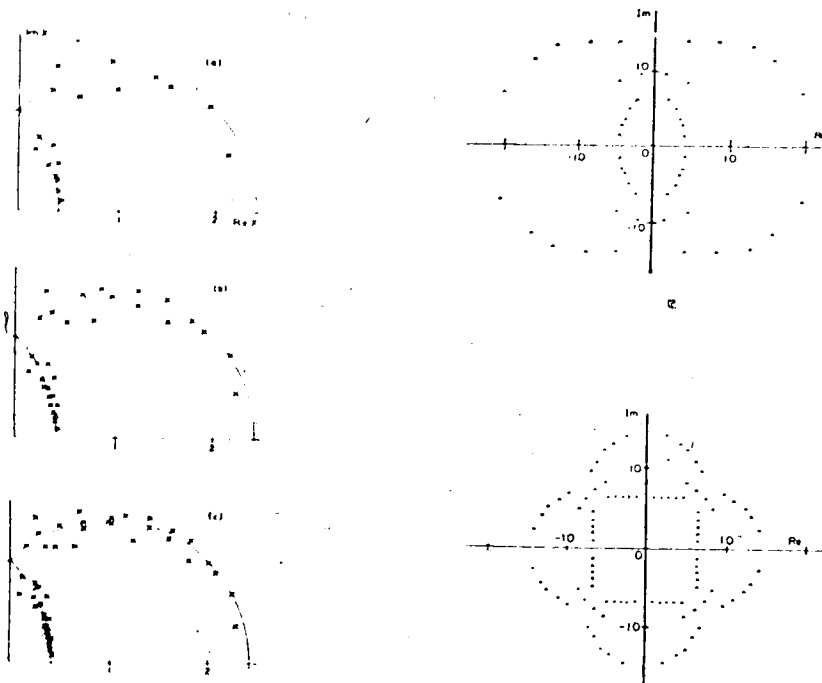


Figure 3.3 (left). Zeros in the $X = \exp(-K)$ plane computed by Abe and Katsura³⁶.
 (a) 6x6 lattice;
 (b) 8x8;
 (c) 10x10.

Figure 3.5 (right). Temperature zeros obtained by Ono et al.⁴⁰ for the 4x6 quadratic lattice.
 (a) $\exp(-2K)$ plane;
 (b) $\exp(-K)$ plane.

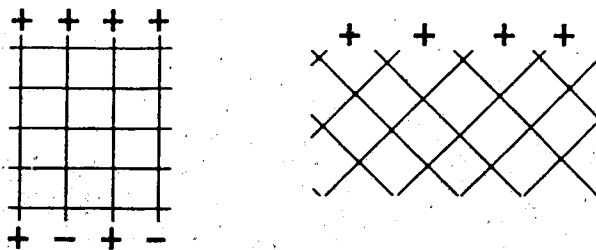


Figure 3.4. Boundary conditions for lattices (A) and (B) in Section 3.5.

BIBLIOGRAPHY

1. C.N. Yang and T.D. Lee, Phys. Rev. 87(1952), 404.
2. T.D. Lee and C.N. Yang, Phys. Rev. 87(1952), 410.
3. R.B. Griffiths, in C. Domb and M.S. Green, eds., Phase Transitions and Critical Phenomena, Vol. 1, p. 7. Academic Press, 1972.
4. R.K. Pathria, Statistical Mechanics. Pergamon Press, 1974.
5. C. Itzykson, R.B. Pearson, and I.B. Zuber, Nucl. Phys. B220(1983), 415.
6. M. Suzuki, Progr. Theor. Phys. 38(1967), 744, 289, 1225.
7. M. Suzuki, Progr. Theor. Phys. 39(1968), 349.
8. S. Ono, M. Suzuki, C. Kawabata, and Y. Karaki, J. Phys. Soc. Japan 26(1969), 96.
9. C.N. Yang, "Special Problems of Statistical Mechanics." Lecture Note, University of Washington 91952, p. 170.
10. S. Katsura, Phys. Rev. 227(1957), 1508; ibid. 129(1968), 2835.
11. C. Domb and R.B. Potts, Proc. R. Soc. A251(1951), 125.
12. C. Fan and F.Y. Wu, Phys. Rev. 179(1969), 560.
13. A. Kawakami and T. Osawa, Prog. Theor. Phys. 42(1969), 196.
14. S. Katsura, Y. Abe, and M. Yamamoto, J. Phys. Soc. Japan 30(1971), 347.
15. C. Kawabata and M. Suzuki, J. Phys. Soc. Japan 27(1969), 1105.
16. C. Kawabata, M. Suzuki, S. Ono, and Y. Karaki, Phys. Lett. 28A(1968), 113.
17. C. Kawabata, M. Suzuki, S. Ono, and Y. Karaki, J. Phys. Soc. Japan 29(1970), 845.
18. J.C. Slater, J. Chem. Phys. 9(1941), 16.

19. E.H. Lieb, Phys. Rev. Lett. 18(1967), 692, 1046;
Ibid. (1967), 108.
20. F.Y. Wu, Phys. Rev. Lett. 18(1967), 608.
21. T. Asano, Progr. Theor. Phys. 40(1968), 1328.
22. T. Asano, J. Phys. Soc. Japan 25(1968), 122.
23. M. Suzuki, J. Math. Phys. 9(1968), 2064.
24. M. Suzuki, Progr. Theor. Phys. 40(1968), 1246.
25. R.B. Briffiths, J. Math Phys. 10(1969), 1559.
26. H.F. Trotter, Proc. Amer. Math. Soc. 10(1959), 545.
27. E.M. Lieb and A.D. Sokal, Commun. Math. Phys. 80(1981),
153.
28. D. Ruelle, J. Stat. Phys. 33(1983), 77.
29. R. Abe, Progr. Theor. Phys. 38(1967), 72, 322.
30. G. Gallavotti, S. Miracle-Sole, and D.W. Robinson,
Phys. Lett. 25A(1967), 493.
31. M.E. Fisher, Phys. Rev. Lett. 40(1978), 1610.
32. P.J. Kortman and R.B. Griffiths, Phys. Rev. Lett. 27
(1971), 1439.
33. G.A. Baker, Jr., L.P. Benofy, and I.G. Enting. Los
Alamos prepring LA-UR 8-805; Submitted to Phys. Rev.
B. (1986).
34. M.E. Fisher, in Boulder Lectures in Theoretical Phy-
sics, Vol. 76, p. 58. University of Colorado Press,
1964.
35. S. Katsura, Progr. Theor. Phys. 38(1967), 1415.
36. Y. Abe and S. Katsura, Progr. Theor. Phys. 43(1970),
1402.
37. H.J. Brascamp and H. Kunz, J. Math Phys. 15(1974), 65.
38. W. Van Saarloos, and D.A. Kurtze, J. Phys. A17(1984),
1301.
39. R. Abe, Progr. Theor. Phys. 37(1967), 1070.
40. S. Ono, Y. Karaki, M. Suzuki, and C. Kawabata, J.
Phys. Soc. Japan 25(1969), 54.

CHAPTER IV

SOME NEW ANALYTICAL RESULTS ON THE TEMPERATURE ZEROS

4.1 Introduction

In the next two chapters we present some recently obtained results regarding the temperature zeros of the triangular Ising lattice; the quadratic lattice will be discussed as a special case, with the third interaction J_3 zero. In this chapter we present the analytical development near the critical points, reported by Stephenson and Couzens¹ and by Stephenson.² In Chapter V we illustrate these results with numerical results for a variety of lattices.³

4.2 General Development Near the Curie Point

We approximate the square of the partition function by one term, and choose the term which arises from the contributions of the "odd" lattice points with

$$\begin{aligned}\phi_r &= (2r-1)\pi/m, & r &= 1, \dots, m; \\ \phi_s &= (2s-1)\pi/n, & s &= 1, \dots, n.\end{aligned}\tag{4.1}$$

This term can be written in the form

$$\begin{aligned}P_4^2 &= 2^{2mn} \prod_{r=1}^m \prod_{s=1}^n \{C_1 C_2 C_3 + S_1 S_2 S_3 - S_1 \cos \phi_r \\ &\quad - S_2 \cos \phi_s - S_3 \cos(\phi_r + \phi_s)\}.\end{aligned}\tag{4.2}$$

where the meaning of C_i and S_i is as in Chapter III, and $i = 1, 2, 3$ for the horizontal, vertical, and diagonal interaction strengths respectively.

$$\text{Define } K = \frac{1}{2}(K_1 + K_2), \text{ and } k = \frac{1}{2}(K_1 - K_2); \quad (4.3)$$

$C_K = \cosh 2K$, $S_K = \sinh 2K$, and similarly for k .

Using the identities

$$C_1 C_2 = C_k^2 + S_K^2 \quad \text{and}$$

$$S_1 S_2 = -C_k^2 + C_K^2, \quad (4.4)$$

the first two terms of the vanishing expression {...}

in equation (4.2) become

$$C_k^2 e^{-2K_3} + S_K^2 e^{2K_3} + S_3.$$

Introducing also $C_{\pm} = \cos \phi_r \pm \cos \phi_s$ (4.5)

one obtains

$$\begin{aligned} \{ \dots \} &= S_K C_k \frac{S_K}{C_k} e^{2K_3} + \frac{C_k}{S_K} e^{-2K_3} - C_+ \\ &\quad - \frac{C_K S_k}{S_K C_k} C_- + \frac{S_3}{S_K C_k} [1 - \cos(\phi_r + \phi_s)] = 0. \end{aligned} \quad (4.6)$$

In terms of the complex variable

$$w \equiv x + iy = \frac{S_K}{C_k} e^{2K_3}, \quad (4.7)$$

this can be written as

$$\begin{aligned} \{ \dots \} &= C_k^2 e^{-2K_3} (1 + w^2 - C_+ w - R_1 C_- \\ &\quad + R_2 [1 - \cos(\phi_r + \phi_s)]) . \end{aligned} \quad (4.8)$$

The symmetry breaking factors R_1 and R_2 are given by

$$R_1 = \frac{C_k S_k}{C_k} e^{2K_3} = w \frac{S_1 - S_2}{S_1 + S_2}, \quad (4.9)$$

and

$$R_2 = S_3 e^{2K_3} / C_k = \frac{2wS_3}{S_1 + S_2}. \quad (4.10)$$

Notice that $R_1 = 0$ if $J_1 = J_2$ and $R_2 = 0$ if $J_2 = 0$.

Next we expand R_1 and R_2 about $w = +1$:

$$\begin{aligned} R_1 &= R_{1C} + R_{1C}' (w-1) + \dots; \\ R_2 &= R_{2C} + R_{2C}' (w-1) + \dots \end{aligned} \quad (4.11)$$

$w = +1$ when $\phi_r = \phi_s = 0$. Approximating also C_{\pm} near $\phi_r = 0$ and $\phi_s = 0$ one obtains from the real part of equation (4.8), with $x = 1$,

$$\begin{aligned} Y = y^2 &= \frac{1}{2}(\phi_r^2 + \phi_s^2) + \frac{1}{2}R_{1C}(\phi_r^2 - \phi_s^2) \\ &+ \frac{1}{2}R_{2C}(\phi_r + \phi_s)^2, \end{aligned} \quad (4.12)$$

and from the imaginary part^{a)}

$$\begin{aligned} X = (1-x) &= \frac{1}{2}(\phi_r^2 + \phi_s^2) + \frac{1}{2}R_{1C}'(\phi_r^2 - \phi_s^2) \\ &+ \frac{1}{2}R_{2C}'(\phi_r + \phi_s)^2. \end{aligned} \quad (4.13)$$

The ' denotes differentiation with respect to w ;
C denotes the Curie point value. X and Y can be written

^{a)} The choice $X = 1 - x$ is more convenient than $X = 2(1 - x)$ in the development near the Néel point, for equation 4.73.

as real, symmetric, quadratic forms:

$$X = (\phi, A\phi); Y = (\phi, B\phi). \quad (4.14)$$

Here,

$$\phi = \begin{bmatrix} \phi_r \\ \phi_s \end{bmatrix}, \quad A = \frac{1}{2} \begin{bmatrix} 1 + R_{1C}' + R_{2C}' & R_{2C}' \\ R_{2C}' & 1 - R_{1C}' + R_{2C}' \end{bmatrix}, \quad \text{and}$$

$$B = \frac{1}{2} \begin{bmatrix} 1 + R_{1C} + R_{2C} & R_{2C} \\ R_{2C} & 1 - R_{1C} + R_{2C} \end{bmatrix} \quad (4.15)$$

It is possible to extract the density of zeros of the partition function if these quadratic forms can be diagonalized simultaneously. This is guaranteed by the following theorem.^{b)}

Theorem 4.1

Let (X, AX) and (X, BX) be real, quadratic forms.

If $(X, BX) \geq 0$, there exists a matrix C such that $X = CY$, and

$$(X, AX) \longrightarrow \lambda_1 Y_1^2 + \dots + \lambda_n Y_n^2,$$

$$(X, BX) \longrightarrow Y_1^2 + \dots + Y_n^2.$$

The λ_j are the solutions of the secular equation $|\lambda B - A| = 0$.

To apply theorem (4.1) to equations (4.14) and (4.15), let

b) S^t denotes the transpose of S .

$$\psi = S\phi . \tag{4.16}$$

The matrix S is determined by the conditions

$$S^t_{AS} = \begin{bmatrix} \lambda_1 & 0 \\ 0 & \lambda_2 \end{bmatrix} \quad \text{and} \quad S^t_{BS} = \begin{bmatrix} 1 & 0 \\ 0 & 1 \end{bmatrix} . \tag{4.17}$$

In terms of the new angles ψ_1 and ψ_2 one has

$$\begin{matrix} X \\ Y \end{matrix} = \begin{matrix} \lambda_1 & \lambda_2 \\ 1 & 1 \end{matrix} \begin{matrix} \psi_1^2 \\ \psi_2^2 \end{matrix} . \quad \text{Inverting this, one has}$$

$$\begin{aligned} (\lambda_1 - \lambda_2)\psi_1^2 &= X - \lambda_2 Y \quad \text{and} \\ (\lambda_1 - \lambda_2)\psi_2^2 &= -X + \lambda_1 Y . \end{aligned} \tag{4.18}$$

It is easy to compute the Jacobians

$$\frac{\partial(\psi_1, \psi_2)}{\partial(X, Y)} = \frac{1}{\sqrt{X - \lambda_2 Y} \sqrt{\lambda_1 Y - X}} \tag{4.19}$$

$$\frac{\partial(X, Y)}{\partial(x, y)} = -2y . \tag{4.20}$$

The minus sign here is not important for the density of zeros; it arises because X decreases as x increases.

We have written the partition function in terms of the angles ϕ_r and ϕ_s , but want to know the locations of the zeros in the w-plane. Hence we need the Jacobian

$$\begin{aligned} \frac{\partial(\phi_r, \phi_s)}{\partial(x, y)} &= \frac{\partial(\phi_r, \phi_s)}{\partial(\psi_1, \psi_2)} \cdot \frac{\partial(\psi_1, \psi_2)}{\partial(X, Y)} \cdot \frac{\partial(X, Y)}{\partial(x, y)} \\ &= \frac{(\det S) y}{2\sqrt{X - \lambda_2 Y} \sqrt{\lambda_1 Y - X}} . \end{aligned} \tag{4.21}$$

Recall from equation (4.17) that $\det(S^t BS) = 1$; so $\det S = (\det B)^{-1/2}$, and does not depend on the derivatives of the symmetry breaking factors R_1 and R_2 .

The cells of the lattice are of size $\frac{2\pi}{m} \cdot \frac{2\pi}{n} = 4\pi^2/mn$.

Therefore the number of zeros in $\Delta\phi_r \Delta\phi_s$ is $\Delta\phi_r \Delta\phi_s \cdot mn/4\pi^2$.

But we have four quadrants and have squared the partition function; so we have to multiply by 2. The number of zeros in $\Delta x \Delta y$ per lattice site is $g(x, y) \Delta x \Delta y$, where $g(x, y)$ is the desired density of zeros. So

$$2\pi^2 g(x, y) \Delta x \Delta y = \Delta\phi_r \Delta\phi_s = \frac{\partial(\phi_r, \phi_s)}{\partial(x, y)} \Delta x \Delta y, \quad (4.22)$$

and

$$g(x, y) = \frac{|y|}{4\pi^2 (\det B)^{1/2} \sqrt{x - \lambda_2 y} \sqrt{\lambda_1 y - x}} \quad (4.23)$$

If $x < \lambda_2 y$ or $x > \lambda_1 y$, $g(x, y)$ is imaginary; if both of these inequalities are satisfied, $g(x, y) < 0$; g then has no meaning. Hence zeros can be located only in regions determined by

$$\lambda_2 y < x < \lambda_1 y; \quad (4.24)$$

the boundaries are given by

$$x_1 = 1 - \lambda_1 y^2 \quad \text{and} \quad x_2 = 1 - \lambda_2 y^2. \quad (4.25)$$

and result from setting $\psi_1 = 0$ or $\psi_2 = 0$ in equation (4.18).

Finally, we must show that $(\phi, B\phi) = 0$.

$$\begin{aligned} \det B &= \frac{1}{4} (1 + 2R_{2C} - R_{1C}^2) = \frac{S_1 S_2 + S_2 S_3 + S_3 S_1}{(S_1 + S_2)^2} \\ &= \frac{1}{(S_1 + S_2)^2} \end{aligned} \quad (4.26)$$

Here we have used the ferromagnetic critical point condition

$$S_1 S_2 + S_2 S_3 + S_3 S_1 = 1. \quad (4.27)$$

Notice that $S_1 + S_2 = 2S_K C_k = 2(S_K e^{2K_3})^2$, so

$$(\det B)^{-1/2} = 2(S_K e^{2K_3})^2. \quad (4.28)$$

4.3 Examples

4.3.1 Partly Isotropic Lattices with $J_1 = J_2$

When $J_1 = J_2$ equations (4.12) and (4.13) reduce to

$$\begin{aligned} Y &= \frac{1}{2} (1 + R_{2C}') \phi_r^2 + \frac{1}{2} (1 + R_{2C}'') \phi_s^2 + R_{2C}' \phi_r \phi_s \\ X &= \frac{1}{2} (1 + R_{2C}') \phi_r^2 + \frac{1}{2} (1 + R_{2C}'') \phi_s^2 + \frac{1}{2} R_{2C}' \phi_r \phi_s \end{aligned} \quad (4.29)$$

so that

$$A = \frac{1}{2} \begin{bmatrix} 1 + R_{2C}' & R_{2C}' \\ R_{2C}' & 1 + R_{2C}' \end{bmatrix}, \quad B = \frac{1}{2} \begin{bmatrix} 1 + R_{2C} & R_{2C} \\ R_{2C} & 1 + R_{2C} \end{bmatrix} \quad (4.30)$$

$$B^{-1}A = \frac{1}{2(2R_{2C} + 1)} \begin{bmatrix} 1 + R_{2C} + R_{2C}' & R_{2C}' - R_{2C} \\ R_{2C}' - R_{2C} & 1 + R_{2C} + R_{2C}' \end{bmatrix}.$$

The secular equation $|\lambda - B^{-1}A| = 0$ has the solutions

$$\lambda_1 = 1/2,$$

$$\lambda_2 = \frac{1}{2} \left(\frac{2R_{2C}' + 1}{2R_{2C} + 1} \right). \quad (4.31)$$

The eigenvectors are easily seen to be $c_1 \begin{bmatrix} 1 \\ -1 \end{bmatrix}$ and $c_2 \begin{bmatrix} 1 \\ 1 \end{bmatrix}$,

and form the columns of S. The normalization factors c_1 and c_2 are obtained by employing equation (4.17). The result is

the basis $\left\{ \begin{bmatrix} 1 \\ -1 \end{bmatrix}, (2R_{2C} + 1)^{-1/2} \begin{bmatrix} 1 \\ 1 \end{bmatrix} \right\}$. In this basis the

vector ϕ has the form $\frac{1}{2} \begin{bmatrix} \phi_r - \phi_s \\ \sqrt{2R_{2C} + 1} (\phi_r + \phi_s) \end{bmatrix}$. Hence,

$$\psi_1 = \frac{1}{2} (\phi_r - \phi_s),$$

$$\psi_2 = \frac{1}{2} \sqrt{2R_{2C} + 1} (\phi_r + \phi_s). \quad (4.32)$$

The boundaries are obtained when $\psi_1 = 0$ or $\psi_2 = 0$, i.e. when $\phi_r = \pm \phi_s$. This means that the unit circle is one of the boundaries. For the quadratic lattice $R_{2C} = 0$, and S corresponds simply to a rotation through $\pi/4$ of the angles ϕ_r and ϕ_s .

4.3.2 Quadratic Lattice

With $J_3 = 0$,

$$P_4^2 = 2^{2mn} \prod_{r=1}^m \prod_{s=1}^n \{C_1 C_2 - S_1 \cos \phi_r - S_2 \cos \phi_s\}. \quad (4.33)$$

Using hyperbolic identities, the vanishing terms can be written as

$$\{\dots\} = S_K C_k \left[\frac{S_K}{C_k} + \frac{C_k}{S_K} - C_+ - \frac{C_K S_K}{S_K C_k} \right]. \quad (4.34)$$

Following section 4.2 we let

$$w = S_K / C_k, \quad (4.35)$$

and obtain

$$\{\dots\} = C_k^2 [w^2 + 1 - C_+ w - R_1], \quad (4.36)$$

where

$$R_1 = \frac{C_K S_K}{S_K C_k} = \frac{S_1 - S_2}{S_1 + S_2}. \quad (4.37)$$

Putting $J_3 = 0$ so $R_{2C} = R_{2C}' = 0$ in equation (4.15), one easily shows that

$$\lambda_1 = \frac{1}{2} \left(\frac{1 + R_{1C}'}{1 + R_{1C}} \right) \quad \text{and} \quad \lambda_2 = \frac{1}{2} \left(\frac{1 - R_{1C}'}{1 + R_{1C}} \right). \quad (4.38)$$

However, X and Y are diagonal in ϕ_r and ϕ_s , so we do not need to apply theorem 4.1:

$$X = \frac{1}{2} (\phi_r^2 + \phi_s^2) + \frac{1}{2} R_{1C}' (\phi_r^2 - \phi_s^2) = a \phi_r^2 + b \phi_s^2,$$

$$Y = \frac{1}{4}(\phi_r^2 + \phi_s^2) + \frac{1}{4}R_{1c}(\phi_r^2 - \phi_s^2) = c\phi_r^2 + d\phi_s^2. \quad (4.39)$$

The density of zeros is

$$g(x, y) = \frac{|y|}{4\pi^2 \sqrt{-cX + aY} \sqrt{dX - bY}}. \quad (4.40)$$

The boundaries are obtained by setting $\phi_r = 0$ and $\phi_s = 0$.

The thermodynamic properties can be obtained from the density of zeros integrated between the boundaries,^{c)} keeping y fixed.

$$\int_{x_2}^{x_1} g(x, y) dx = \frac{1}{4\pi^2} |y| \int_{\frac{b}{d}y}^{\frac{a}{c}y} \frac{dx}{\sqrt{-cdx^2 + (bc + ad)x - aby^2}}$$

$$= |y|/4\pi\sqrt{cd} \quad ; \quad (4.41)$$

$$cd = 1/4(1 - R_{1c}^2) = \frac{4}{(S_1 + S_2)^2}, \text{ where we have used the}$$

critical point condition, equation (4.27), with $S_3 = 0$.

Writing $S_1 + S_2 = 2S_K C_K$ and using the definition of w , with

$w = +1$, one finds that $(cd)^{-1/2} = 2(\sinh 2K_C)^2$. Hence

$$\int_{x_2}^{x_1} g(x, y) dx = \frac{1}{2\pi} |y| (\sinh 2K_C)^2. \quad (4.42)$$

c) The integration can be carried out similarly for more general lattices; the numerical values of the parameters are then modified by the nature of the lattice.

4.3.3 Isotropic Quadratic Lattice

With $J_1 = J_2$, the equation (4.33) reduces further to

$$P_4^2 = 2^{2mn} \prod_{r=1}^m \prod_{s=1}^n \{ \cosh^2 2K - \sinh 2K (\cos \phi_r + \cos \phi_s) \}. \quad (4.43)$$

The appropriate variable is now

$$W = \sinh 2K. \quad (4.44)$$

Zeros in the w -plane are now located on the unit circle

$W = \exp(\pm i\phi)$, where ϕ is defined by

$$2\cos\phi = \cos\phi_r + \cos\phi_s. \quad (4.45)$$

The density of zeros is now one-dimensional, and is given everywhere on the unit circle by

$$g(\phi) = (\sin\phi/\pi^2) \int_0^{\cos^{-1}(2|\cos\phi| - 1)} \frac{d\phi_r}{\sqrt{1 - (2|\cos\phi| - \cos\phi_r)^2}}. \quad (4.46)$$

Near $\phi = \pi/2$, $g(\phi) \sim -\frac{1}{\pi} \ln|\pi/2 - \phi|$, so g has a logarithmic

singularity near $w = \pm i$. For small ϕ $g(\phi) \sim \phi/2\pi$, which is proportional to $|y|$.

4.3.4 Partly Isotropic Lattices with $J_2 = J_3$

When $J_2 = J_3$ one can proceed as in Section 4.3.1.

Let

$$K = \frac{1}{2}(K_2 + K_3), \quad k = \frac{1}{2}(K_2 - K_3), \quad \text{and}$$

$$\tilde{C}_{\pm} = \cos(\phi_r + \phi_s) \pm \cos\phi_s. \quad (4.47)$$

Instead of equation (4.8),

$$\begin{aligned} \{ \dots \}' = C_k^2 e^{-2K_1} [1 + \tilde{w}^2 - \tilde{w}C_+ - \tilde{R}_1 \tilde{C}_- \\ + \tilde{R}_2 [1 - \cos \phi_r]] = 0. \end{aligned} \quad (4.48)$$

Here,

$$\tilde{w} = \frac{S_k}{C_k} e^{2K_1}, \quad (4.49)$$

$$\tilde{R}_1 = -C_k S_k e^{2K_1} / C_k^2 = \tilde{w} \left(\frac{S_3 - S_2}{S_3 + S_2} \right), \quad (4.50)$$

and

$$\tilde{R}_2 = S_1 e^{2K_1} / C_k^2 = \frac{2\tilde{w}S_1}{S_3 + S_2}. \quad (4.51)$$

In the \tilde{w} -plane, the unit circle is part of every zero distribution, and arises from $\phi_r = 0$; the ferromagnetic critical point is at $\tilde{w} = +1$.

The density of zeros can be extracted in the same way as in Section 4.3.1. The eigenvalues of A are

$$\begin{aligned} \lambda_1 &= 1/2 \\ \lambda_2 &= \frac{1}{2} \left(\frac{2\tilde{R}_2 C_k + 1}{2\tilde{R}_2 C_k + 1} \right). \end{aligned} \quad (4.52)$$

Note that this description (in terms of \tilde{w}) results from the one with $J_1 = J_2$ under the transformations $\phi_r \rightarrow \phi_r + \phi_s$,

$K_1 \rightarrow K_3$, and $\tilde{w}(K_1, K_2, K_3) = w(K_3, K_2, K_1)$.

4.4 Development Near the Néel Point

The antiferromagnetic critical point is at $w = -1$, and is located by setting $\phi_r = \phi_s = \pi$. Let us therefore introduce the supplementary angles ϕ_r^* , ϕ_s^* and the functions C_{\pm}^* as follows:

$$\phi_r^* = \pi - \phi_r, \quad \phi_s^* = \pi - \phi_s, \quad C_{\pm}^* = \cos \phi_r^* \pm \cos \phi_s^* . \quad (4.53)$$

Instead of equation (4.8), one now obtains

$$\{ \dots \} = C_k^2 e^{-2K_3} \{ 1 + w^2 + C_{\pm}^* w + R_1 C_{\pm}^* + R_2 [1 - \cos(\phi_r^* + \phi_s^*)] \} . \quad (4.54)$$

The structure of this expression is identical with equation (4.8), provided that one changes $\phi_r^* \leftrightarrow \phi_s^*$ and $w \rightarrow w^* = -w$. Expanding R_1 and R_2 about $w^* = +1$, and C_{\pm}^* about $\phi_r^* = 0$ and $\phi_s^* = 0$,

$$X^* \equiv (1 + x) = \frac{1}{4} (\phi_s^{*2} + \phi_r^{*2}) + \frac{1}{4} R_{1N} (\phi_r^{*2} - \phi_s^{*2}) + \frac{1}{4} R_{2N} (\phi_r^* + \phi_s^*)^2 \quad (4.55)$$

and

$$Y \equiv y^2 = \frac{1}{4} (\phi_r^{*2} + \phi_s^{*2}) + \frac{1}{4} R_{1N} (\phi_r^{*2} - \phi_s^{*2}) + \frac{1}{4} R_{2N} (\phi_r^* + \phi_s^*)^2 . \quad (4.56)$$

R_{1N} is the value of R_1 at the Néel point.

The development of the density of zeros proceeds as near the ferromagnetic critical point, with the exception that in order to prove that the matrix B is positive definite, one employs the critical point condition for the Néel point.

$$S_1 S_2 - S_2 S_3 - S_3 S_1 = 1. \quad (4.57)$$

4.5 Temperature Zeros for $J_1 < J_2 = J_3 < 0$

From equation (4.28) it is clear that $(\det B)^{-1/2} = \infty$ when $T = 0$. Therefore one cannot obtain the density of zeros as in the last section when T is low.

The antiferromagnetic critical point is approached when T is low and the interaction strengths are all negative. From equation (4.7), we have

$$w = \frac{e^{2(K_1 + K_2)} - 1}{e^{2(K_1 - K_2)} + 1}. \quad (4.58)$$

We neglect the exponential in the numerator in comparison with the one in the denominator to obtain

$$w \approx -1/(1 + z_2/z_1). \quad (4.59)$$

To the same approximation,

$$\frac{S_1 - S_2}{S_1 + S_2} \approx (1 - \frac{z_2}{z_1}) / (1 + \frac{z_2}{z_1}) = -(2w + 1) \quad \text{and} \quad R_1 \approx -w(2w + 1)$$

and $R_2 \approx 2w(w + 1)$. Equation (4.54) can now be written entirely in terms of w :

$$\begin{aligned}
 \{\dots\} &= z_p C_k^2 [1 + w^2 + w C_+^* - w(2w + 1) C_-^* \\
 &\quad + 2w(w + 1) [1 - \cos(\phi_R^* + \phi_S^*)] , \\
 &= z_p C_k^2 \{ [1 + 2(\cos\phi_R + \cos\phi)] w^2 + 2\cos\phi w + 1 \} , \quad (4.60)
 \end{aligned}$$

where

$$\cos\phi = 1 - \cos\phi_S - \cos(\phi_R + \phi_S) \quad (4.61)$$

Taking the real and imaginary parts of equation (4.60), one has

$$y^2 = \frac{[1 + 2(\cos\phi_R + \cos\phi)] x^2 + 2\cos\phi x + 1}{1 + 2(\cos\phi_R + \cos\phi)} \quad (4.62)$$

and

$$1 + 2(\cos\phi_R + \cos\phi) = -\cos\phi/x \quad (4.63)$$

Combining these results one obtains

$$x^{*2} + y^2 = \frac{2(1 + \cos\phi_R)}{1 + 2(\cos\phi_R + \cos\phi)} \equiv R^2 \quad (4.64)$$

Expanding R^2 about $\phi_R = \pi$, keeping ϕ_S arbitrary, one obtains

the equation of a circle centered on $w = -1$, with radius

$$R = |\phi_R^*| :$$

$$x^{*2} + y^2 = |\phi_R^*|^2 \quad (4.65)$$

$$X^* = 1 + x = R^2 + \frac{\cos\phi - 1}{1 + 2(\cos\phi_R + \cos\phi)} \quad (4.66)$$

Expanding the RHS to second order in ϕ_R^* ,

$$X^* = \phi_R^* \sin\phi_S + (\cos 2\phi_S - \frac{1}{2} \cos\phi_S) \phi_R^{*2} \quad (4.67)$$

and

$$y = \phi_r^* \cos \phi_s \quad (4.68)$$

The last two equations allow the interpretation of ϕ_s as the angle which parameterizes the circle, equation (4.65).

If ϕ_s is also near π , one expands equation (4.67) about $\phi_s = \pi$ to the lowest vanishing order to obtain

$$X^* = \phi_r^* \phi_s^* + \frac{3}{2} \phi_r^{*2} \quad (4.69)$$

If $\phi_s^* = 0$,

$$X^* = \frac{3}{2} y^2, \quad (4.70)$$

and zeros lie on a parabola for small y .

Proceeding slightly differently, Stephenson² obtained equations (4.65) and (4.68) to (4.70). Approximating the denominator in X^* by unity to first order in ϕ_r^* , he arrived at

$$X^* = (1 - \cos \phi_r^*) (2 + \cos \phi_s^*) + \sin \phi_r^* \sin \phi_s^* \quad (4.71)$$

If ϕ_r^* becomes slightly larger, equation (4.63) is no longer correct. Let

$$\alpha = 2(1 - \cos \phi_r^*), \quad \beta = \alpha / (1 - \alpha) \quad (4.72)$$

Adding $2X^* + \beta^2$ to both sides of equation (4.64) and rearranging the RHS, one obtains

$$(X^* + \beta)^2 + y^2 = \beta(1 + \beta) \quad (4.73)$$

This equation does not depend explicitly on ϕ_s , and describes a family of circles. Each circle has radius

$R = \sqrt{\beta(1 + \beta)}$ and is centered at $X^* = -\beta$.

A trivial computation shows that $\frac{\partial(X^*, Y)}{\partial(\phi_r, \phi_s)} = \phi_r^* + O(\phi_r^{*2})$, so the leading term of the density of zeros is given by

$$2\pi^2 g(x, y) = \frac{\partial(\phi_r, \phi_s)}{\partial(x, y)} = \frac{1}{|\phi_r^*|} = \frac{1}{R}. \quad (4.74)$$

Circles centered on $X^* = -\beta$ and spaced according to equation (4.74) are illustrated in Figure 4.1. Notice that the partition function has no real zeros away from the critical points, so a zero-free cusp is expected to extend from $w \leq -1$ and $w \geq -1$.

Stephenson² has shown that the energy derived from the density of zeros, equation (4.74), agrees with the thermodynamic derivation, starting from Houtappel's double-integral formula for the partition function. For the singular part of the energy per site, he obtains

$$\frac{E}{N} \approx \frac{2}{\pi} (J_2 - J_1) \exp \{2\beta(J_1 - J_2)\}, \quad J_1 < J_2 < 0. \quad (4.75)$$

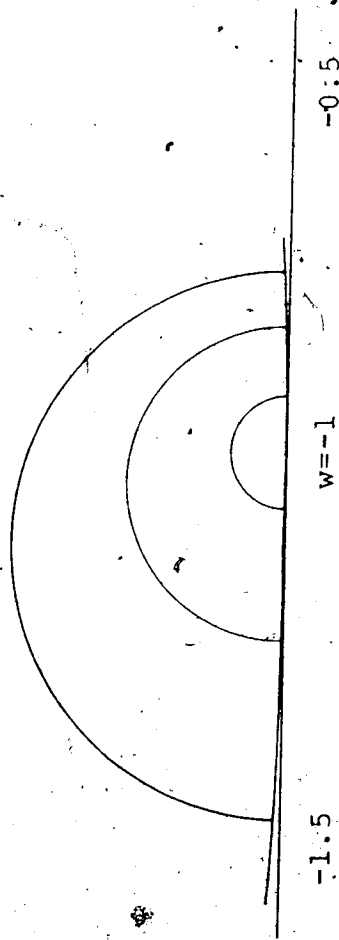


Figure 4.1. Circles centered on $-8 = \frac{\alpha}{\alpha-1}$ for $r=1$, 2 , and 3 . $m = n = 48$ in this drawing.

BIBLIOGRAPHY

1. J. Stephenson and R. Couzens, *Physica* 129A (1984), 201.
2. J. Stephenson, *Physica* (accepted, to appear), 1986.
3. J. Stephenson and J. Van Aalst, *Physica* (accepted, to appear), 1986.
4. F. Ayres, Jr., Theory and Problems of Matrices, Schaum Publishing Company, 1962.

CHAPTER V

SOME NEW NUMERICAL RESULTS ON THE TEMPERATURE ZEROS^{a)}

5.1 Location of the Temperature Zeros

In this chapter, we continue the study of the temperature zeros of the Ising model partition function which we began in Chapter IV, reporting our numerical results. One term of the square of the partition function is cast in polynomial form; the roots of this function are calculated, from which zeros in the w -plane are constructed.^{b)}

In order to write equation (4.2) in polynomial form, we set

$$J_1 = aJ, J_2 = bJ, J_3 = cJ \quad (5.1)$$

for the smallest possible integers a, b, c with $a \geq b \geq c \geq 0$; the triple (a, b, c) then identifies the lattice under consideration. Next we put

$$z = e^{-2K}, \quad K = J/kT. \quad (5.2)$$

For real temperatures the range $0 < z < 1$ describes the ferromagnet, $J > 0$, and the range $1 < z < \infty$ the corresponding

^{a)} A condensed version of this chapter has been accepted for publication. See J. Stephenson and J. Van Aalst, *Physica* 1986.

^{b)} All the computations were performed using FORTRAN. The roots of $P(z)$ were calculated using the routine ZRPOLY in *IMSLIB, and the plotting routines are in *PLOTLIB.

antiferromagnet. The powers of z in equation (4.2) then depend only on the combinations d, e, f of a, b, c as follows:

$$d = a + b, \quad e = a + c, \quad f = b + c. \quad (5.3)$$

Notice that $d \geq e \geq f \geq 0$ if $a \geq b \geq c \geq 0$.

The vanishing factors in equation (4.2) become, when written in descending order of power of z ,

$$\begin{aligned} \{ \dots \} &= [z^{2d} + z^{2e} + z^{2f} + 2z^{d+e} \cos \phi_r + 2z^{d+f} \cos \phi_s \\ &\quad + 2z^{e+f} \cos(\phi_r + \phi_s) - 2z^d \cos(\phi_r + \phi_s) \\ &\quad - 2z^e \cos \phi_s - 2z^f \cos \phi_r + 1] / 4z^{d+f} \\ &\equiv P(z) / 4z^{d+f}. \end{aligned} \quad (5.4)$$

The polynomial which results when $a \geq c$ in equation (5.1), so that $d \geq f$, also written in descending order of powers of z , is identical with equation (5.4), provided that also $\cos(\phi_r + \phi_s) \geq \cos \phi_r$. Hence, distributions of zeros in the z -plane of lattices related to each other in this way have the same boundaries. The locations of the zeros within these boundaries will be shifted slightly because, unlike ϕ_r , $\phi_r + \phi_s$ does not locate a lattice point in the (ϕ_r, ϕ_s) diagram.

As in Chapter IV, we choose the "odd" term with

$$\begin{aligned} \phi_r &= (2r - 1)\pi/m \quad r = 1, \dots, m, \\ \phi_s &= (2s - 1)\pi/n \quad s = 1, \dots, n \end{aligned} \quad (5.5)$$

and choose $m = n = 24$ for all lattices to be considered.

Hence the lattice spacing is always the same, although the amount of computation will differ from one lattice to another. A reduction in the amount of calculation is provided by the following lemma.

Lemma 5.1

If z is a zero of the partition function, so is $-z$.

Proof. If a , b , and c are all odd, d , e , and f are all even. In this case the polynomial is one in z^2 , and the lemma is trivially true. All terms which can be odd are proportional to the cosine of one of ϕ_r , ϕ_s , or $\phi_r + \phi_s$. A change $z \rightarrow -z$ can then be compensated by adding π to one or both of ϕ_r and ϕ_s .

All possible polynomials fall into four classes (i) - (iv), according to the required transformation of ϕ_r and ϕ_s . In Table 5.1 we list these classes, the corresponding transformations, and the minimum ranges of ϕ_r and ϕ_s sufficient for complete knowledge of all of the roots of $P(z) = 0$. The roots of $P(-z)$ are then put in automatically. These regions are easily deduced from symmetry arguments.

In terms of z the ferromagnetic (Curie) critical point is located by the condition

$$z^d + z^e + z^f = 1, \quad (5.6)$$

which has one real, positive root z_c in $0 < z < 1$, and

occurs when $\phi_r = \phi_s = 0$. The corresponding antiferromagnet

with J_3 weakest has a Néel point located by the real, positive root z_N of

$$z^d - z^e - z^f = 1, \quad (5.7)$$

which occurs when $\phi_r = \phi_s = -\pi$. If e and f are odd and d is even, there are non-physical, real, negative roots of equations (5.6) and (5.7) at $-z_N$ and $-z_C$, respectively.

In the partly isotropic case with $b = c$, $J_2 = J_3$, so $d = e$ and $f = 2c$, there is no longer a proper antiferromagnetic critical point; equation (5.7) yields $z^{2c} = -1$, so $z = \pm i$ if c is odd. Numerical values of z_N and z_C are listed in Table 5.2.

In terms of z , equation (4.7) is

$$w \equiv x + iy = \frac{1 - z^{a+b}}{z^c (z^a + z^b)} = \frac{1 - z^d}{z^e + z^f}, \quad (5.8)$$

which also depends only on the combinations d , e , and f in equation (5.3). An unfortunate feature of using w for locating zeros away from the critical point(s) is that there can be unphysical, spurious, real zeros, which arise from negative values $-z_C$ and $-z_N$ of z .

When $\phi_r = -\phi_s$, zeros lie on the unit circle in the w -plane, so the unit circle is part of every zero distribution in the w -plane. Furthermore, there are always zeros at $z = \pm i$, which arise from $\phi_r = -\phi_s = \pi/2$. These zeros frequently map into $w = \pm i$, as listed in Table 5.2.

Zero distributions are always symmetrical under sign

reversal of z by Lemma 5.1, but in general symmetry under $w \rightarrow -w$ arises from the transformation $z \rightarrow -z$ only in those cases (iv) in which e and f are odd, but d is even. In these cases the unphysical, real w zeros no longer occur at distinct locations, since now $w(-z_C) = -1$ and $w(-z_N) = +1$ (when present). Examples are (221), (332), and (421).

5.2 Anisotropic Quadratic Lattices

In this section, we look at lattices with $J_3 = 0$, $c = 0$, so that $d = e + f$. Deplacing z by $1/z$ and multiplying through by z^{2d} in equation (5.4), we obtain

$$\begin{aligned} \{ \dots \} = & [z^{2d} + z^{2f} + z^{2e} - 2z^{d+f} \cos \phi_S - 2z^{d+e} \cos \phi_R \\ & + 2z^e \cos \phi_S + 2z^f \cos \phi_R + 1] . \end{aligned} \quad (5.9)$$

Changing $\phi_R \rightarrow \phi_R + \pi$ and $\phi_S \rightarrow \phi_S + \pi$, it is clear that the distribution of zeros in the z -plane is invariant under $z \rightarrow 1/z$. It is also easy to check that under $z \rightarrow 1/z$ $w \rightarrow -w$, so zero distributions in the w -plane are symmetrical in both the real and imaginary axes.

In Figures 5.1 to 5.3, we show the zero distributions of the quadratic lattices (310), (320), and (210), respectively, in the z -plane, and in Figures 5.4 to 5.6 the corresponding distributions in the w -plane.

Dividing the ferromagnetic critical point condition, equation (5.6) with $c = 0$, by z^{a+b} , and rearranging, one obtains

$$\frac{1}{z^{a+b}} - \frac{1}{z^a} - \frac{1}{z^b} = 1. \quad (5.10)$$

This is the condition for the corresponding antiferromagnetic critical point. Hence, for the quadratic lattice $z_C z_N = 1$, the physical critical points are at $w = \pm 1$. Unphysical roots $-z_C$ and $-z_N$ map to symmetrical positions on the real axis in w , since under $z \rightarrow 1/z$, $w \rightarrow -w$. For the isotropic, quadratic lattices (110) and (310), $w(-z_C) = -1$ and $w(-z_N) = +1$. For (320) and (210), real w zeros arising from $w(-z_C)$ and $w(-z_N)$ are at $w = \pm 4.678574$ and $w = \pm 7.942920$ respectively.

Noting that $c = 0$, so that at least one of a and b must be odd, it is obvious that $z = i$ maps into $w = \pm i$ with the following exception: if both a and b are odd, and their sum d is a multiple of 4, then the transformation to w , equation (5.8), contains a vanishing numerator and denominator at $z = \pm i$, the limiting form of the map as $z \rightarrow \pm i$ is

$$w(i) = \left(\frac{a+b}{a-b}\right) i^a. \quad (5.11)$$

Examples are (310) and (530) in Table 5.2.

5.3 Class (i) Lattices

If a , b , and c are all odd, the polynomial $P(z)$ is one in z^2 . In this case, to reduce the amount of calculation, roots in the z^2 -plane are calculated, from which roots in the z -plane are constructed. Writing $z^2 = \xi + i\zeta$ and $z = u + iv$, one easily shows that

$$u = \pm \frac{1}{\sqrt{2}} [\xi + \sqrt{\xi^2 + \zeta^2}]^{1/2}$$

$$v = \pm \frac{1}{\sqrt{2}} (\text{sign } \xi) [-\xi + \sqrt{\xi^2 + \zeta^2}]^{1/2} \quad (5.12)$$

The factor sign ξ in v ensures that $u^2 - v^2 + 2iuv = z^2$.

To obtain all the zeros of the partition function in the z -plane, it is sufficient to construct z from $s = \xi + i|\zeta|$ instead of z^2 , and then use equation (5.12) to construct z . Diagrams obtained in this way were checked against diagrams for which the roots z were calculated directly from the polynomial.

We illustrate zero distributions of class (i) lattices with (311), (113), (311), and the completely isotropic lattice (111). In Figures 5.7 to 5.10 we show the z -plane distributions; in Figure 5.11 the w -plane distribution of (311); in Figures 5.12 and 5.13 the w -plane of (113) and the \tilde{w} -plane of (311) respectively; in Figure 5.14 the w -plane of (113). Observe that the w -plane distribution of (113) has the same boundaries as the \tilde{w} -plane distribution of (311), but the zeros are shifted slightly in positions. This shifting in positions is somewhat more evident in the z -plane distributions of (113) and (311). The completely isotropic lattice (111) has relatively simple zero distributions, and is included here only in the interest of completeness.

All of the z -plane distributions considered here have a line of imaginary zeros, which arise from real,

negative roots z^2 , say $z^2 = -r$. The range of r can be determined directly from the polynomial. For (331) the polynomial in r reduces to

$$P(r) = 4r^3(r+1)\cos^2\phi_1 - 4r^2(r^3+1)\cos\phi_2\cos\phi_1 + (r^3-1)^2, \quad (5.13)$$

where

$$\phi_1 = \frac{1}{2}(\phi_r + \phi_s) \quad \text{and} \quad \phi_2 = \frac{1}{2}(\phi_r - \phi_s). \quad (5.14)$$

$P(r)$ may be regarded as a quadratic in $\cos\phi_1$. In order for $\cos\phi_1$ to be real, in the range $[-1,1]$, we require that

$$\left(\frac{r^3-1}{r^3+1}\right)^2 [1+1/r] \leq \cos^2\phi_2 \leq 1. \quad (5.15)$$

This inequality restricts r to the range

$$r_1 = \frac{1}{2}(\sqrt{5}-1) = 0.618034 \dots \leq r \leq r_2 = 2.205569 \dots \quad (5.16)$$

Here r_1 and r_2 are the positive, real roots of the factors

$r^2 + r - 1$ and $r^3 - 2r^2 - 1$ respectively, which occur in

$P(r)$ when extreme equality holds in equation (5.15). The corresponding value of w obtained from

$$w = \frac{1-z^6}{2z^4} = \frac{1+r^3}{2r^2} \quad (5.17)$$

are:

$$w_1 = 1/r_1 = \frac{1}{2}(\sqrt{5}+1) = 1.618034 \dots,$$

$$w_2 = r_2 - 1 = 1.205569 \dots$$

w_1 gives the upper end of the line of real w zeros, but the lower end comes not from w_2 but $r = 2^{1/3}$, where w attains its minimum value $\frac{3}{2^{5/3}} = 0.94491$ in equation (5.17).

For (113) the polynomial in r reduces to

$$P(r) = 4r(r^3 + 1)\cos^2\phi_1 - 4r^2(r + 1)\cos\phi_2 \cos\phi_1 + (r - 1)^2. \quad (5.18)$$

In order for $\cos\phi_1$ to be real, in the range $[-1, 1]$, we require that

$$\left(\frac{r-1}{r+1}\right)^2 [1 + 1/r^3] \leq \cos^2\phi_2 \leq 1. \quad (5.19)$$

This inequality restricts r to the range

$$r_1 = 1/2 \leq r < \infty; \quad (5.20)$$

the corresponding range of w is

$$0 < w \leq 3. \quad (5.21)$$

The lattices (113) and (311) are related to each other by a π c, so inequality (5.20) also holds for (311); the range of w in the latter case is

$$-3 \leq w < -1. \quad (5.22)$$

5.4 Partly Anisotropic Ferromagnetic Lattices

The partly anisotropic cases $a = b > c > 0$ also have distinct ferro- and anti-ferromagnetic critical points. For lattices with $J_1 = J_2$, in the vicinity of the critical point in the w -plane, the cusp-like region containing zeros has the unit circle as one of its boundary lines. Moreover,

zeros near $w = +1$ lie inside (outside) the unit circle when J_3 is the strongest (weakest) interaction; cross-over occurs at the completely isotropic lattice.

In Figures 5.15 and 5.16, we show the z -plane distributions of (221) and (112) respectively, and in Figures 5.17 and 5.18 the corresponding w -plane distributions; in Figures 5.19 and 5.20 the z -plane distributions of (332) and (223), and in Figures 5.21 and 5.22 the corresponding w -plane distributions.

For the lattice (331) $R_2 = S_3 e^{2K_3} = \frac{1}{z} \left(\frac{1}{2} - 1 \right)$, and $w = S_K e^{2K_3} = \frac{1}{z} \left(\frac{1}{4} - z^2 \right)$. Using the critical value z_C from Table 5.2, we obtain $R_{2C} = \frac{3 - \sqrt{5}}{\sqrt{5} - 1}$, $R_{2C}' = \frac{\sqrt{5} - 1}{2\sqrt{5}}$, and

$\lambda_2 = \frac{1}{2} \left(\frac{R_{2C}' + 1}{R_{2C} + 1} \right) = 0.34714 \dots < 1/2 (= \lambda_1)$. The boundaries are given by

$$x_1 = 1 - \lambda_1 y^2 \quad \text{and} \quad x_2 = 1 - \lambda_2 y^2. \quad (5.23)$$

One of the boundaries is the unit circle; the other one lies outside the unit circle. Hence zeros lie exterior to the unit circle, as is evident from Figure 5.12.

For the lattice (113) we have $R_{2C} = 1.618034 \dots$, $R_{2C}' = 2.1708205 \dots$, and $\lambda_2 = 0.630495 \dots$. So $\lambda_2 > \lambda_1$, and zeros are interior to the unit circle.

5.5 Partly Anisotropic Antiferromagnetic Lattices

Interest in the class of lattices with the two weaker interactions equal arises from the need to check the theoretical result near the antiferromagnetic zero point, which is at $z = +\infty$, see also Section 4.5. The predicted circular distributions around $w = -1$ can be seen in the w -plane distributions of the lattices (211), (322), and (311) in Figures 5.23, 5.24, and 5.14, respectively. These examples exhibit a zero-free cusp, extending from $w = -1$ along the real axis for $w > -1$, although with some difficulty for (311) (see insert). The latter lattice also has a non-physical real zero at $w(\pm 1) = -2$.

The z -plane distributions of (211) and (322) are shown in Figures 5.25 and 5.26:

The reverse lattice (112) has a symmetrical distribution in the w -plane. Here $w = 0$ corresponds to both zero and infinite temperatures. On the negative, real axis, the physical range of w is in the subinterval $(-w_0, 0)$ of $(-1, 0)$. The expression for w reduces to

$$w = \sinh 2K_1 \cdot e^{2K_3} \quad (5.24)$$

where $J_1 = J_2 = aJ$, and $J_3 = cJ$ with $c > a$, is the strongest interaction. The minimum value of w is located by $dw/dK = 0$, or

$$\tanh 2K_1 = -a/c \quad (5.25)$$

which has a negative real solution for K_1 , and can be

rearranged to give

$$z_0 = \left(\frac{c+a}{c-a}\right)^{1/2a}, \text{ and } w_0 = \frac{-a}{\sqrt{c^2 - a^2}} \left(\frac{c-a}{c+a}\right)^{c/2a}. \quad (5.26)$$

For (112) $z_0 = \sqrt{3}$, $w_0 = -1/3\sqrt{3} = -0.192450 \dots$; for (223) $z_0 = 5^{1/4} = 1.495349 \dots$, $w_0 = -0.267496 \dots$; and for (113) $z_0 = \sqrt{2}$, $w_0 = -1/8$. There do not seem to be any partition function zeros close to z_0 or w_0 in the diagrams.

5.6 Completely Anisotropic Lattices

Finally we consider the completely anisotropic lattices. Generally $z = +i$ maps into $w = \pm i$, except:

a) when a and b are both odd, but their sum d is a multiple of 4, as for the quadratic lattices:

$$w(i) = \left(\frac{a+b}{a-b}\right) i^{a-c}, \text{ e.g. (311)}; \text{ or} \quad (5.27)$$

b) when both a and b are even, c now being odd, so that

$$w(i) = \begin{cases} 0, & \text{if } d \text{ is a multiple of 4, e.g. (221)} \\ \pm i^\infty, & \text{if } d \text{ is not a multiple of 4, e.g. (421)}. \end{cases} \quad (5.28)$$

We illustrate zero distributions of completely anisotropic lattices with the example which has the polynomial of lowest degree, (321). Figure 5.27 shows the z -plane distribution, and Figure 5.28 the w -plane.

Table 5.1

Classification of lattices, and transformations used to prove symmetry under $z \rightarrow -z$ and to reduce the range of ϕ_r and/or ϕ_s required in numerical calculations

| a | b | c | d | e | f | Class | Transformation | Range of ϕ_r, ϕ_s |
|------|------|------|------|------|------|-------|--|--|
| even | even | even | even | even | even | (i) | $z \rightarrow -z$: a, b, c by 2. | $0 < \phi_r < 2\pi$ $0 < \phi_s < \pi$ |
| even | odd | even | odd | even | odd | (ii) | $\phi_r \rightarrow \phi_r + \pi, z \rightarrow -z$ | $0 < \phi_r, \phi_s < \pi$ |
| odd | even | odd | even | odd | even | (iii) | $\phi_s \rightarrow \phi_s + \pi, z \rightarrow -z$ | $0 < \phi_r, \phi_s < \pi$ |
| even | even | odd | even | odd | odd | (iv) | $\phi_r \rightarrow \phi_r + \pi, z \rightarrow -z$ $\phi_s \rightarrow \phi_s + \pi$ | $\phi_s - \pi < \phi_r < \pi - \phi_s$ $0 < \phi_s < \pi$ |

Table 5.2

Lattice classification data, critical point values z_C , z_N and associated unphysical real w zeros for selected quadratic (upper part) and triangular (lower part) lattices

| a | b | c | d | e | f | Class | $w(i)$ | z_C | z_N | w zeros ^b |
|---|---|---|---|---|---|-------|-----------------|-----------------------------|-----------------------------|---|
| 1 | 1 | 0 | 2 | 1 | 1 | (iv) | -1 | $\sqrt{5} - 1$ | $\sqrt{5} + 1$ | ± 1 |
| 2 | 1 | 0 | 3 | 2 | 1 | (iii) | -1 | 0.543689 | 1.839287 | ± 4.678574 |
| 3 | 1 | 0 | 4 | 3 | 1 | (iv) | -2 ^a | $\frac{1}{2}(\sqrt{5} - 1)$ | $\frac{1}{2}(\sqrt{5} + 1)$ | ± 1 |
| 3 | 2 | 0 | 5 | 3 | 2 | (iii) | 1 | 0.699737 | 1.429108 | ± 7.942920 |
| 4 | 1 | 0 | 5 | 4 | 1 | (ii) | -1 | 0.667961 | 1.497094 | ± 2.416273 |
| 5 | 3 | 0 | 8 | 5 | 3 | (iv) | 4 ^d | 0.798675 | 1.252073 | ± 1 |
| 1 | 1 | 1 | 2 | 2 | 2 | (i) | -1 | $1/\sqrt{3}$ | - | ± 1 |
| 2 | 1 | 1 | 3 | 3 | 2 | (iii) | -1 | 0.657298 | - | 8.671954 |
| 2 | 2 | 1 | 4 | 3 | 3 | (iv) | 0 | 0.716673 | 2.106919 | ± 1 |
| 3 | 1 | 1 | 4 | 4 | 2 | (i) | -2 ^a | $1/\sqrt{2}$ | - | $\pm 1, (-2)^c$ |
| 3 | 2 | 1 | 5 | 4 | 3 | (ii) | 1 | 0.754878 | 1.705903 | -11.808629 $+4.490805$ 15.97184 |
| 3 | 2 | 2 | 5 | 5 | 4 | (iii) | -1 | 0.789161 | - | ± 1 |
| 3 | 3 | 1 | 6 | 4 | 4 | (i) | 1 | 0.786151 ^d | 1.485116 | ± 1 |
| 3 | 3 | 2 | 6 | 5 | 5 | (iv) | -1 | 0.813134 | 2.029074 | ± 1 |
| 4 | 1 | 1 | 5 | 5 | 2 | (iii) | -1 | 0.741912 | - | 3.761027 |
| 4 | 2 | 1 | 6 | 5 | 3 | (iv) | $\pm i$ | 0.782122 | 1.538497 | ± 1 |

- a. A factor of $(1+z^2)$ cancels out of the algebraic expression for w .
- b. Unphysical real w zeros arising from $w(-z_C)$ and $w(-z_N)$.
- c. The unphysical real w zero at -2 arises from $z = \pm i$.
- d. Exactly $\sqrt{(\sqrt{5} - 1)/2}$

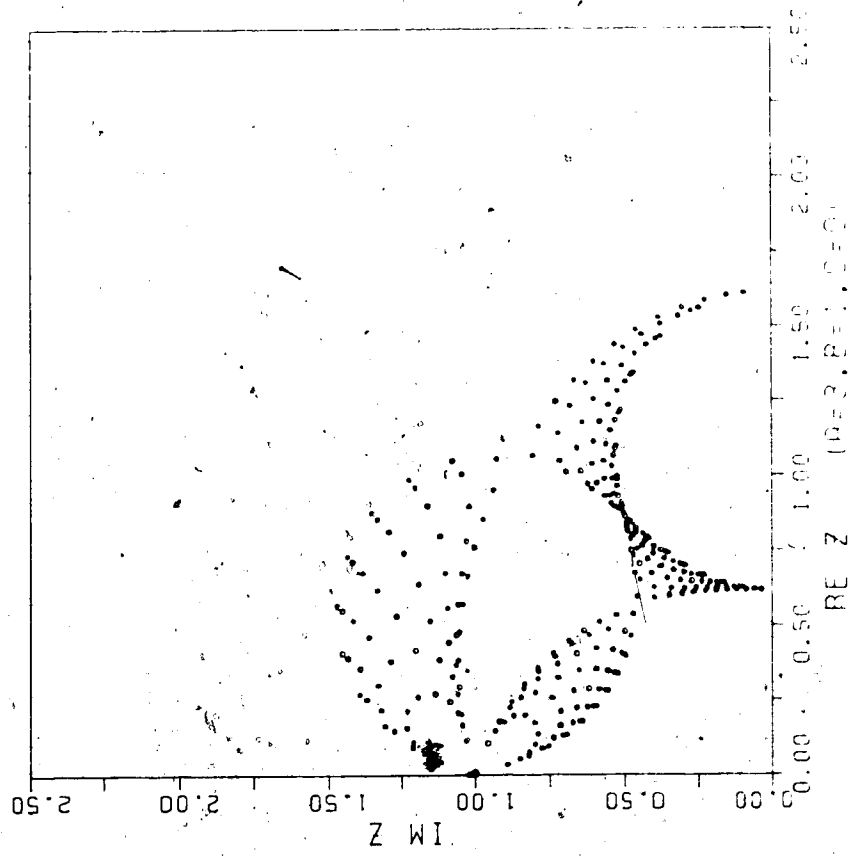


Figure 5.1. Zero distribution for $(3,1,0)$ in the z -plane.

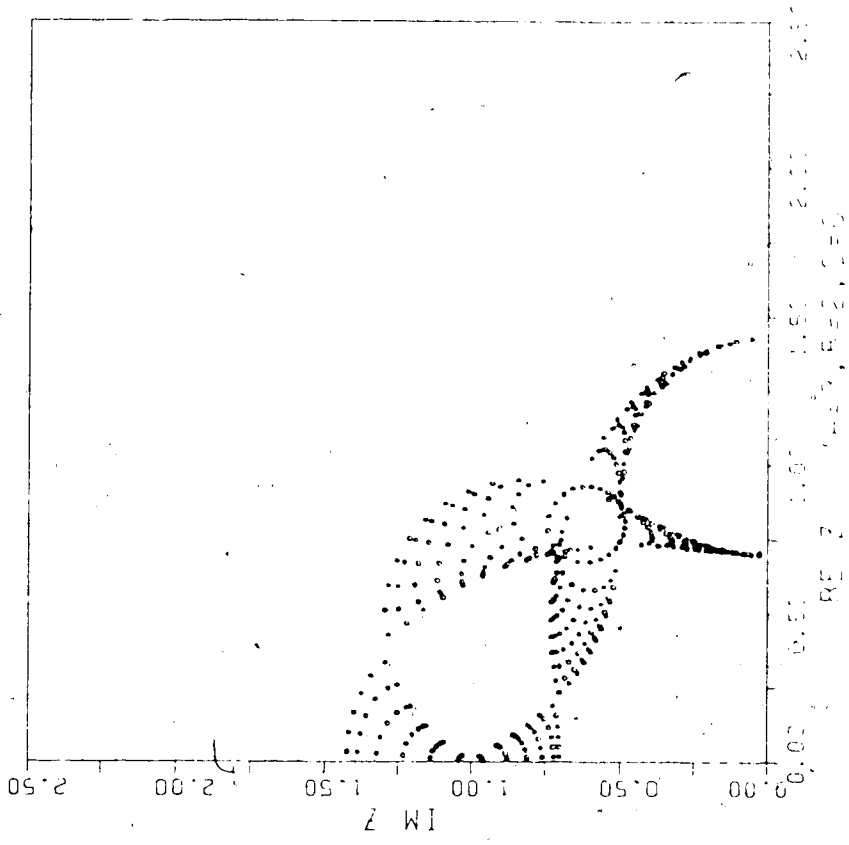


Figure 5.2. Zero distribution for $(3,2,0)$ in the z -plane.

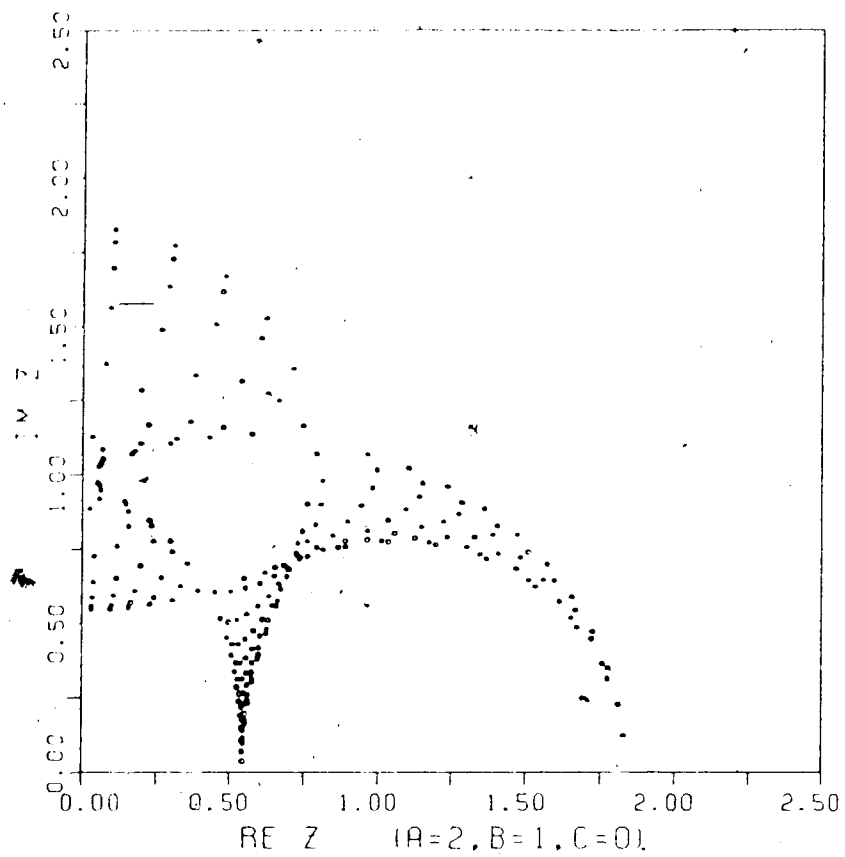


Figure 5.3. Zero distribution for (210) in the z-plane.

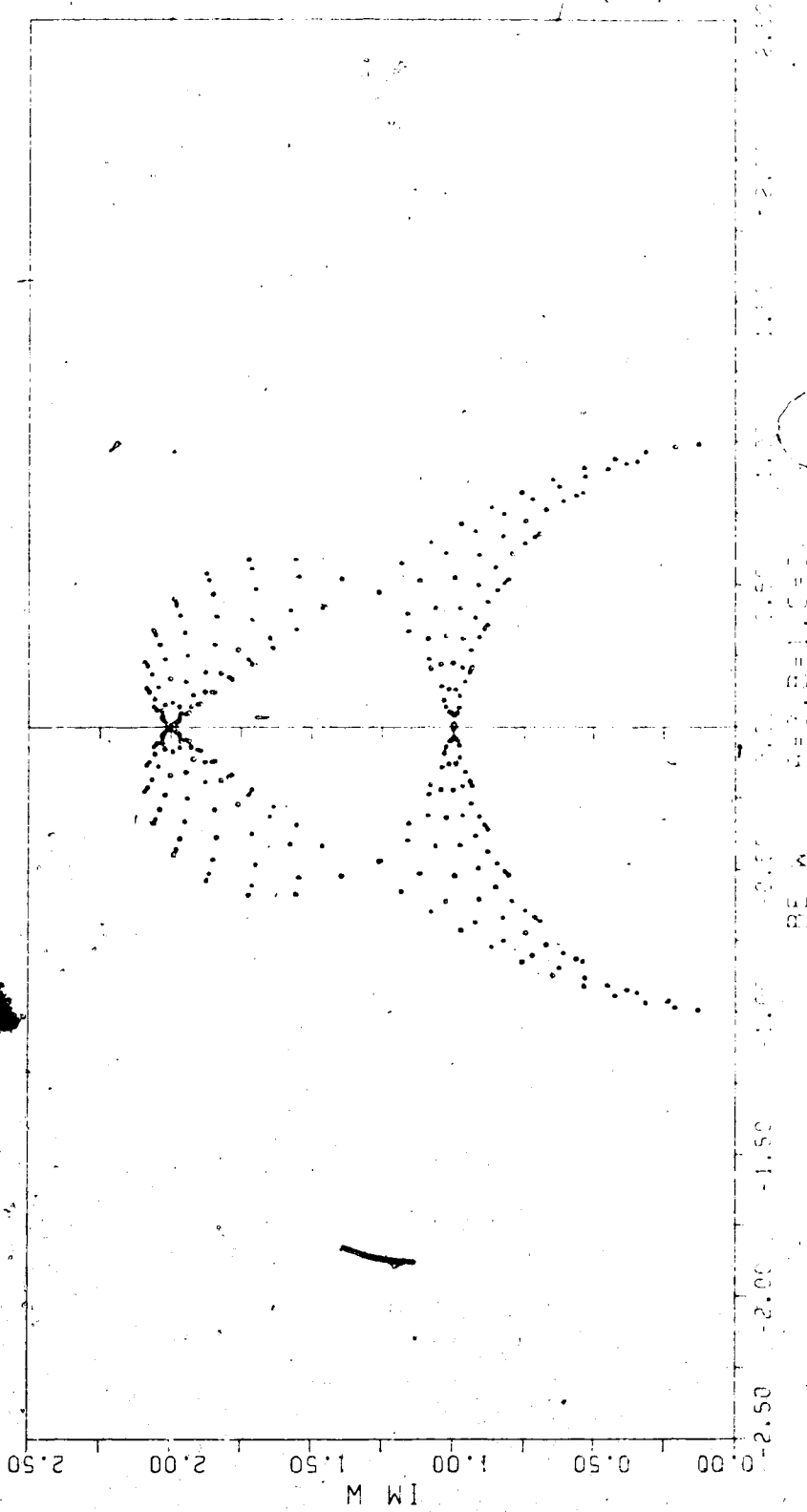


Figure 5.4. Zero distribution for (310) in the w-plane.

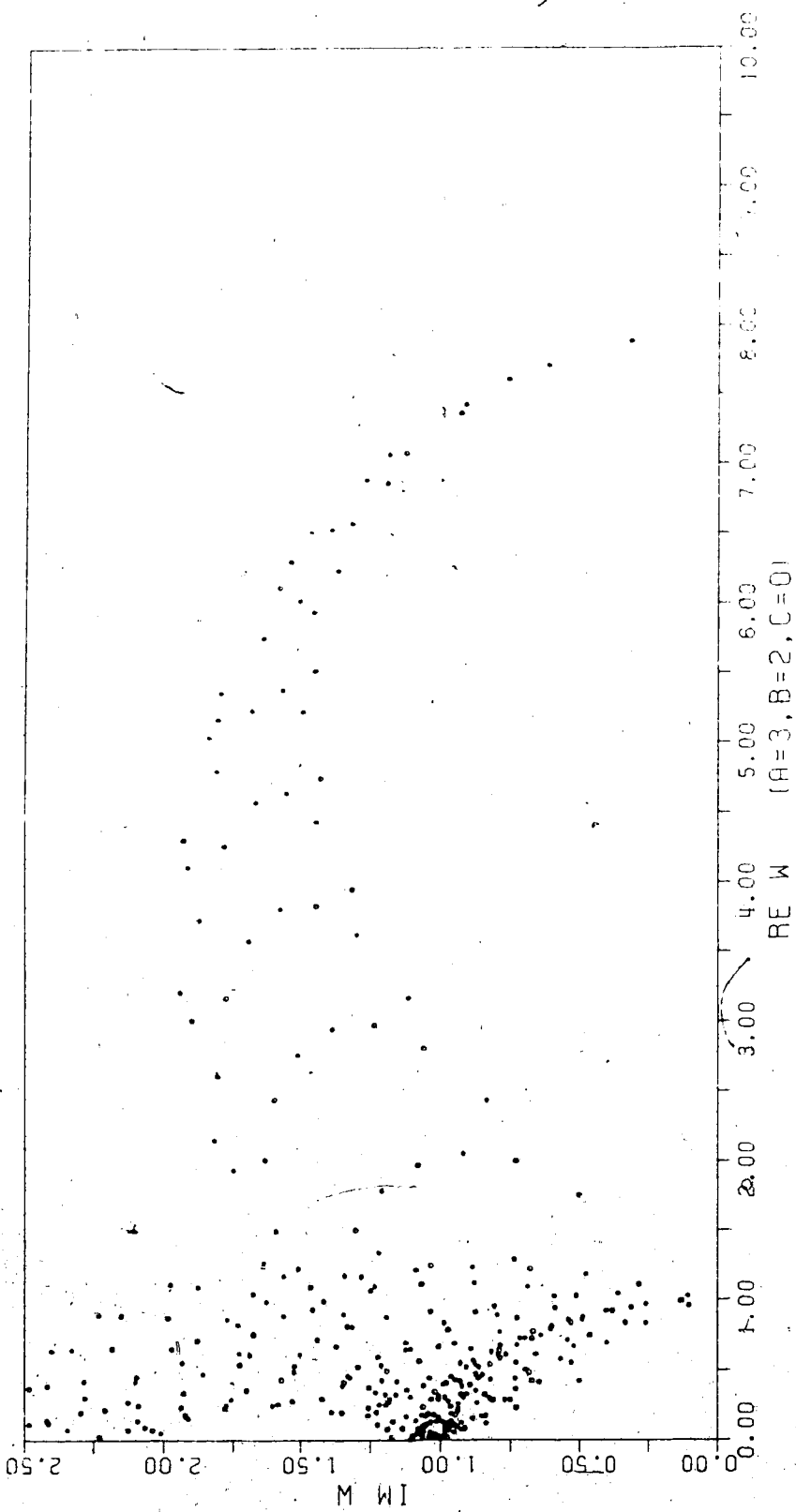


Figure 5.5. Zero distribution for (320) in the w-plane.
This quadratic lattice has unphysical zeros at $w = \pm 7.942920i$.

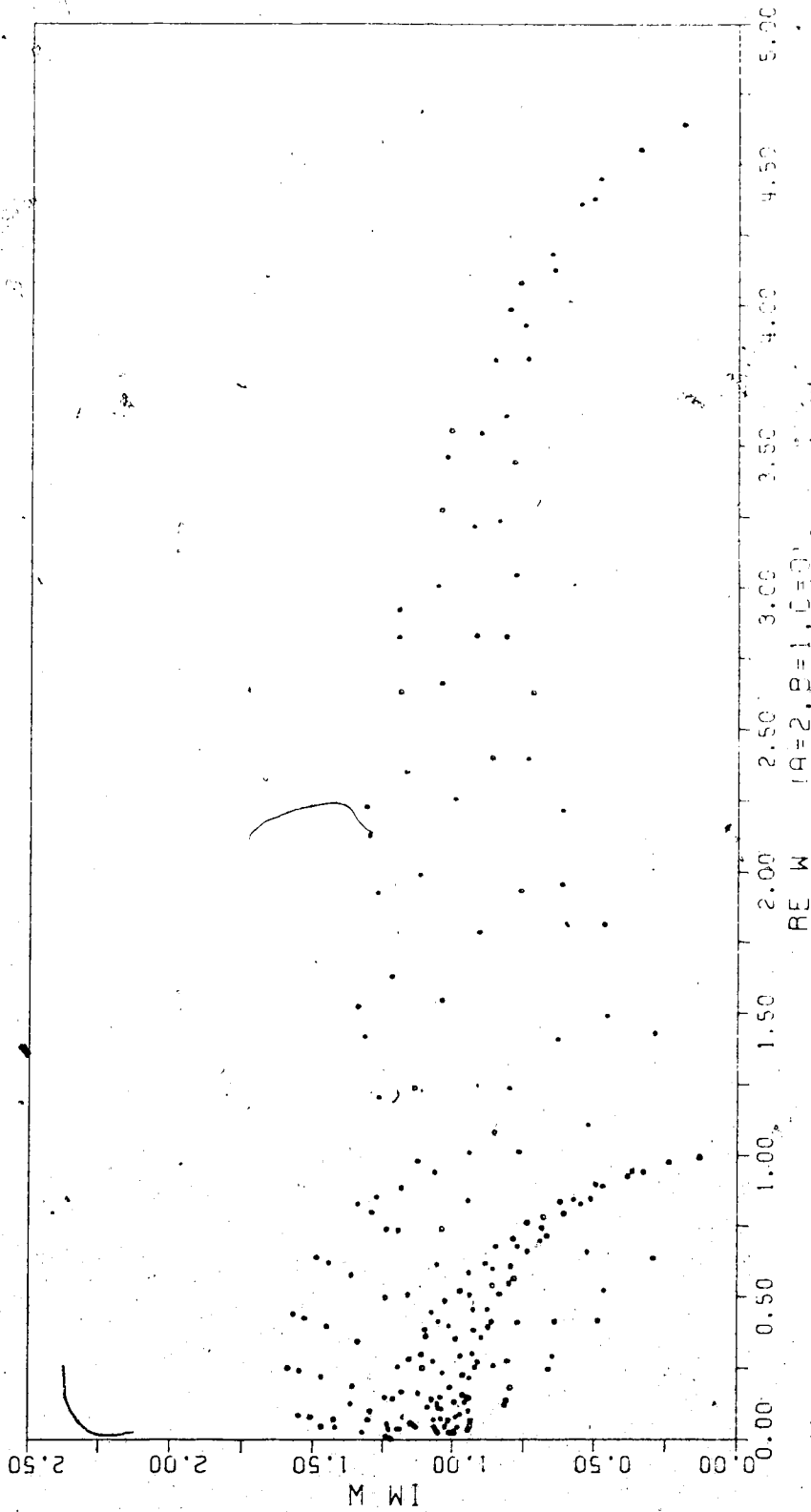


Figure 5.6. Zero distribution for (210) in the w -plane.
This lattice has unphysical zeros at $w = \pm 4.678574$.

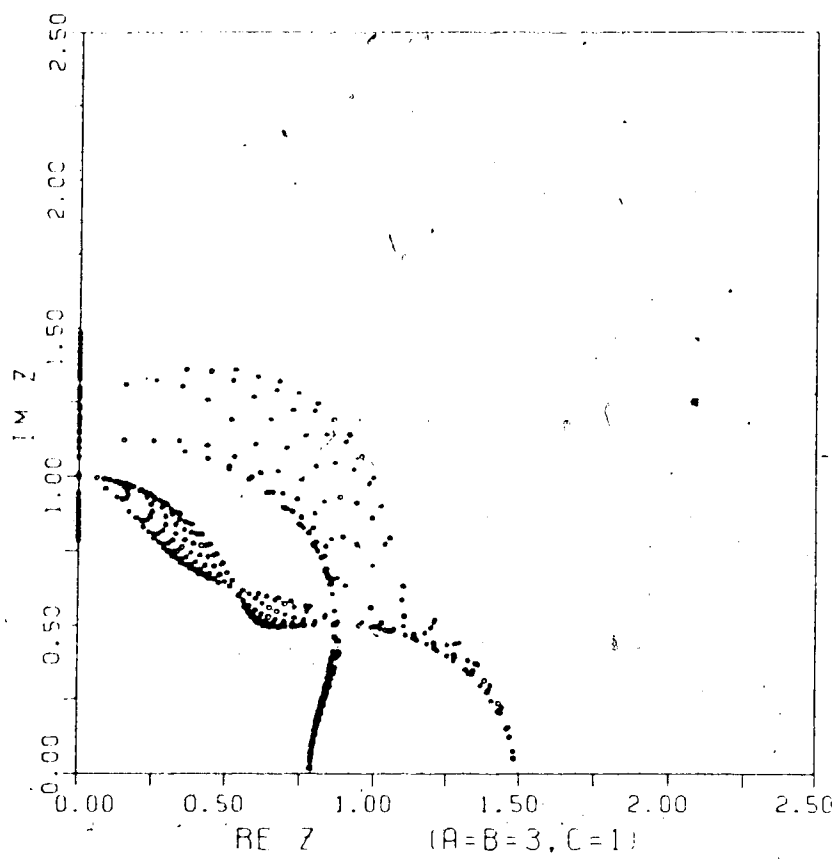


Figure 5.7. Zero distribution for (331) in the z -plane.

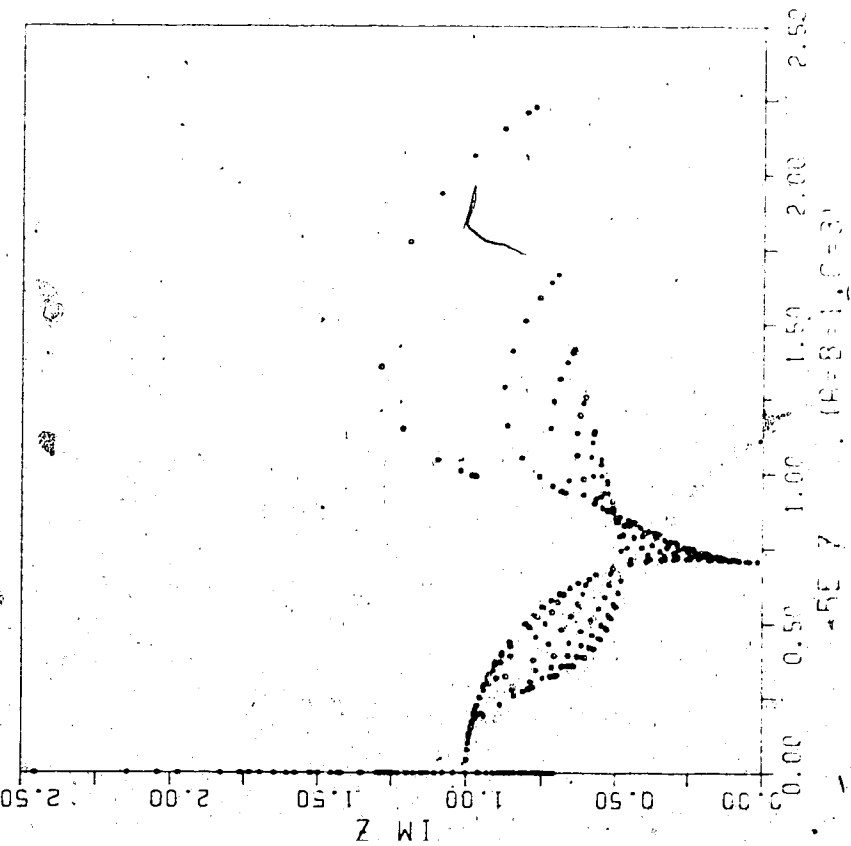


Figure 5.8. Zero distribution for (113) in the z-plane.

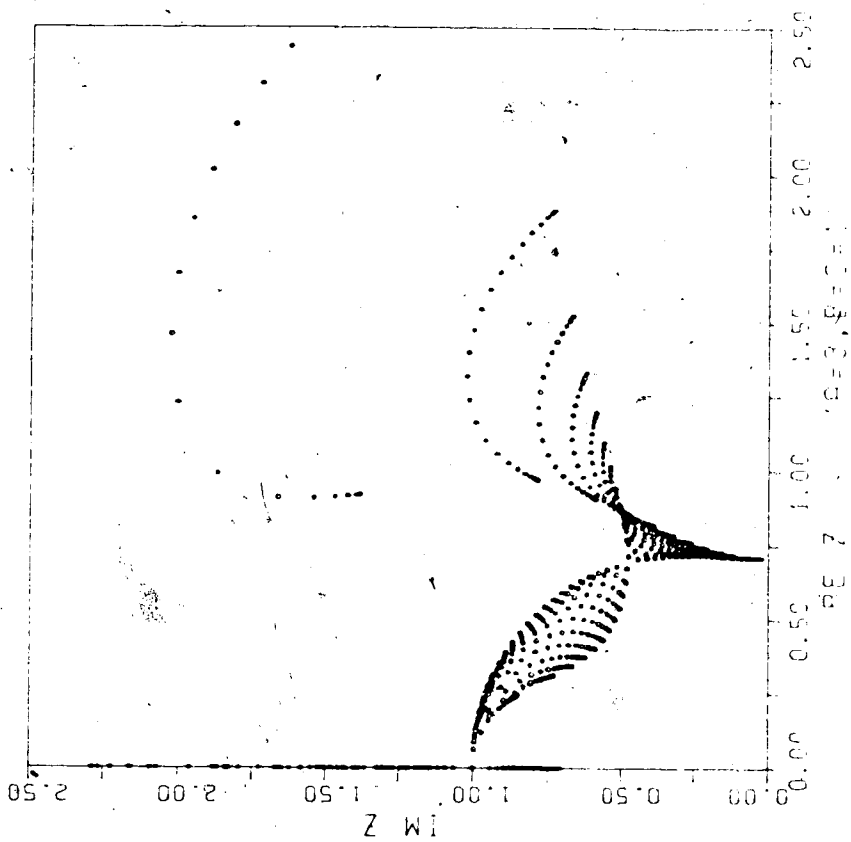


Figure 5.9. Zero distribution for (311) in the z-plane.

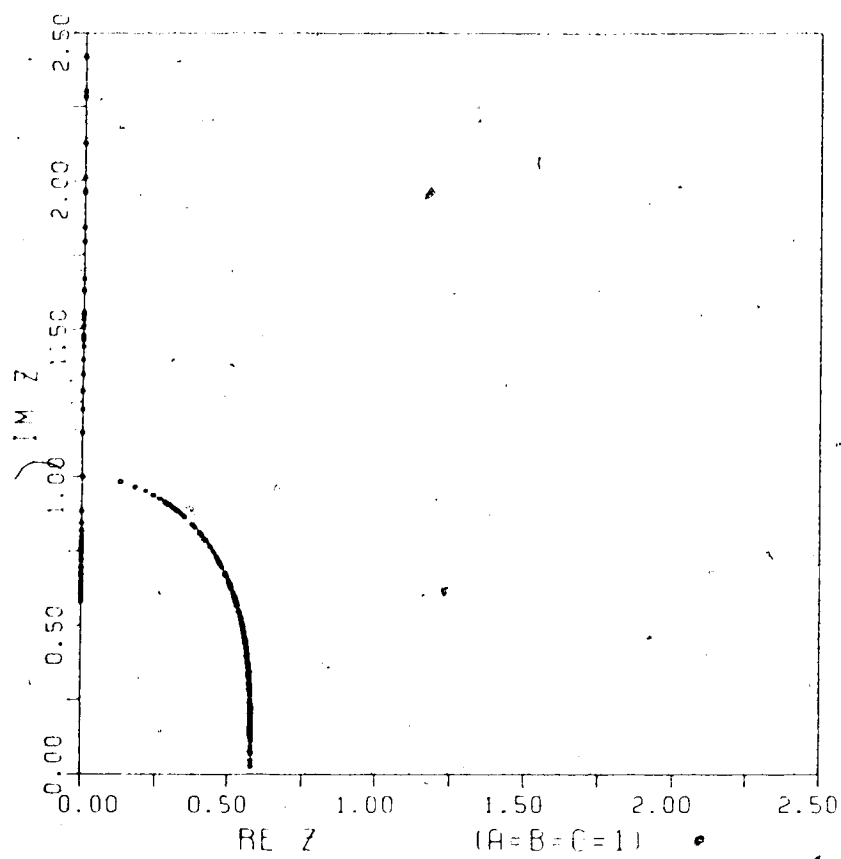


Figure 5.10. Zero distribution of the completely isotropic lattice (111) in the z-plane.

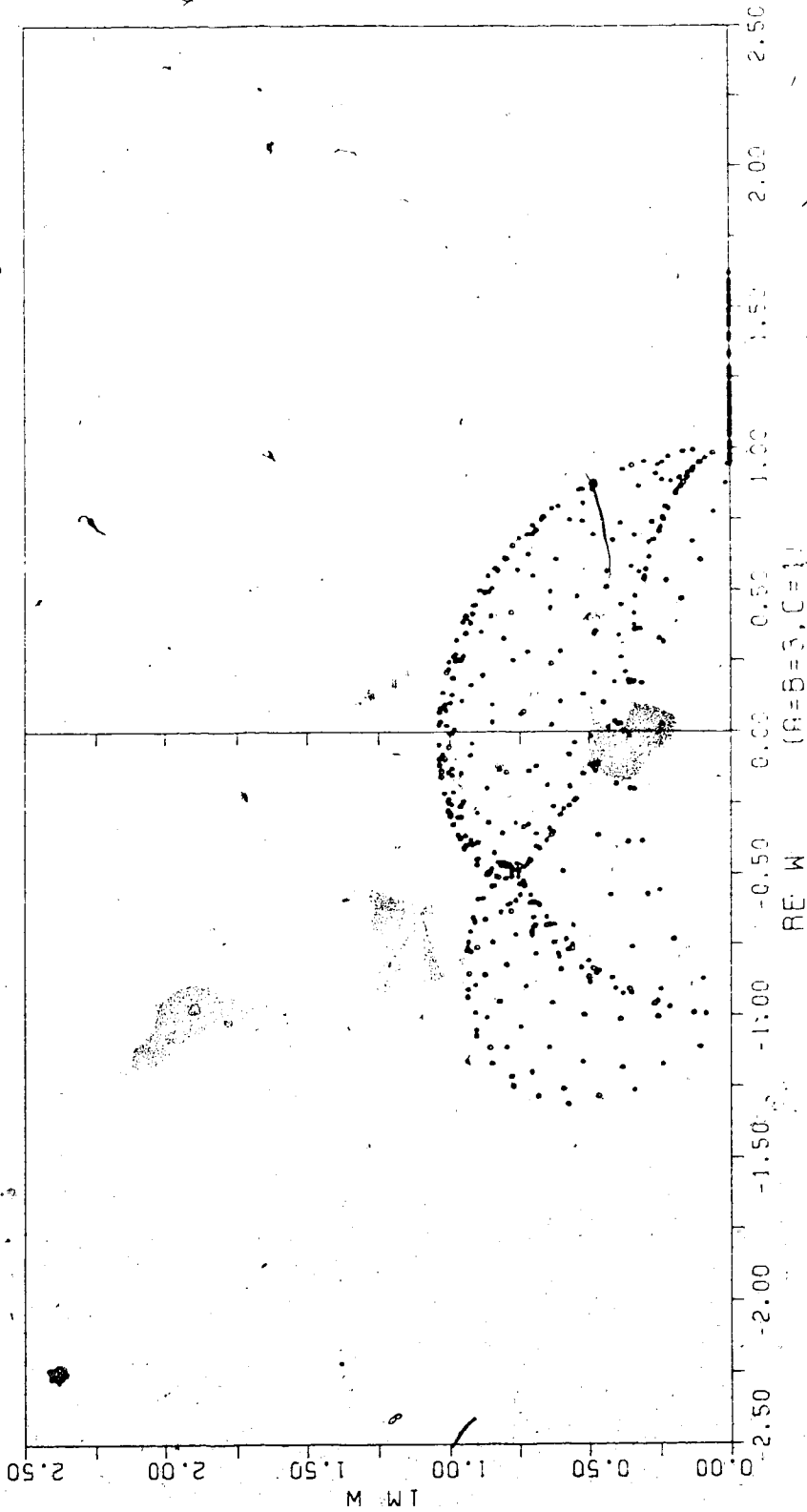


Figure 5.11. Zero distribution for (331) in the w -plane. The line of positive real zeros arises from a line of pure imaginary z -plane zeros. Also $z=ii$ maps to $w=1$.

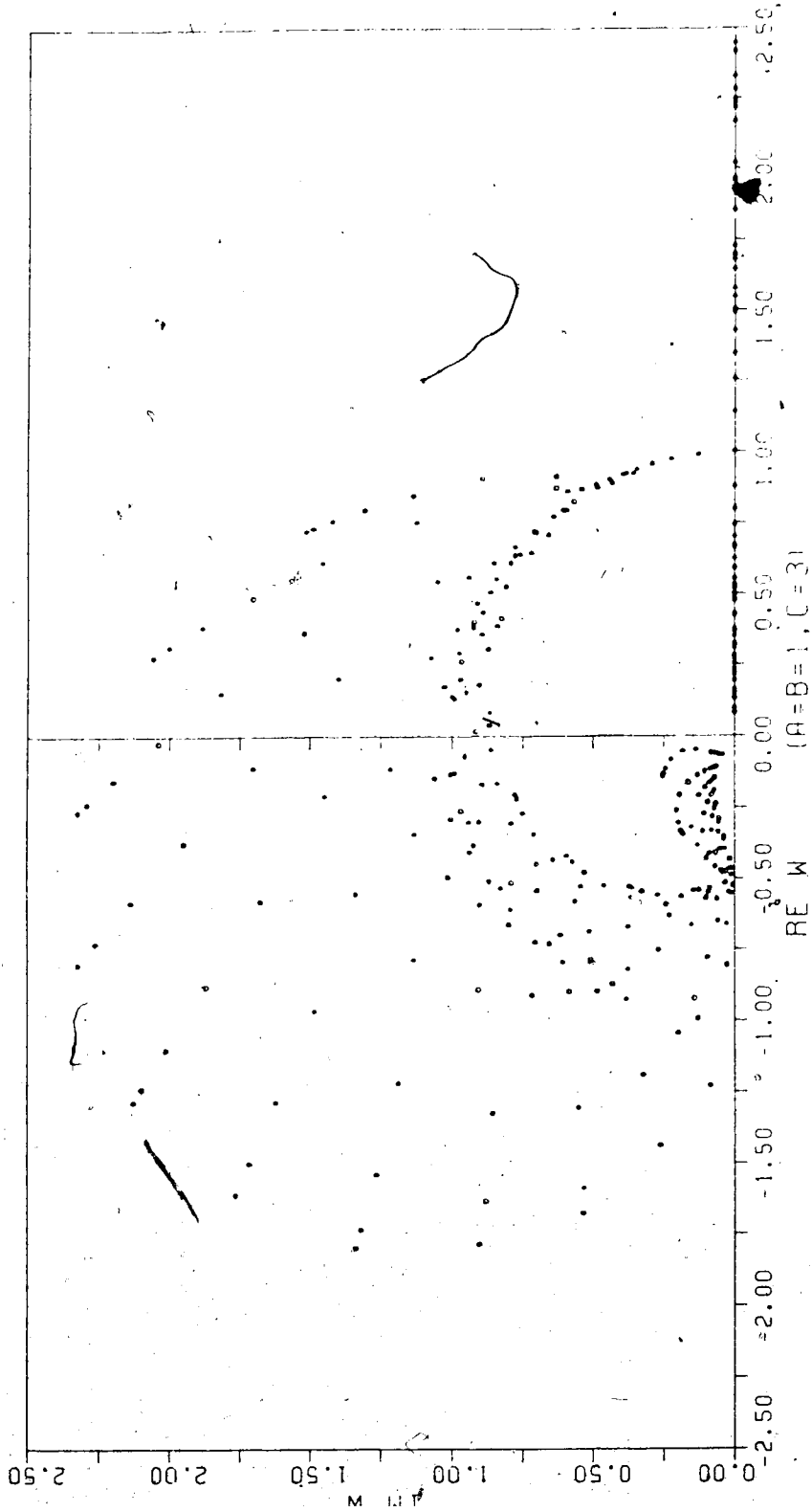


Figure 5.12. Zero distribution for (113) in the w -plane. A line of pure imaginary z -plane zeros maps into a line of positive real zeros in $(0,3)$.

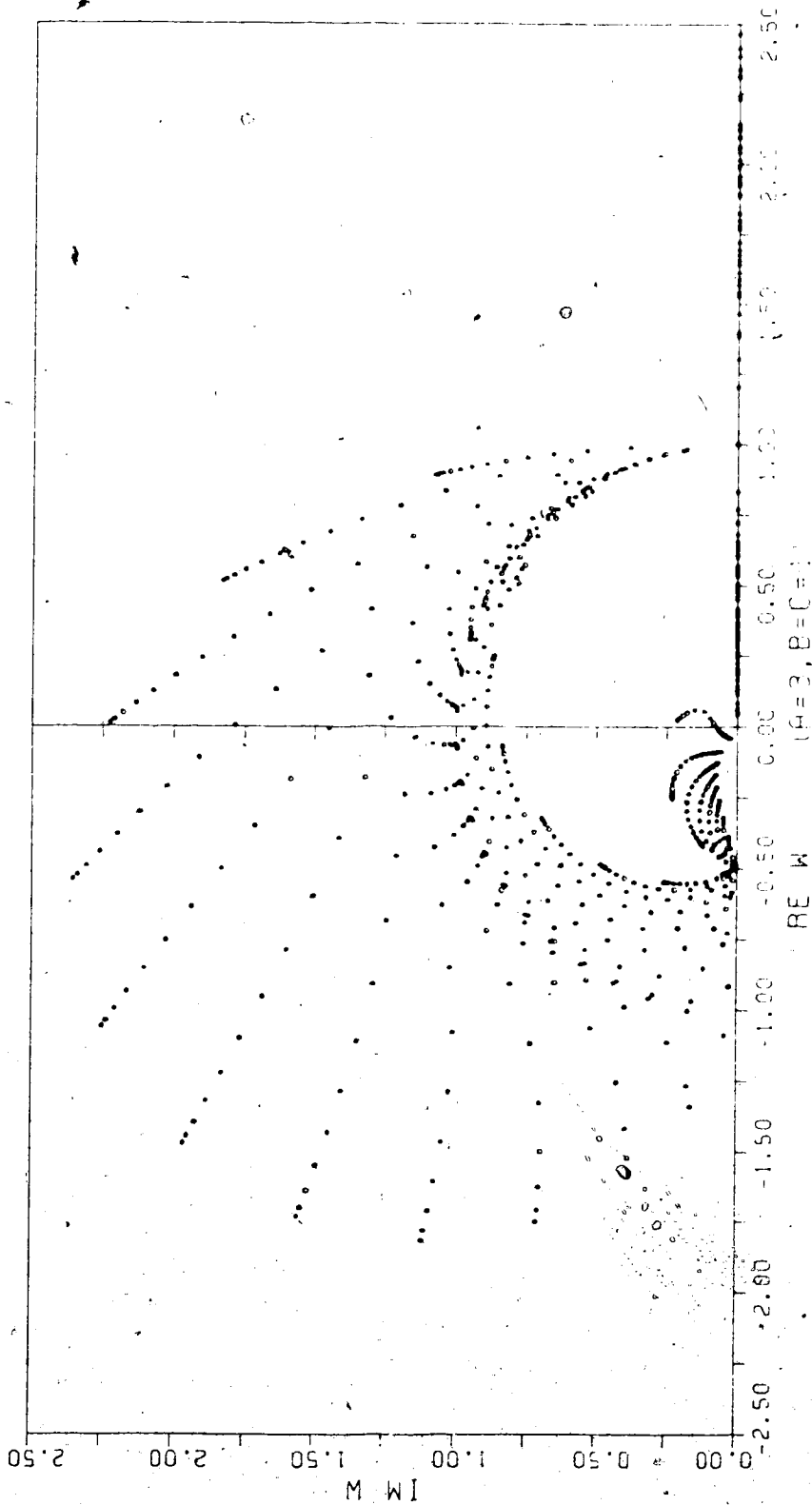


Figure 5.13. Zero distribution for (3.11) in the \bar{w} -plane.

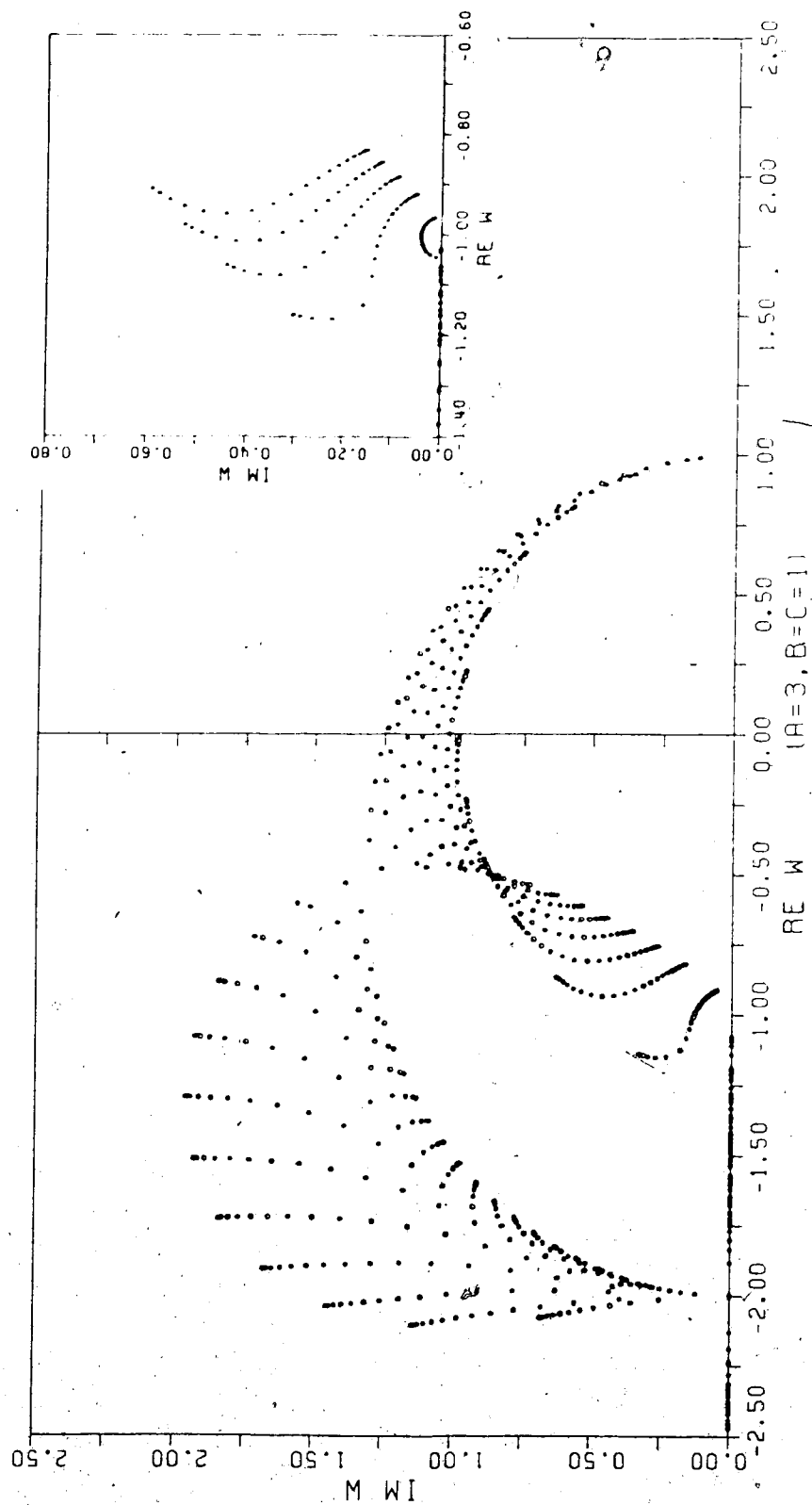


Figure 5.14. Zero distribution for (311) in the w -plane. The inset shows in more detail the circular pattern of zeros around the antiferromagnetic critical point $w = -1$; the unphysical zero at $w = -2$ arises from $z = \pm i$. A line of pure imaginary z -plane zeros maps into a line of negative real zeros in $(-3, -1]$.

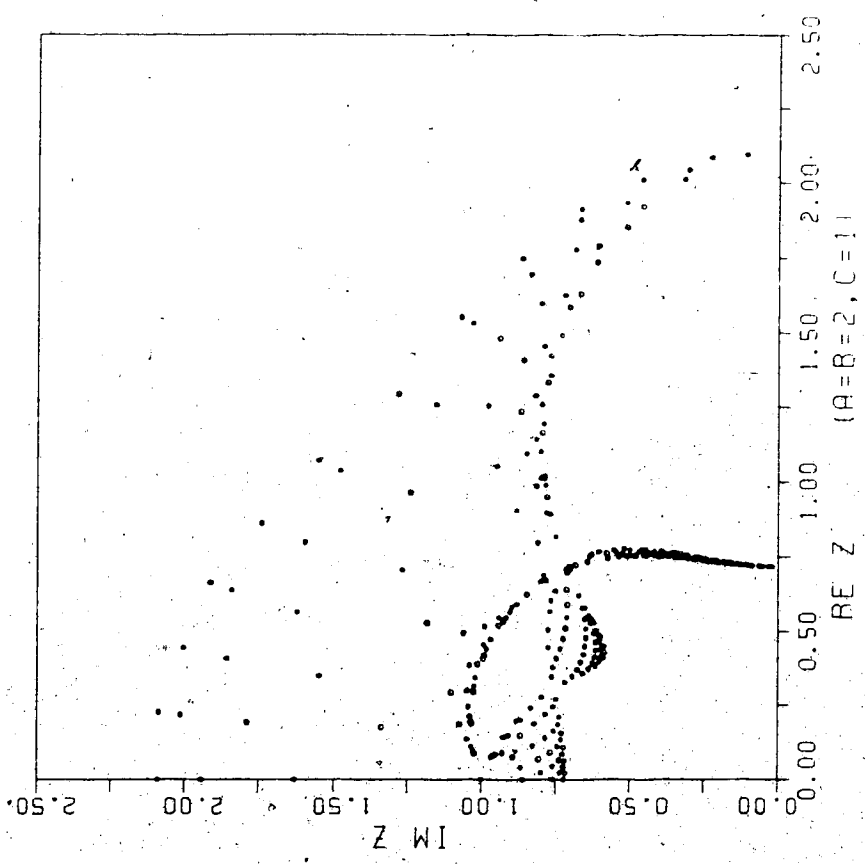


Figure 5.15. Zero distribution for (221) in the z-plane.

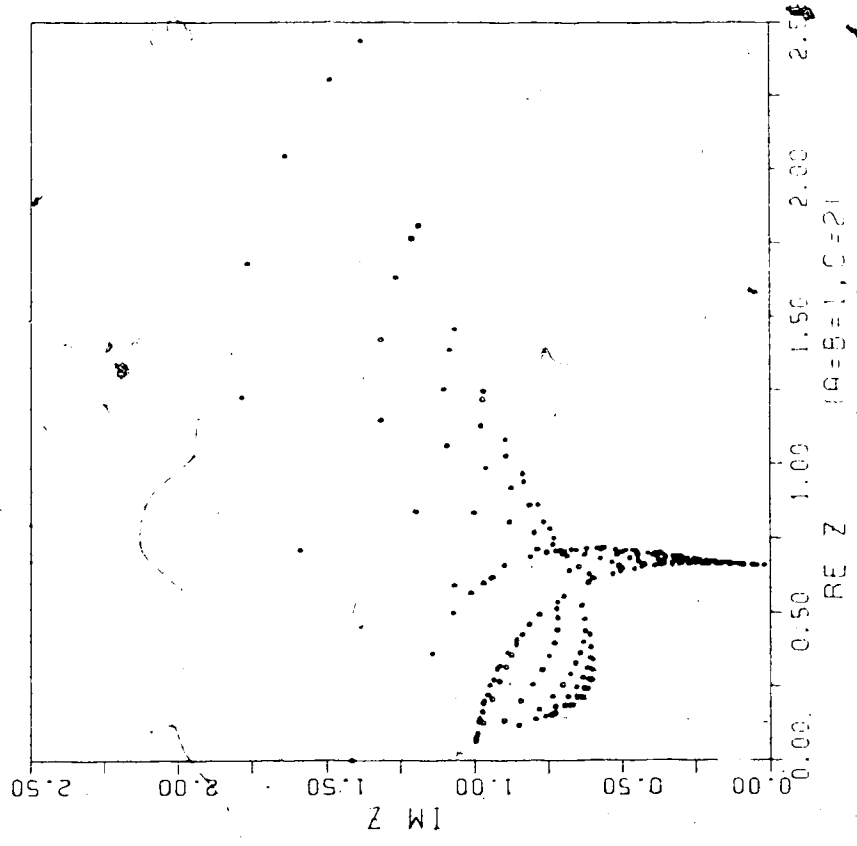


Figure 5.16. Zero distribution for (112) in the z-plane.

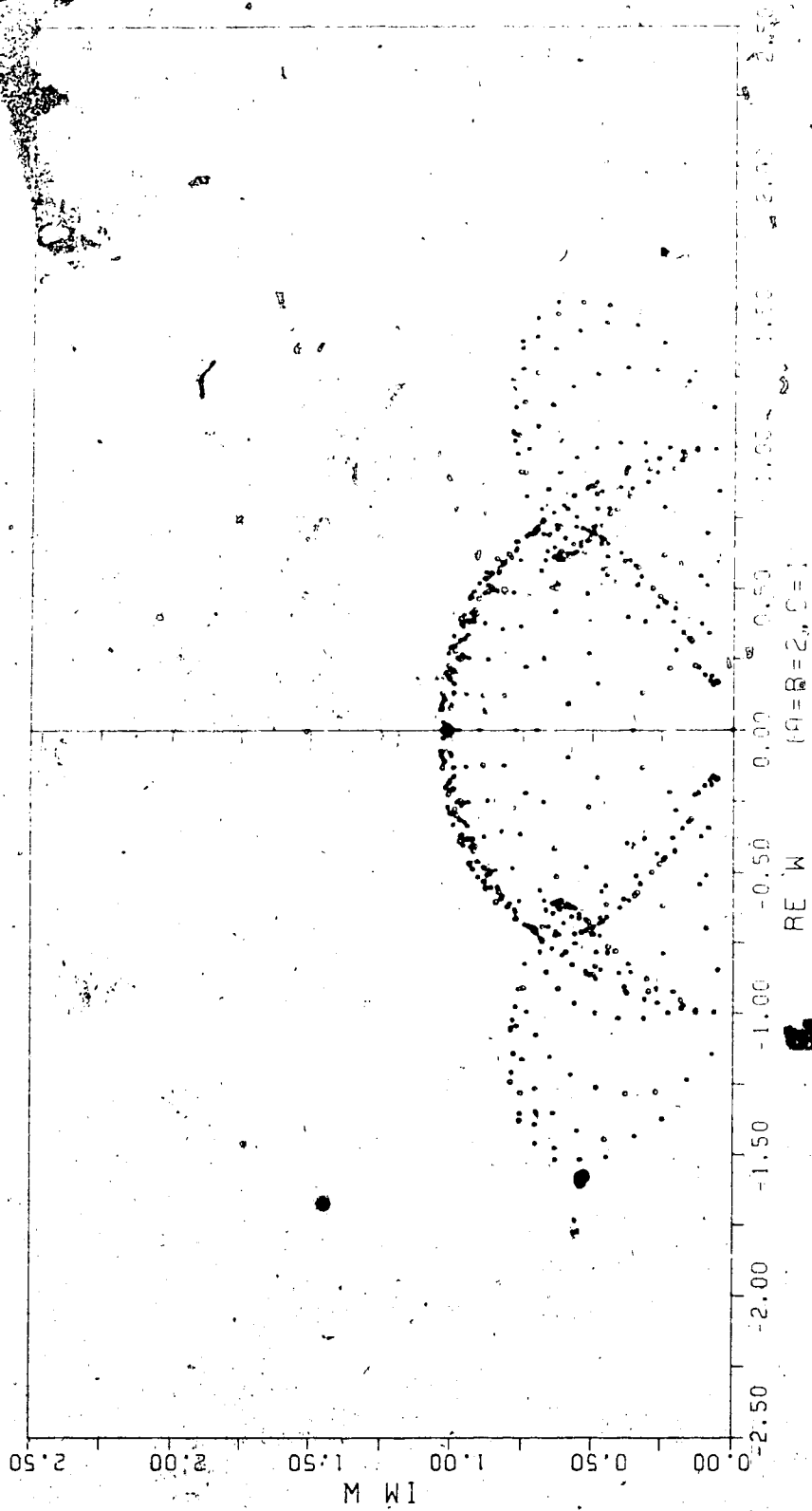


Figure 5.17. Zero distribution for (221) in the w -plane.
 $z = ti$ maps to $w = 0$.

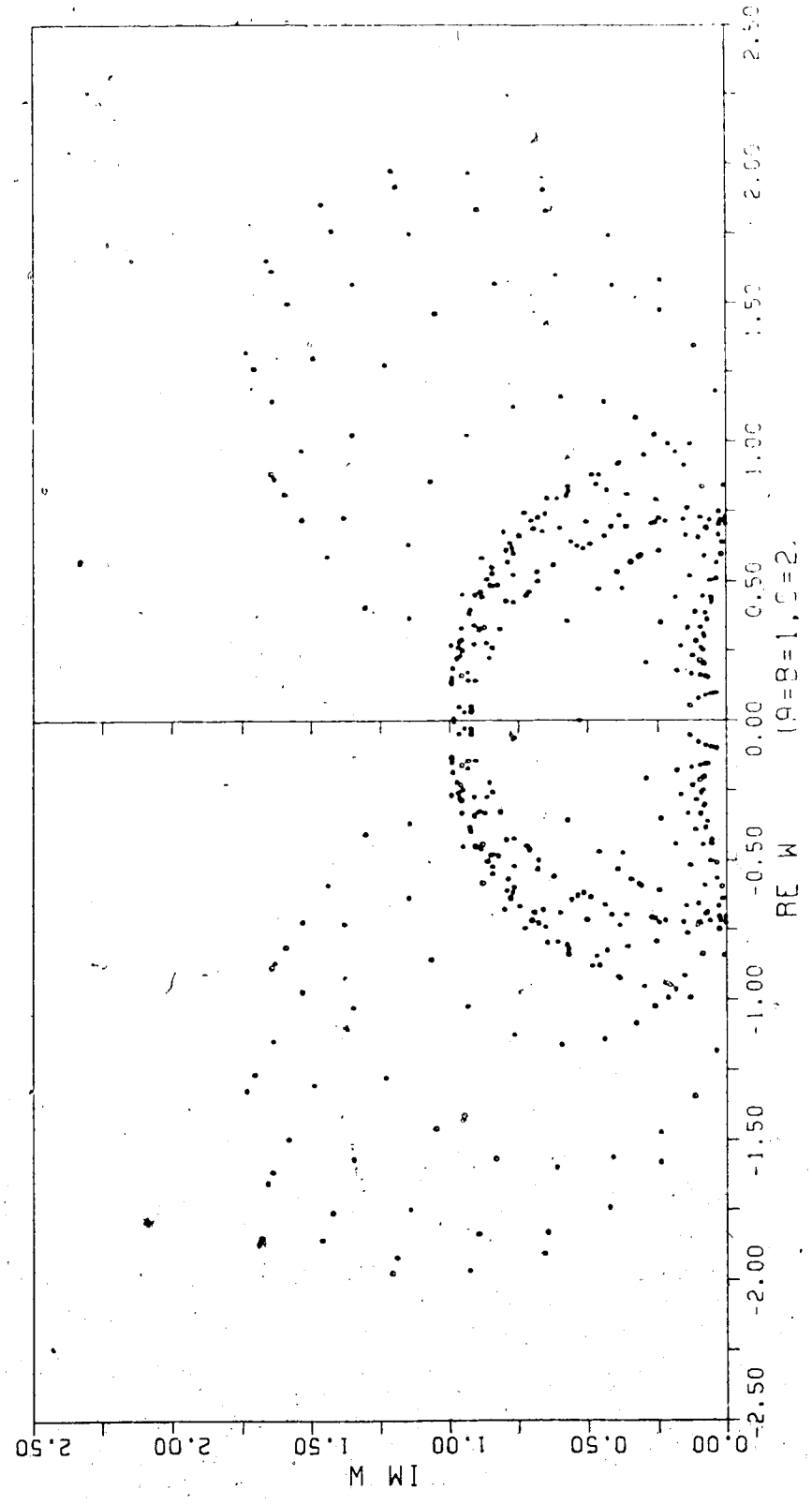


Figure 5.18. Zero distribution for (112) in the w -plane.
Zeros cluster inside the unite circle.

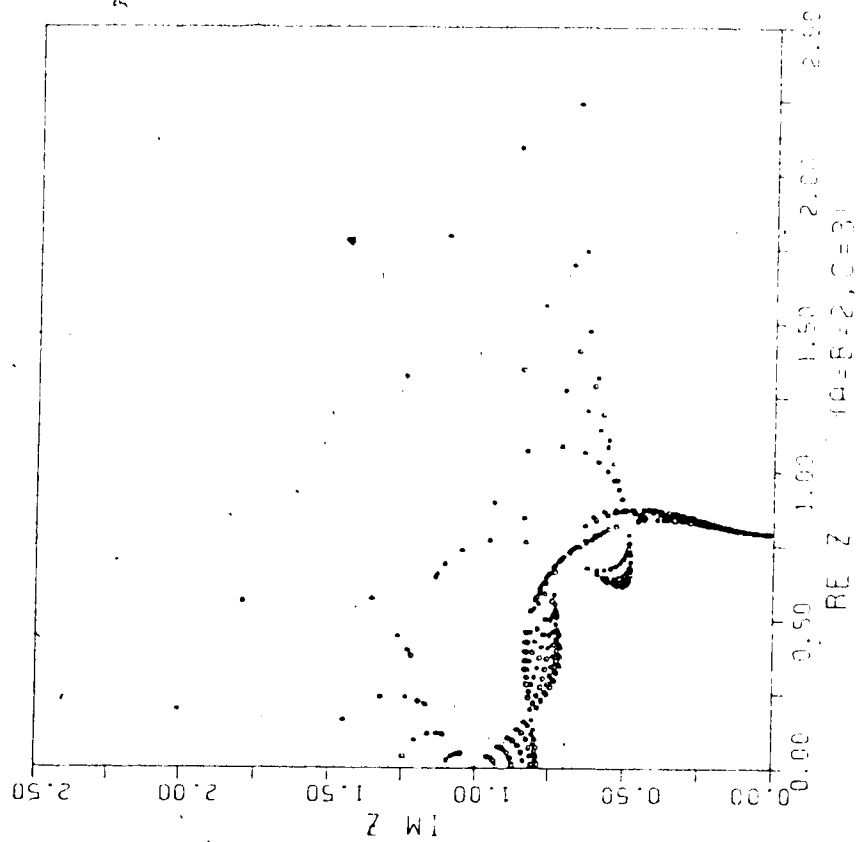


Figure 5.20. Zero distribution for (223) in the z -plane.

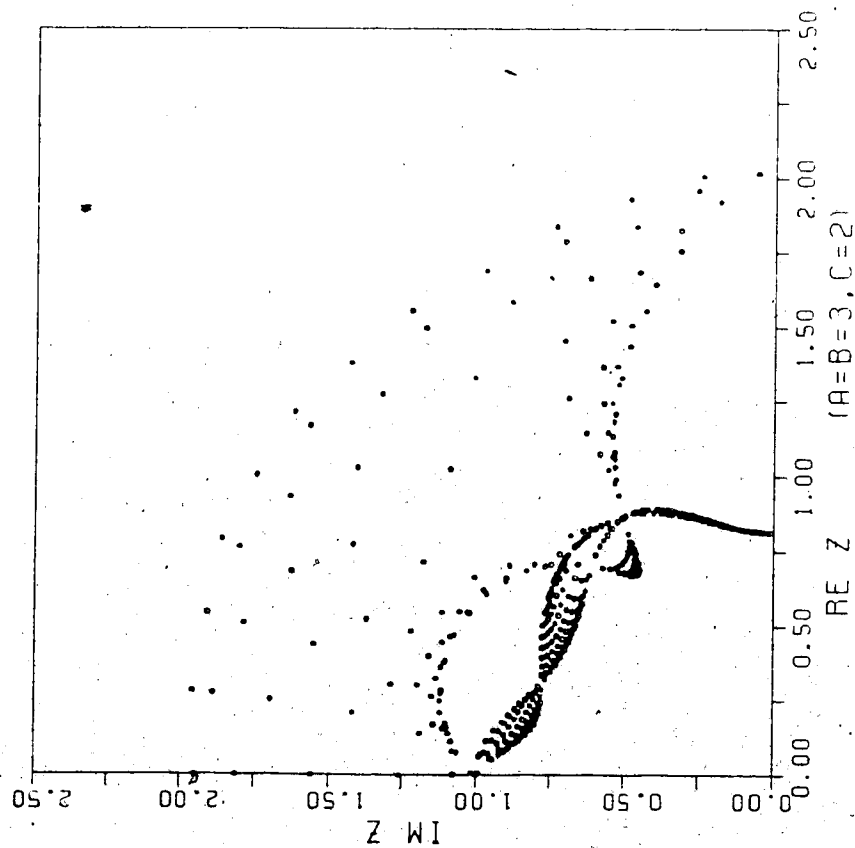


Figure 5.19. Zero distribution for (332) in the z -plane.

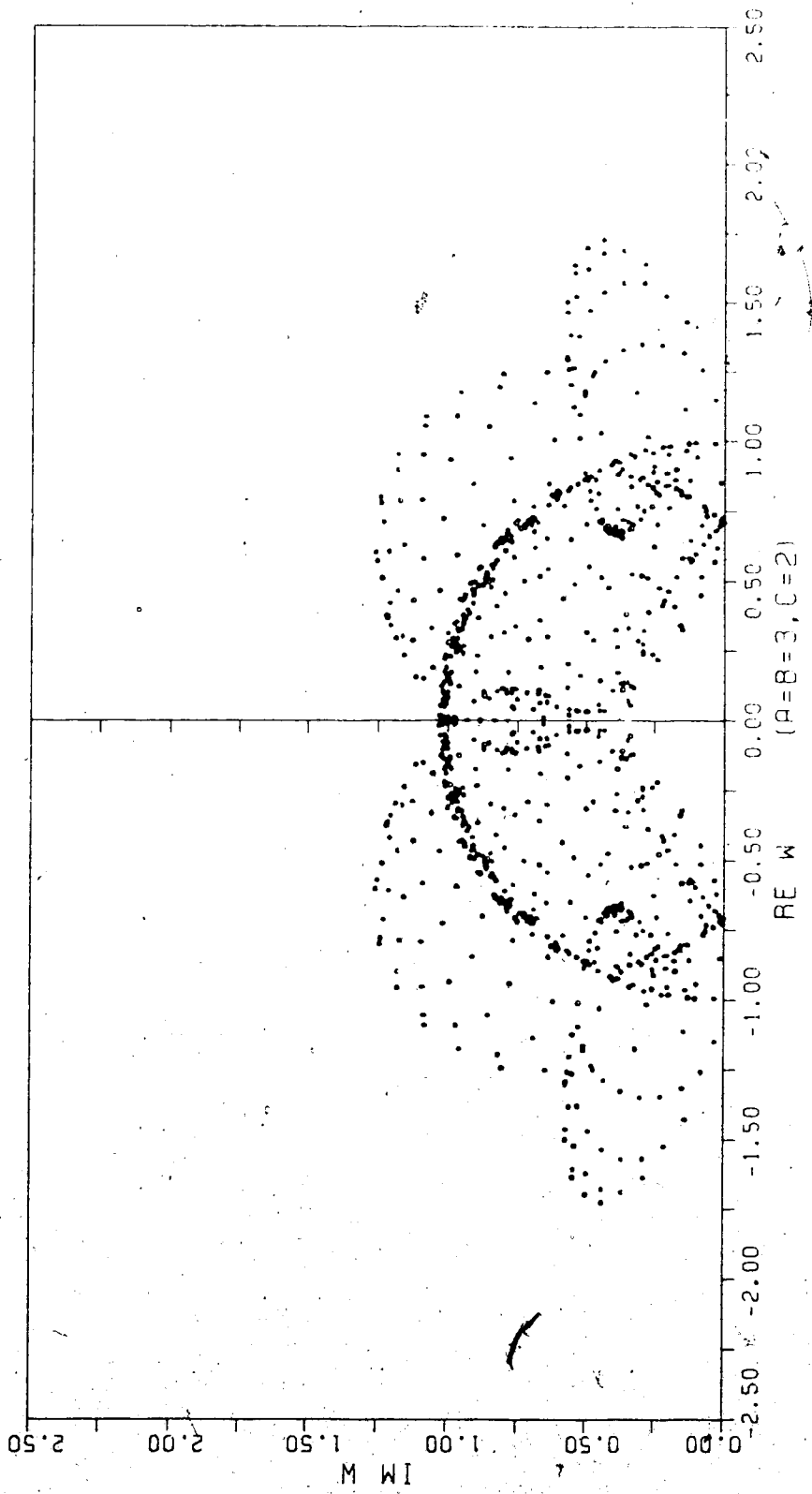


Figure 5.21. Zero distribution for (332) in the w-plane. This lattice has unphysical zeros at $w = \pm 1/\sqrt{2}$.

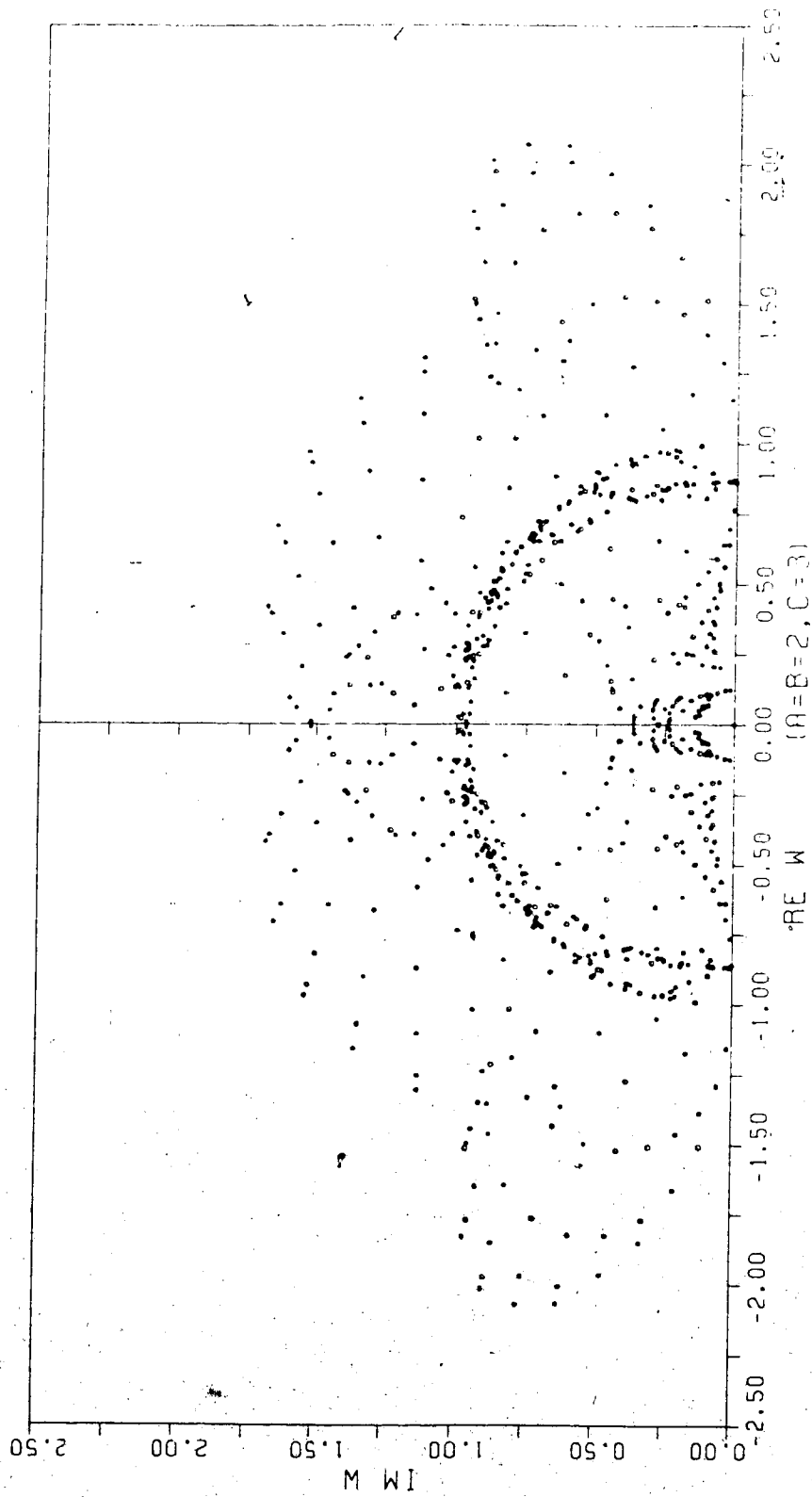


Figure 5.22. Zero distribution for (223) in the w -plane.

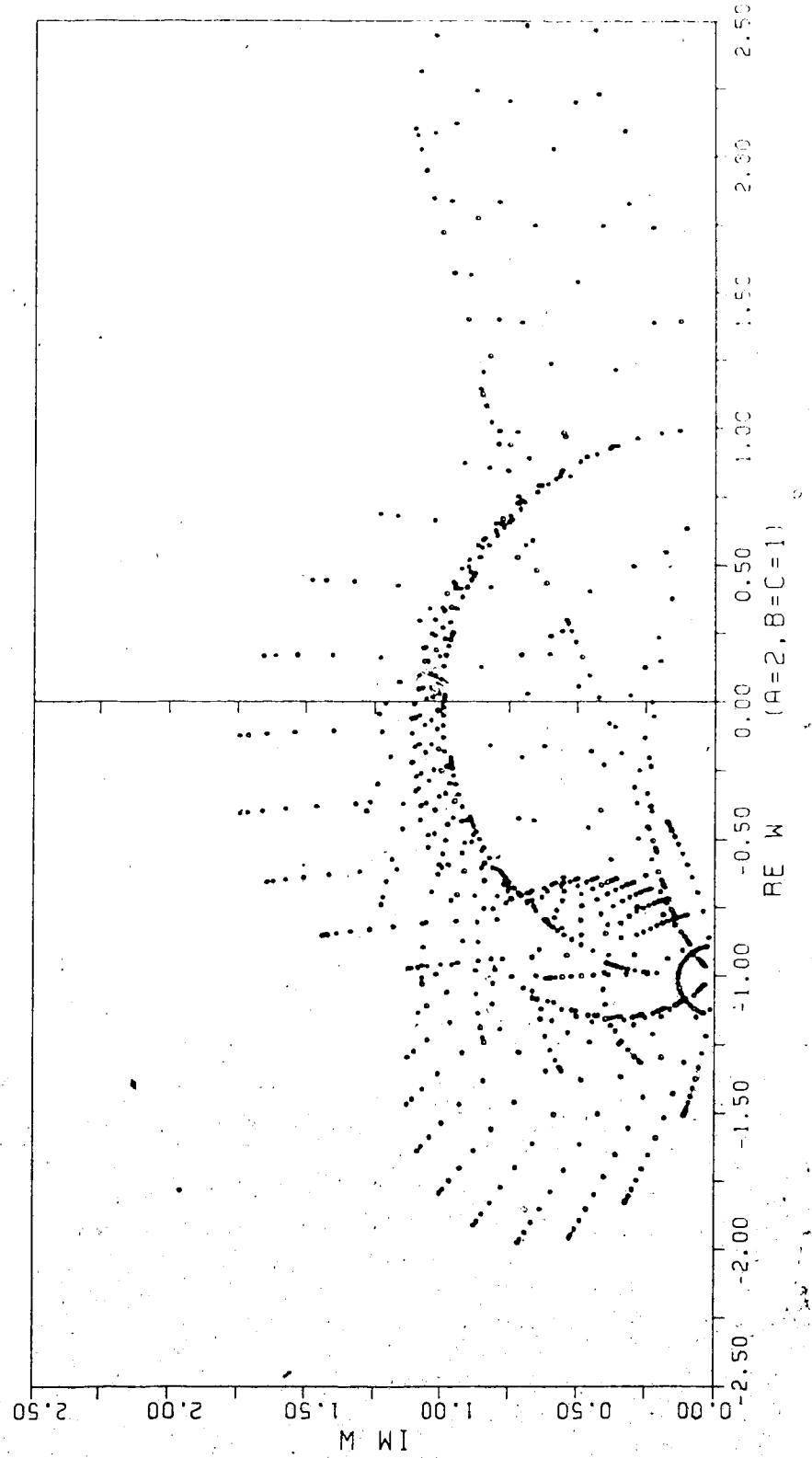


Figure 5.23. Zero distribution for (211) in the w-plane. This lattice has an unphysical real zero at $w = 8.671954$. Zeros cluster outside the unit circle, and the circular distribution near $w = -1$ is clearly visible.

6

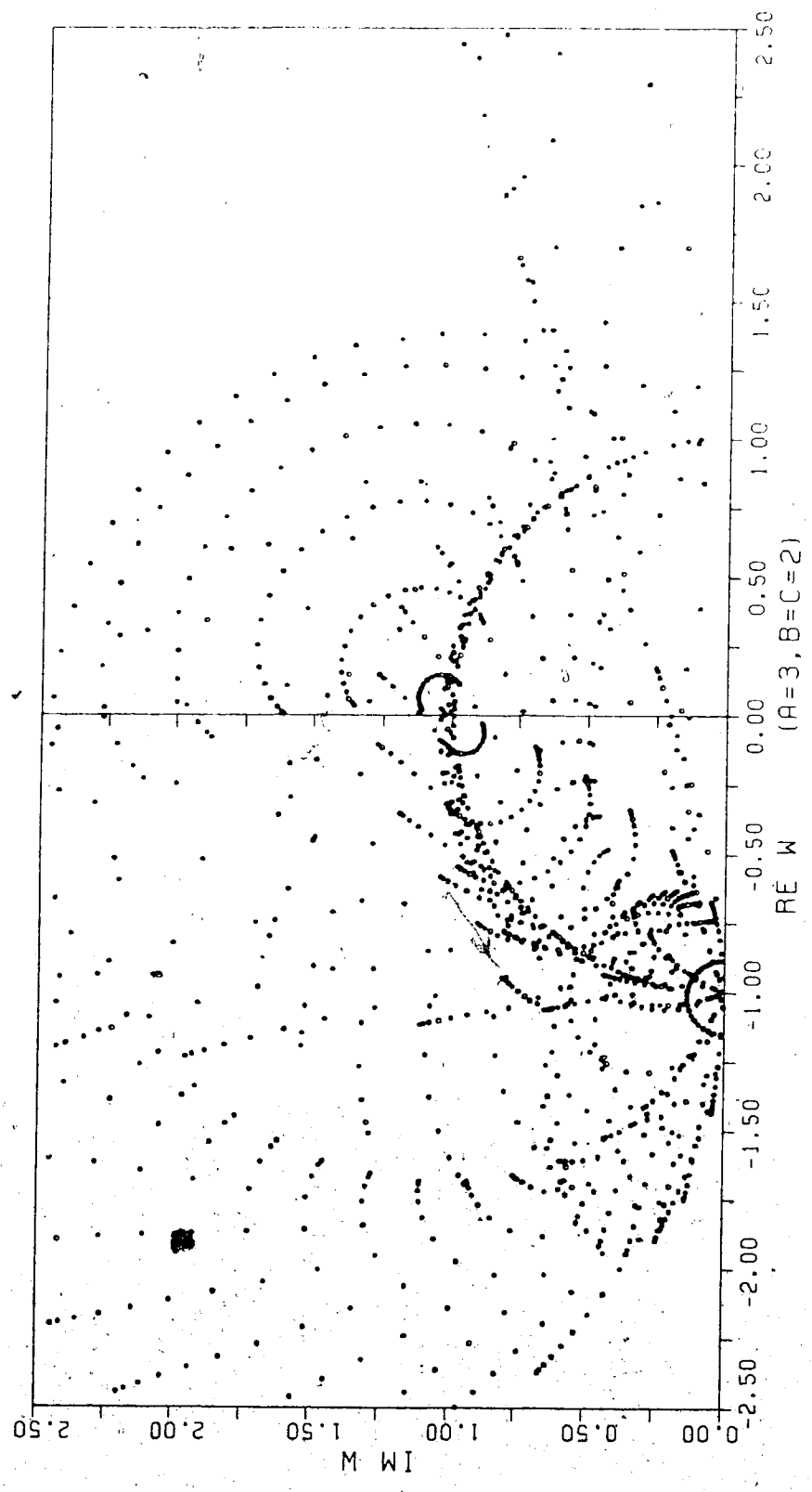


Figure 5.24. Zero distribution for (322) in the w -plane. This lattice also shows the circular distribution near $w = -1$.

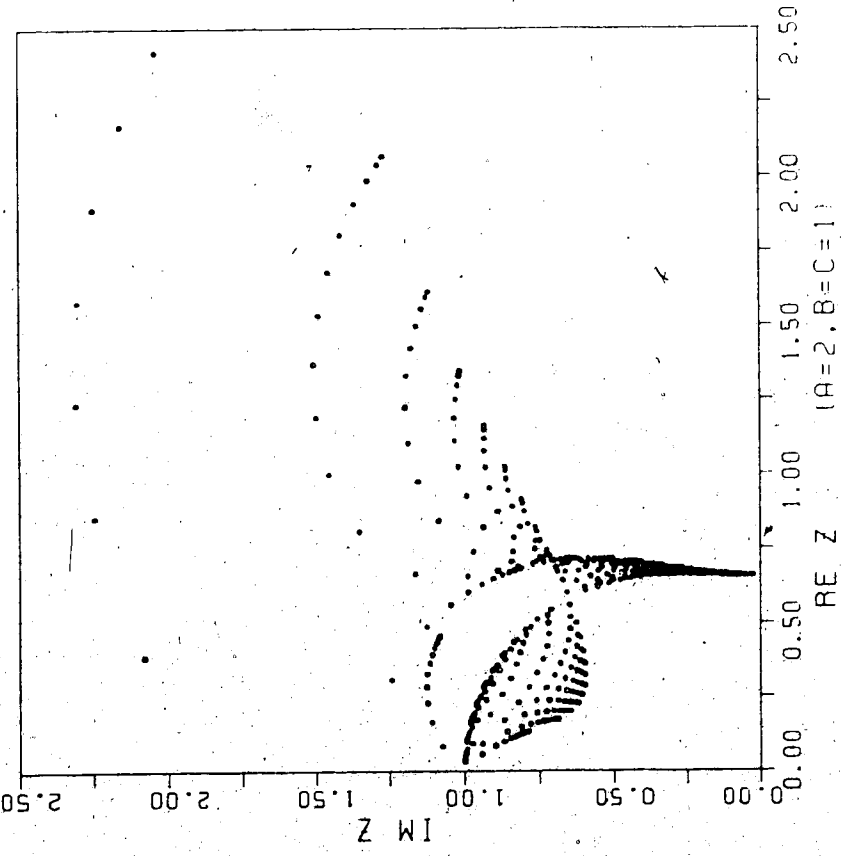


Figure 5.25. Zero distribution for (211) in the z-plane.

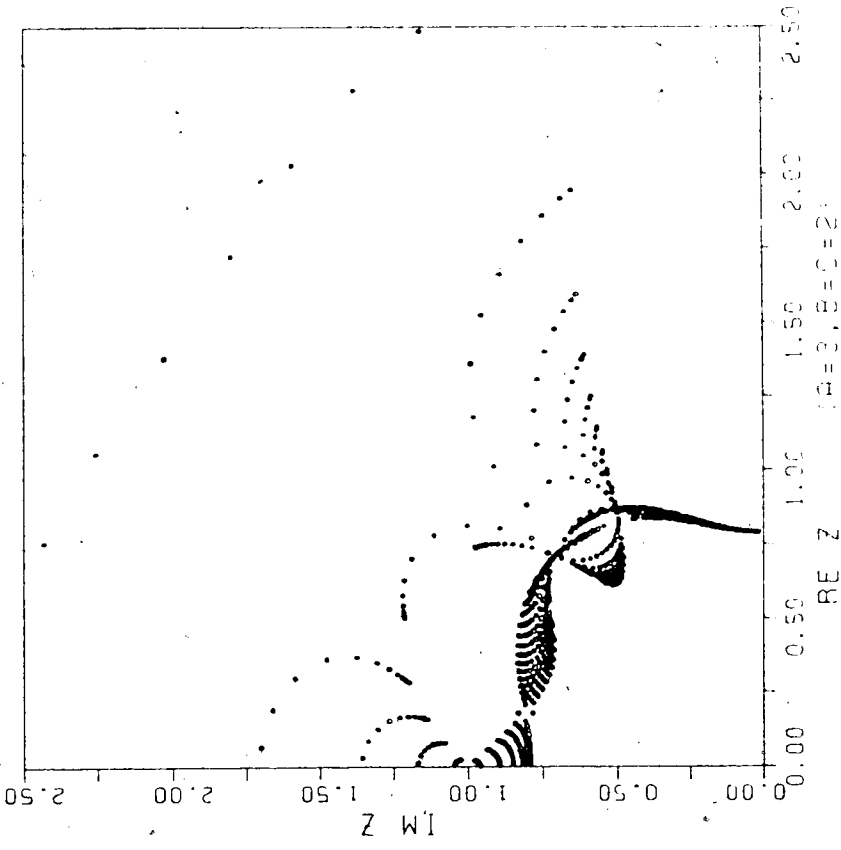


Figure 5.26. Zero distribution for (322) in the z-plane.

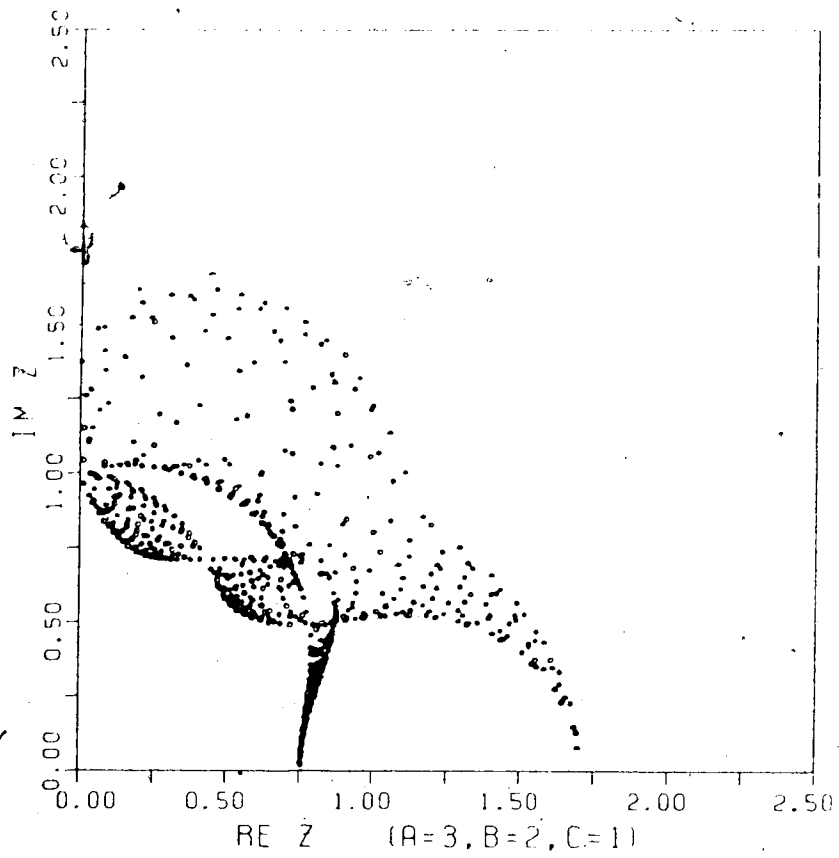


Figure 5.27. Zero distribution for the completely anisotropic lattice (321) in the z-plane.

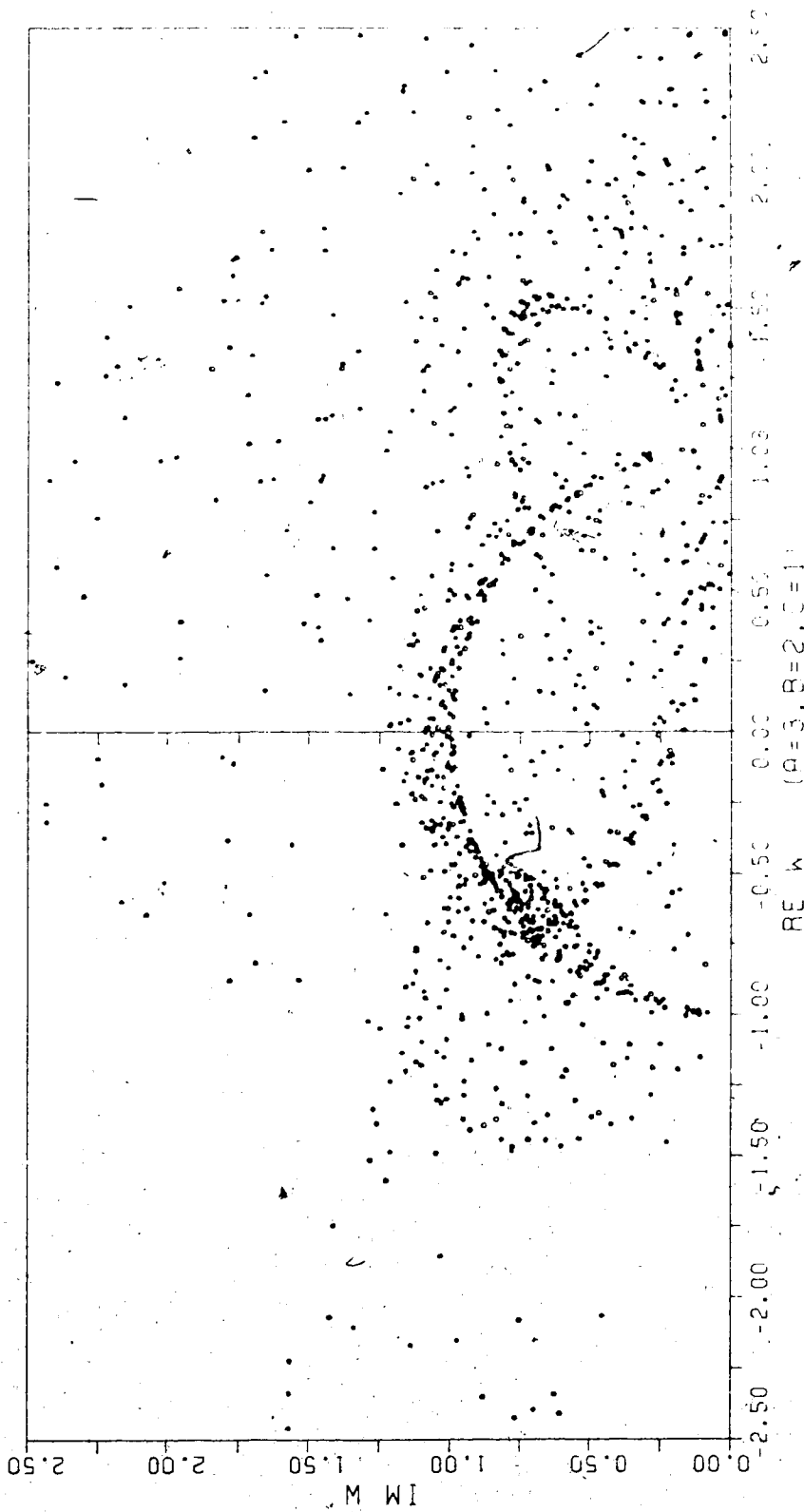


Figure 5.28. Zero distribution for the completely anisotropic lattice (321) in the w-plane.

CHAPTER VI

DISCUSSION AND CONCLUSIONS

For a finite lattice consisting of N spins, the partition function can be written as a polynomial. Usually one fixes the temperature or magnetic field, and discusses zeros of this polynomial in terms of the remaining variable. The coefficients of the remaining variable are always positive. This means that in the $\exp(-2h)$ plane there are no zeros on the positive real axis; in the $\exp(-2K)$ plane there are no zeros on the entire real axis in view of Lemma 5.1. In the thermodynamic limit zeros can approach the real axis, and one can discuss the occurrence of a phase transition.

We have seen that in the $\exp(-2h)$ plane zeros of the ferromagnetic Ising lattice lie on the unit circle. In Chapter III we discussed that this result can be extended to the Heisenberg model, the Ising model of general spin, and several other situations.

For the temperature zeros we do not have a theorem regarding their locations. For the isotropic quadratic lattice zeros lie on the unit circle in the $\sinh 2K$ plane, or on two circles of radius $\sqrt{2}$ centered on ± 1 in the $\tanh K$ plane. For the isotropic quadratic and triangular lattices zeros lie

on lines, and for the anisotropic triangular lattices they cover two-dimensional regions.

In Chapter IV we showed that if the square of one term of the partition function is written in terms of an appropriately chosen variable w , then it is possible to extract the density of zeros near the critical points in the w -plane. In the w -plane, the unit circle is part of every zero distribution. Unfortunately, the mapping from the $\exp(-2K)$ to the w -planes can introduce real zeros in the w -plane. These zeros are genuine, but they do not lead to the conclusion that a phase transition occurs. Since the completion of the work discussed in Chapter V, Stephenson has obtained an equation for the location of the boundary zeros everywhere in the $\exp(-2K)$ plane, and has shown that the density of zeros is infinite everywhere on the boundaries.^{a)}

The partition function zero approach to phase transitions is exact for finite lattices. In Chapter III it was shown that this approach leads to a logarithmic singularity in the specific heat for the Ising model, in agreement with the specific heat known from the Onsager solution and the series expansions. This justifies calculating the zeros of a finite lattice, and then passing to the thermodynamic limit to discuss the onset of a phase transition.

a) J. Stephenson, in preparation for publication.

The partition function zero distributions fit into the scaling theory. Fisher and Barber¹ have discussed finite size scaling, and Itsykson, Pearson, and Zuber² used the finite size scaling theory to discuss the Lee-Yang edge in the context of scaling. Stephenson and Couzens³ have also related the density of zeros in terms of the w -variable to scaling theory by scaling the real and imaginary parts of w separately. Finally, we mention that Derrida, De Seze, and Itzykson⁴ have shown that for a diamond hierarchical lattice the zeros of the partition function in the thermodynamic limit are contained in the so-called Julia set of the renormalization transformation. It is not known if this also holds for other lattices. Much remains to be done in this area.

BIBLIOGRAPHY

1. M.E. Fisher and M.N. Barber, *Phys. Rev. Lett.* 28 (1972), 1516.
2. C. Itzykson, R.B. Pearson, and J.B. Zuber, *Nucl. Phys.* B220 (1983), 415.
3. J. Stephenson and R. Couzens, *Physica* 129A (1984), 201.
4. B. Derrida, L. De Seze, and C. Itzykson, *J. Stat. Phys.* 33 (1983), 559.